LONG TERM ADAPTATION SCENARIOS

TOGETHER DEVELOPING ADAPTATION RESPONSES FOR FUTURE CLIMATES

CLIMATE TRENDS AND SCENARIOS

environmental affairs

Department:
Environmental Affairs
REPUBLIC OF SOUTH AFRICA

giz

On behalf of
Federal Ministry for the Environment, Nature Conservation and Nuclear Safety
of the Federal Republic of Germany

SANBI
Biodiversity for Life

LONG-TERM ADAPTATION SCENARIOS
FLAGSHIP RESEARCH PROGRAMME (LTAS)

CLIMATE TRENDS AND SCENARIOS FOR SOUTH AFRICA

LTAS Phase 1, Technical Report (no. 1 of 6)

The project is part of the International Climate Initiative (ICI), which is supported by the German Federal Ministry for the Environment, Nature Conservation and Nuclear Safety.

environmental affairs
Department:
Environmental Affairs
REPUBLIC OF SOUTH AFRICA

giz

On behalf of
Federal Ministry for the Environment, Nature Conservation and Nuclear Safety
of the Federal Republic of Germany

SANBI
Biodiversity for Life

When making reference to this technical report, please cite as follows: DEA (Department of Environmental Affairs). 2013. Long-Term Adaptation Scenarios Flagship Research Programme (LTAS) for South Africa. Climate Trends and Scenarios for South Africa. Pretoria, South Africa.

TABLE OF CONTENTS

LIST OF FIGURES

LIST OF TABLES

LIST OF ABBREVIATIONS

AAO	Antarctic Oscillation
ACCESS1-0	Australian Community Climate and Earth System Simulator (Centre for Australian Weather and Climate Research)
AR4	Fourth Assessment Report of the IPCC
AR5	Fifth Assessment Report of the IPCC
CABLE	Atmosphere Biosphere Land Exchange model
CABLE	CSIRO Atmosphere Biosphere Land Exchange model
CCAM	conformal-cubic atmospheric model
CCSM4	Community Climate System Model, version 4 (University Corporation for Atmospheric Research, USA)
CGCM	Coupled Global Circulation Model
CHPC	Centre for High Performance Computing
CIP	Climate Information Portal (CSAG, UCT)
CMIP5	Coupled Model Intercomparison Project Phase 5
CMIPX	Coupled Model Intercomparison Project phase X
CNRM-CM5	National Centre for Meteorological Research (France) Coupled Global Climate Model, version 5
CO_2e	carbon dioxide equivalent
CORDEX	Coordinated Regional Downscaling Experiment
CRU TS3.1	Climatic Research Unit (University of East Anglia) Time Series 3.1
CRU	Climate Research Unit (Hadley Centre/University of East Anglia)
CSAG	Climate System Analysis Group
CSIR	Council for Scientific and Industrial Research
CSIRO	Commonwealth Scientific and Industrial Research Organisation
DJF	December, January, February
dtr	diurnal temperature range (the difference between daily tmax and tmin)
ECHAM5/MPI-OM	coupled climate model consisting of atmospheric general circulation model (ECHAM5) and MPI-OM ocean-sea ice component, Max Planck Institute for Meteorology (MPIM), Hamburg, Germany
ENSO	El Niño-Southern Oscillation
GCM	general circulation model
GFDL-CMX	Geophysical Fluid Dynamics Laboratory Coupled Model, versionX (National Oceanic and Atmospheric Administration (NOAA), Geophysical Fluid Dynamics Laboratory USA)

IOD	Indian Ocean Dipole
IPCC	Intergovernmental Panel on Climate Change
IPSL-CM5A-MR	Institute Piere Simon Laplace Climate Modelling Centre Coupled Model
JJA	June, July, August
LTAS	Long-Term Adaptation Scenarios Flagship Research Programme
MAM	March, April, May
MAP	Mean annual precipitation
MIROC3.2-medres	Model for Interdisciplinary Research on Climate, medium resolution (Centre for Climate System Research (CCSR) of the University of Tokyo, National Institute for Environmental Studies (NIES), Frontier Research Centre for Global Change (FRCGC), Japan Agency for Marine-Earth Science and Technology (JAMSTEC))
MIROC4h	Model for Interdisciplinary Research on Climate (Atmosphere and Ocean Research Institute (AORI) of the University of Tokyo, the National Institute for Environmental Studies (NIES) and the Japan Agency for Marine-Earth Science and Technology (JAMSTEC))
MIT	Massachusetts Institute of Technology
IGSM	Integrated Global System Model
MJO	Madden-Julian Oscillation
MPI-ESM-LR	Coupled Max Planck Institute Earth System Model at base resolution
MRI-GCM3	Meteorological Research Institute Global Climate Model, version 3 (Japan Meterological Agency (JMA))
NorESM1-M	Norwegian Earth System Model, Part 1 (Norwegian Climate Centre)
PDF	Probability density function
ppm	Parts per million
ppt	Precipitation
RCP	Representative concentration pathway
SOI	Southern Oscillation Index
SON	September, October, November
SRES	Special report on emissions scenarios
SST	Sea-surface temperature
tmax	Maximum Temperature
tmin	Minimum Temperature
UCT	University of Cape Town
UKMO-HadCM3	United Kingdom Met Office, Hadley Centre Coupled Model, version 3
WMA	Water Management Area

ACKNOWLEDGEMENTS

The first phase of the Long Term Adaptation Scenario Flagship Research Programme (LTAS) involved numerous people and organisations, and was characterised by a spirit of collaboration and cooperation across organisational and disciplinary boundaries. The Department of Environmental Affairs (DEA) and the South African National Biodiversity Institute (SANBI) would like to thank the Deutsche Gesellschaft für Internationale Zusammenarbeit (GIZ) for technical and financial assistance, under the supervision of Dr Michaela Braun and Mr Zane Abdul, who also served on the Project Management Team.

DEA and SANBI would specifically like to thank the groups, organisations and individuals who participated and provided technical expertise and key inputs to the *Climate trends and scenarios* technical report, Dr Francois Engelbrecht (Council for Scientific and Industrial Research [CSIR]), Prof. Bruce Hewitson and Mr Chris Jack (Climate SysteMs Analysis Group [CSAG]), Dr Mark Tadross (UNDP), Professor Mark New (African Climate and Development Initiative) and Dr Adam Schlosser and Dr Kenneth Strzepek (Massachusetts Institute of Technology [MIT]), LTAS Technical Working Group members, and members of the Climate and Impacts task teams.

DEA and SANBI would also like to acknowledge other members of the Project Management Team who contributed their time and energy to the development of this technical report, namely Mr Shonisani Munzhedzi[i] and Mr Vhalinavho Khavhagali who provided key guidance on behalf of the DEA, Prof. Guy Midgley (SANBI), Ms Sarshen Scorgie and Ms Petra de Abreu (Conservation South Africa) who were key editors of the technical report. Ms Gigi Laidler served as the SANBI project administrator with assistance from Ms Faslona Martin, Mr Nkoniseni Ramavhona who served as DEA project administrator and Ms Gwendolin Aschmann from GIZ who provided additional project management support. Ms Jaqui Stephenson (Environmental Resources Management) and Mr Dick Cloete (Media Directions) provided preliminary and final editing of phase 1 products respectively, and Studio 112 conducted the layout.

i Mr Shonisani Munzhedzi, Department of Environmental Affairs, Climate Change Branch, Chief Directorate Adaptation • Tel: +27 (0) 12 395 1730 • Cell: +27 (0) 76 400 0637 • email: SMunzhedzi@environment

THE LTAS PHASE 1

The Long-Term Adaptation Scenarios (LTAS) Flagship Research Programme (2012–2014) is a multi-sectoral research programme, mandated by the South African National Climate Change Response White Paper (NCCRP, para 8.8). The LTAS aims to develop national and sub-national adaptation scenarios for South Africa under plausible future climate conditions and development pathways. During its first Phase (completed in June 2013), fundamental climate modelling and related sector-based impacts and adaptation scoping were conducted and synthesised. This included an analysis of climate change trends and projections for South Africa that was compared with model projections for the same time period, and the development of a consensus view of scenarios for three time periods (short-, medium- and long-term). Scoping of impacts, adaptation options and future research needs, identified in the White Paper and guided by stakeholder engagement, was conducted for primary sectors namely water, agriculture and forestry, human health, marine fisheries, and biodiversity. This modelling and scoping will provide a basis for cross-sectoral and economic assessment work needed to develop plausible adaptation scenarios during Phase 2 (scheduled for completion in April 2014).

Six individual technical reports have been developed to summarise the findings from phase 1, including one technical report on **climate trends and scenarios for South Africa** and five summarising the climate change implications for primary sectors, water, agriculture and forestry, human health, marine fisheries, and biodiversity. A description of the key messages emerging from the LTAS Phase 1 has been developed into a summary for policy-makers; as well as into seven factsheets comprising the LTAS *Climate and Impacts Factsheet Series*.

REPORT OVERVIEW

This technical report presents the LTAS Phase 1 findings on climate trends and scenarios for South Africa. It represents the most significant step forward in consolidating locally relevant data available for South African climate change modelling since the original South African Country Studies carried out during the 1990s. This includes presenting future climate trends for South Africa over the short-, medium and long-term simulated by three distinct methods (including statistical and dynamical downscaling), and driven by different emissions scenarios generally representing an unmitigated and a mitigated future energy pathway. The report also summarises observed climatological trends for South Africa from 1960 to 2010 and compares them to trends produced by modelling approaches used to project future trends in climate.

Climate trends and projections are presented in the form of maps and statistics, and then summarised for the short-, medium-, and long -term future (~2025, ~2050, ~2090) both at national scale, and at a locally relevant scale, in relation to six hydrological zones of South Africa (see Figure 1). This approach was followed on the well-supported basis that a majority of climate change impacts across South African economic and other sectors will be mediated through primary impacts on the water sector. The six hydrological zones were developed as part of the National Water Adaptation Strategy process, reflecting boundaries defined by water management areas (WMAs) in South Africa, grouped according to their climate and hydrological characteristics. These include:

- **Zone 1:** the Limpopo, Olifants and Inkomati WMAs in the northern interior (Limpopo/Olifants/Inkomati);
- **Zone 2**: the Pongola-Umzimkulu WMA in KwaZulu-Natal in the east (Pongola-Umzimkulu);
- **Zone 3:** the Vaal WMA in the central interior (Vaal);
- **Zone 4:** the Orange WMA in the north west (Orange);
- **Zone 5:** the Mzimvubu-Tsitsikamma WMA in the south east (Mzimvubu-Tsitsikamma);
- **Zone 6:** Breede-Gouritz and Berg Olifants WMAs in the south west (Breede-Gouritz/Berg).

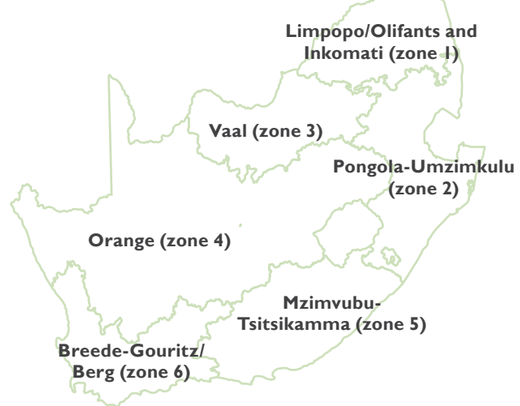

Figure 1. Six hydrological zones have been developed as part of the National Water Adaptation Strategy process, reflecting boundaries defined by water management areas (WMAs) in South Africa and grouped according to their climatic and hydrological characteristics. These zones can be appropriately modelled and analysed for direct impacts on the water sector, and related indirect effects on other sectors.

Based on the consolidated climate data and spatial projections, as well as the wide range of other relevant climate information presented, a set of climate scenarios for South Africa and the southern African region is provided. Four fundamental climate scenarios are presented for South Africa nationally, and further elaborated on sub-national level for the six hydrological zones (Figure 1) up to 2050 and beyond. Specifically, the four fundamental scenarios are: warmer/wetter, warmer/drier, hotter/wetter, and hotter/drier at national scale, with different degrees of change and likelihood that capture the impacts of global mitigation and the passing of time. Climate scenarios developed during LTAS Phase 1 presented in this report reflect as full a range of plausible climate risks and opportunities as possible, given the current state of knowledge. The development of scenarios makes for better communication of climate risks and opportunities outside of purely technical impacts and adaptation applications, and allows for qualitative assessments of risks and opportunities in addition to the technical and quantitative assessments.

A brief description of each chapter of the technical report is provided below.

Chapter 1 (Introduction) describes the progression of work on climate change scenarios for South Africa including a description of the progress in modelling approaches and scenarios for South Africa with reference to the 1990s South African Country Studies Programme, South Africa's Initial National Communication (2003), the Fourth Assessment Report of the Intergovernmental Panel on Climate Change (IPCC) (AR4, 2007), South Africa's Second National Communication (2011), the Fifth Assessment Report of the IPCC (AR5, 2013/2014) and the LTAS Phase 1 climate modelling work and fundamental climate scenarios.

Chapter 2 (South Africa's observed climatology) summarises observed climatological trends for South Africa from 1960 to 2010 including providing a narrative overview of the results of previous trends assessments (section 2.1.1); and describing types of climate variability at intraseasonal and interannual timescales (2.1.2). This chapter also presents the methodology and results of the LTAS trend analysis of past climate for 1960–2012 (2.1.3 and 2.1.4) and compares this to past trend analyses.

Chapter 3 (Comparison of model and observed trends for South Africa) compares observed climatological trends for South Africa from 1960 to 2010 described in Chapter 2 to modelled trends for the same period produced by modelling approaches used to project future trends in climate. An assessment of the strengths and weaknesses of modelled projections is presented i.e. how well climate models have simulated observed trends.

Chapters 4 and 5 (Statistical and dynamically downscaled climate projections for South Africa, respectively) present downscaled South African climate projections (temperature and rainfall) for the time-period 2015 to 2035 (centred on ~2025) and into the future (centred on ~2050 and ~2090) conducted by national and international institutions using statistical and dynamical/mechanistic downscaling methodology based on outputs from AR4 (A2 and B1 emissions scenarios – see 4.1, 4.2 and 5.2) and AR5 (RCP 8.5 and 4.5 Wm^{-2} pathways, see 4.3, 4.4, 5.2 and 5.3); and representing an unmitigated (unconstrained, A2 and RCP8.5) and mitigated (constrained, B1 and RCP4.5) future energy pathway. These results provide the basis for the key messages presented in Chapters 6 and 7.

Chapter 6 (Key messages at national and sub-national scales) summarises key messages at national and sub-national scale for South Africa's six hydrological zones from the detailed statistical and dynamical downscaling presented in Chapters 4 and 5, and further analyses of this at sub-regional scale. The projected envelope of changes in temperature and rainfall as a function of time is presented for each of the hydrological zones. The interpretation of the regional messages presented is complemented through figures which show the ensemble of simulated annual anomalies in temperature and rainfall, for the period 1961–2100, relative to the 1971–2005 baseline period.

Chapter 7 (Massachusetts Institute of Technology (MIT) pattern-scaling projections and comparison to the high-resolution regional downscalings) provides the results of a comparison of South African climate model projections with projections from a statistical downscaling approach developed at MIT, which involves thousands of model realisations of temperature and rainfall obtained through a pattern-scaling technique applied to coupled general circulation model (CGCM) data with a global climate model. Probability density functions (PDFs) are presented for each of the hydrological zones, separately for the projected temperature and rainfall anomalies.

Chapter 8 (Climate scenarios) presents four fundamental climate scenarios at national scale further elaborated with rainfall projections at sub-national level e.g. for South Africa's six hydrological zones based on climate projections, regional analyses and other relevant climate information presented in Chapters 1–7.

Chapter 9 (Conclusion) concludes the report highlighting the need to explore the cross-sectoral socio-implications of South Africa's future climate scenarios on water and food security to develop appropriate adaptation scenarios to inform national and sub-regional response strategies.

EXECUTIVE SUMMARY

The LTAS Phase 1 climate trends and scenarios work developed a consensus view of the range of plausible climate scenarios for three time-periods for South Africa at national and sub-national scales under a range of global emissions scenarios. The time-periods considered were 2015 to 2035 (centred on ~2025, so-called short-term) in addition to the previously followed approach of exploring climate change over several decades into the future (centred on ~2050 (medium-term) and ~2090 (long-term)).

These scenarios were developed through local and international climate modelling expertise using both statistical and dynamical downscaling methodologies based on outputs from IPCC AR4 (A2 and B1 emissions scenarios) and IPCC AR5 (RCP 8.5 and 4.5 Wm^{-2} pathways). These represent an unmitigated future energy pathway (unconstrained, A2 and RCP8.5) and mitigated future energy pathway (constrained, B1 and RCP4.5, or emissions scenarios equivalent to CO_2e levels stabilising between 450 and 500ppm).

The LTAS also revisited observed climate trends (1960–2012) and current climatology for South Africa and compared these with projected trends by using a subset of the models. This is an initial effort to identify potential strengths and weaknesses in modelling approaches employed so far to provide a qualitative basis for assessing the credibility of future projections, and to guide efforts to address potential shortcomings.

Climatic trends and projections are summarised nationally, and for six hydrological regions of South Africa (Figure 1) due to the acknowledged importance of the water sector as the basis for understanding cross-sectoral impacts of climate change.

Observed climate trends for South Africa (1960–2010)

Over the last five decades the following climate trends have been observed in South Africa.

- Mean annual **temperatures** have increased by at least 1.5 times the observed global average of 0.65°C reported by IPCC AR4 for the past five decades.
- Maximum and minimum temperatures show significant increases annually, and in almost all seasons. A notable exception is the central interior (zone 3, Vaal), where minimum temperatures have been increasing less strongly, and some decreases have been observed.
- High temperature extremes have increased significantly in frequency, and low temperatures have decreased significantly in frequency annually and in most seasons across the country, but particularly in the western and northern interior of the country.
- The rate of temperature change has fluctuated, with the highest rates of increase from the middle 1970s to the early 1980s, and again in the late 1990s to middle 2000s.
- **Rainfall** has shown high interannual variability, with smoothed rainfall showing an amplitude of about 300 mm, about the same as the national average.
- Rainfall trends are similar in all the hydrological zones, with rainfall being above average in the 1970s, the late 1980s, and mid to late 1990s, and below average in the 1960s and in the early 2000s, reverting to mean towards 2010.
- Annual rainfall trends overall are weak and non-significant, but there is a tendency towards a significant decrease in the number of rain days in almost all hydrological zones.
- This implies a tendency towards an increase in the intensity of rainfall events and increased dry spell duration.
- There has also been a marginal reduction in rainfall for the autumn months in almost all hydrological zones.

Strengths and weaknesses of model simulations of the recent historical climate (1960–2010)

Based on comparisons of observed and modelled trends for 1960–2010, some key climatic processes relevant for South Africa appear not to be adequately represented by the GCMs or the downscaling methods currently in use. Key findings in this regard are that:

- Observed temperature trends are more closely matched by modelled simulations than are rainfall trends, a tendency noted in the IPCC fifth Assessment Report.
- Observed temperature trends since 2000 have not increased as steeply as projected by model simulations.
- Observed temperature trends in the central interior (zone 3, Vaal) are flat, but modelled trends are significantly positive, matching all the other zones.
- The observed reductions in autumn rainfall are not reproduced by the models, and the models tend to show opposite trends.

Projected rainfall and temperature changes for South Africa

Climate scenarios were summarised from the results of applying three different climate modelling techniques to derive a range of future climate scenarios under two main emissions scenarios representing relatively constrained and unconstrained global emissions.

Overall, there is far less uncertainty in temperature than rainfall projections. All modelling approaches project warming trends until the end of this century, but most approaches project the possibility of both drying and wetting trends in almost all parts of South Africa. Nonetheless, effective global mitigation action is projected generally to reduce strongly the risk of extreme warming trends, and to reduce the likelihood of extreme wetting and drying outcomes by at least mid-century.

Climate change projections for South Africa up to 2050 and beyond under high emission scenarios include:

- Very significant warming, as high as 5–8°C, over the South African interior by the end of this century. Warming would be somewhat reduced over coastal zones.
- A general pattern of a risk of drier conditions to the west and south of the country and a risk of wetter conditions over the east of the country
- Many of the projected changes are within the range of historical natural variability, and uncertainty in the projections is high.

An effective global emissions reduction pathway would largely eliminate the risk of extreme rainfall changes, both increases and decreases, by mid-century. High resolution regional modelling suggests even larger benefits of effective global mitigation by the end of this century, when regional warming of 5–8°C could be more than halved to 2.5–3°C.

Projected climate futures for South Africa (2015–2035, 2040–2060 and 2070–2090)

South Africa's climate future up to 2050 and beyond can be described using four fundamental climate scenarios at national scale, with different degrees of change and likelihood that capture the impacts of global mitigation and the passing of time.

1. **warmer (<3°C above 1961–2000) and wetter** with greater frequency of extreme rainfall events.
2. **warmer (<3°C above 1961–2000) and drier**, with an increase in the frequency of drought events and somewhat greater frequency of extreme rainfall events.
3. **hotter (>3°C above 1961–2000) and wetter** with substantially greater frequency of extreme rainfall events.
4. **hotter (>3°C above 1961–2000) and drier**, with a substantial increase in the frequency of drought events and greater frequency of extreme rainfall events.

The effect of strong international mitigation responses would be to reduce the likelihood of scenarios 3 and 4, and increase the likelihood of scenarios 1 and 2 during the course of this century. In both wetter and drier futures a higher frequency of flooding and drought extremes could be expected, with the range of extremes exacerbated significantly under unconstrained emissions scenarios. These scenarios can be further elaborated in terms of rainfall projections at sub-national level e.g. for South Africa's six hydrological zones (see Table A).

Summary and linkages

Global climate model ensembles summarised for South Africa suggest a significant benefit from effective mitigation responses (e.g. global CO_2e stabilisation at between 450 and 500 ppm) relative to unconstrained emission pathways by as early as mid-century. Even under strong international mitigation responses, significant socio-economic implications would be expected for vulnerable groups and communities in South Africa under both wetter and drier climate futures. These implications would largely be felt through impacts on water resources, such as changes in water resource availability and a higher frequency of natural disasters (flooding and drought), with cross-sectoral effects on human settlements, disaster risk management and food security.

Table A. Rainfall projections for each of South Africa's six hydrological zones

Scenario	Limpopo/ Olifants/ Inkomati	Pongola-Umzimkulu	Vaal	Orange	Mzimvubu-Tsitsikamma	Breede-Gouritz/ Berg
1: warmer/ wetter	↑ spring and summer	↑ spring	↑ spring and summer	↑ in all seasons	↑ in all seasons	↓ autumn, ↑ winter and spring
2: warmer/drier	↓ summer, spring and autumn	↓ spring and strongly ↓ summer and autumn	↓ summer and spring and strongly ↓ autumn	↓ summer, autumn and spring	↓ in all seasons, strongly ↓ summer and autumn	↓ in all seasons, strongly ↓ in the west
3: hotter/wetter	Strongly ↑ spring and summer	Strongly ↑ spring	↑ spring and summer	↑ in all seasons	Strongly ↑ in all seasons	↓ autumn, ↑ winter and spring
4: hotter/ drier	Strongly ↓ summer, spring and autumn	↓ spring and strongly ↓ summer and autumn	↓ summer and spring and strongly ↓ autumn	↓ summer, autumn and spring	↓ all seasons, strongly ↓ in summer and autumn	↓ all seasons, strongly ↓ in the west

1. INTRODUCTION

The projection of climate change scenarios over South Africa began earnestly during the 1990s, based on extensive work over the previous decades that quantified the climatology of South Africa (Tyson et al., 1975), and that explored the role of oceanic and atmospheric drivers of regional and local climate (Reason et al., 2004), and particularly the pattern of decadal and multi-decadal climate variability such as that resulting from the El Nino Southern Oscillation (ENSO) and other characteristic features of the Southern Hemisphere climate (Reason and Rouault, 2002).

In the course of the South African Country Studies Programme during the 1990s, and in preparation for South Africa's Initial National Communication, a series of climate projections was developed. These were of two kinds, namely a simple spatial interpolation of global climate models, and a statistically downscaled set of projections. The overall view from these approaches was that South Africa faced a considerably drier and warmer future overall by mid-century, with some indication of an increased risk of intense rainfall events. Modelling approaches developed extensively after this initial effort, including far better representation of oceanic influences on global and regional climates and, as a consequence, a more moderate view of future climate change resulted during the development of climate scenarios for the Fourth Assessment Report (AR4) of the Intergovernmental Panel on Climate Change (IPCC).

It became clear that there was far more uncertainty relating to rainfall projections in the summer rainfall regions of South Africa, while the winter rainfall region continued to show a high likelihood of drying projections by mid to end century. Statistical downscaling of these results showed a far higher likelihood of increased rainfall over the summer rainfall eastern regions of South Africa (e.g. Hewitson and Crane, 2006), though the impacts of rising temperature would lead in many (but not all) regions to a net drop in water availability. These better supported projections were summarised in the work that informed South Africa's Second National Communication, and have gone on to inform some national sectoral strategy development, most notably in the water sector.

Computationally more expensive dynamic downscalings over southern Africa have been obtained subsequently using regional climate models to downscale the output of AR4 global climate models to high resolution (Tadross et al., 2005; Engelbrecht et al., 2009, 2011; Engelbrecht et al., 2012; Malherbe et al., 2013). These projections provided insight into potential changes in atmospheric circulation over southern Africa under climate change. Plausible scenarios are the southern displacement of frontal systems in winter, leading to reduced rainfall over the south-western Cape (e.g. Christensen et al., 2007; Engelbrecht et al., 2009) and the more frequent occurrence of mid-level anti-cyclones between spring and autumn, resulting in the southern African region becoming generally drier (e.g. Engelbrecht et al., 2009; Malherbe et al., 2013).

With the development of the IPCC Fifth Assessment Report (AR5), a new set of emissions scenarios and global climate scenarios has been developed by the international community. This provided the LTAS process with the opportunity to engage local and international climate modellers with further updated scenarios. Through the course of a series of Technical Working Group meetings and expert task team workshops, it was decided to develop a set of scenarios based as far as possible on updated emission scenarios representing high and mitigated pathways, namely the RCP 8.5 and 4.5 Wm^{-2} pathways. These are roughly comparable to the IPCC AR4 A2 and B1 emissions scenarios, which have been extensively used in South Africa, thus providing a link between scenario, impacts and adaptation work done previously. In addition to the previously followed approach of exploring impacts over several decades into the future (i.e. 2050 and 2090), the LTAS has also undertaken to explore short term scenarios, for the time-period 2015 to 2035 (centred on ~2025), and to explore recent climate trends and revisit a current climatology for South Africa.

2. SOUTH AFRICAN OBSERVED CLIMATOLOGY

The Hadley Centre Climate Research Unit (CRU) TS2.0 monthly 50km resolution observed dataset (Hulme et al. 1999) has been used to produce the following figures illustrating South African historical climate statistics, and to develop a current climatology. The updated CRU dataset extends from 1901 to 2006 and uses all available station observations through the period to interpolate rainfall and temperatures onto a 50km grid globally.

It is important to note the limitations of station interpolation both through time and spatially. As the number of available observing stations fluctuates through the dataset time period this data is not suitable for robust trend analysis. Additionally, due to the lack of station observations in many areas, particularly mountainous and remote terrain, the interpolated values do not capture the complexity of temperature and rainfall in such areas. However, this dataset is well suited as a general representation of pattern and variability and has been used extensively for climate variability related studies globally.

The following figures are intended to illustrate both the mean climate conditions across South Africa during the four major seasons of (December–February: DJF), (March–May: MAM), (June–August: JJA), and (September–November: SON), and the statistical range of variability across the same seasons. The range of variability is represented as maps of the statistical 10th and 90th percentiles for each grid point for the season in question through the full time period. The 10th and 90th percentile are good representatives of the range of variability while excluding the very extreme years in the record.

In the figures provided (Figure 2, Figure 3, and Figure 4), the columns represent the four seasons (left to right: DJF, MAM, JJA, SON), while the rows represent the 90th percentile, the mean, and the 10th percentile statistics (top to bottom: 90th percentile, mean, 10th percentile).

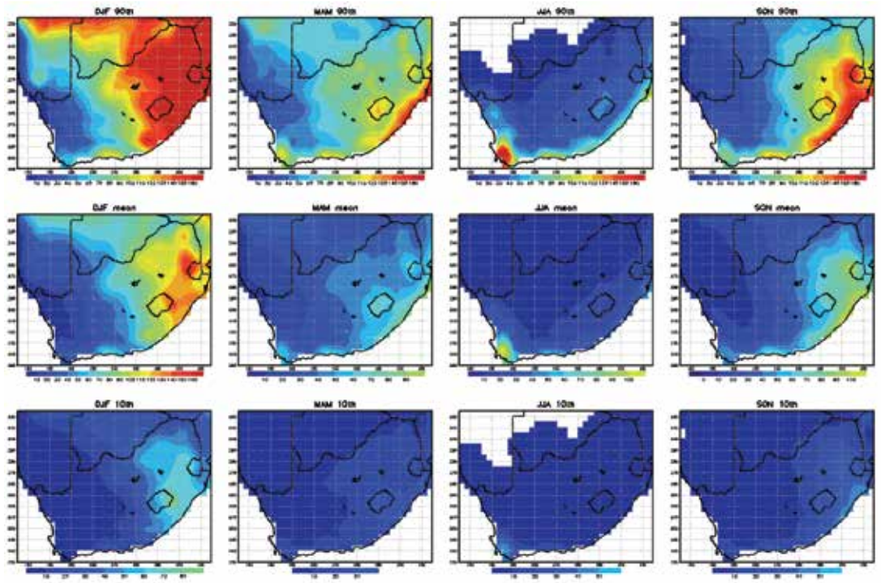

Figure 2. CRU Observed Monthly Total Rainfall for DJF, MAM, JJA, and SON. Top row: 90th percentile, middle row: mean, bottom row: 10th percentile.

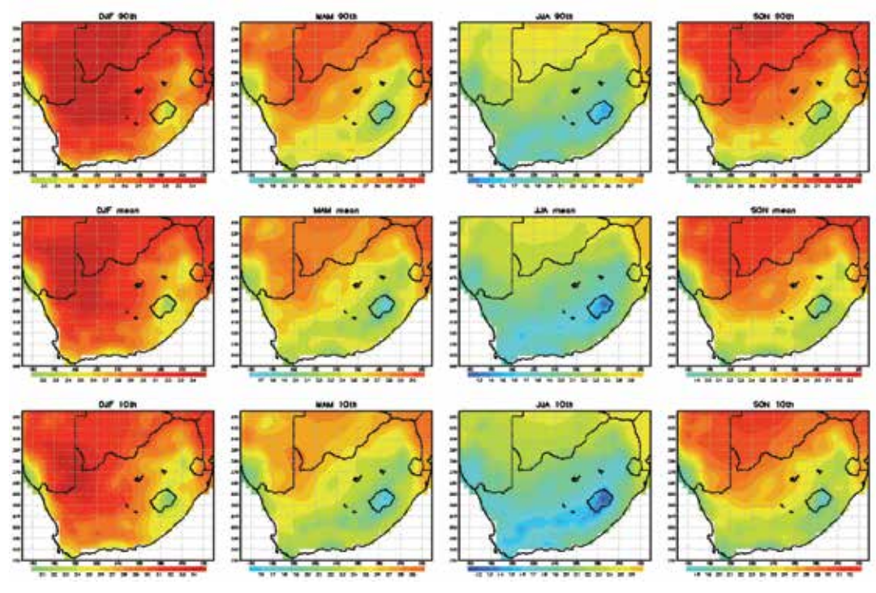

Figure 3. CRU Observed Monthly mean maximum temperatures for DJF, MAM, JJA, and SON. Top row: 90th percentile, middle row: mean, bottom row: 10th percentile.

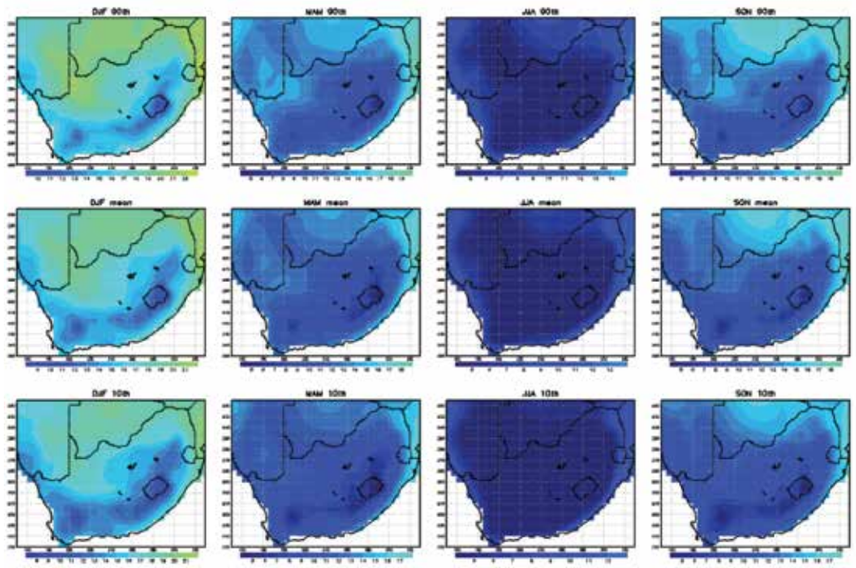

Figure 4. CRU Observed Monthly mean minimum temperatures for DJF, MAM, JJA, and SON. Top row: 90th percentile, middle row: mean, bottom row: 10th percentile

2.1 Historical trends in South Africa's climate

This section presents an analysis of climatic trends in rainfall and temperature for South Africa. First, a review of relevant published literature is presented in order to put the current results in the context of previous trend analyses. This is followed by a brief summary of the various timescales of natural climate variability and linkages between SA's climate and global climate modes (sometimes termed "tele-connections"). A description of the data and methods used in the current analyses is then presented, after which the key results are summarised.

2.1.1 Review of previous trend analyses for South Africa

The greatest restriction to the study of historical climate is the availability of long-term meteorological station observations that have sufficient coverage to give an adequate representation of the variations of a region's climate in both space and time. South Africa has a relatively good network of rainfall and temperature recording stations compared to the rest of Africa and much of the Southern Hemisphere (Hughes and Balling, 1995; Easterling et al., 2000; New et al. 2006). This makes it possible to investigate trends and variability over multiple decades. A number of recent studies, both global in scope and more regionally focused, have given insight into how the rainfall and temperature characteristics of SA have varied over the last century.

Because South Africa's mean annual precipitation (MAP) is highly variable from year to year (Tyson, 1986; Mason and Jury, 1997), few spatially coherent or statistically significant trends in this have been observed (New et al., 2006; Nel, 2009; Kruger, 2006). However, of more relevance than MAP are the characteristics of how rainfall is distributed throughout the year. These include the timing of the onset and end of the rainy season, the typical duration of wet and dry periods and the occurrence of extreme heavy rainfall events. A review by Easterling et al. (2000) indicates a tendency for increased extreme precipitation in the south-western and eastern parts of South Africa during most of the 20th century. This is supported by Groisman et al. (2005), who show a significant increase in the annual frequency of very heavy rainfall events over eastern SA from 1906–1997. Furthermore, Mason et al. (1999) demonstrate increases in the intensity of high rainfall events in the 1961–1990 period relative to 1931–1960 over much of SA. Kruger (2006) shows increases in extreme rainfall indices over the southern Free State and parts of the Eastern Cape from 1910–2004. New et al. (2006) also show some evidence for increased rainfall extremes over parts of SA for the 1961–2000 period. Nel (2009) demonstrated a shift in seasonality for stations in the Kwazulu-Natal (KZN) Drakensberg for 1955–2000. In that study, MAP showed no significant trend, but an increase in summer rainfall was accompanied by decreased autumn and winter rainfall resulting in a shorter wet season and a more pronounced seasonal cycle. This is consistent with results from Thomas et al. (2007) for north-west KZN, where an increase in early-season rainfall has been observed along with a decrease in late-season rainfall between 1950 and 2000. Seasonal shifts were also observed by Thomas et al. (2007) in Limpopo for the same period, where there has been a tendency for a later seasonal rainfall onset accompanied by increased dry spells and fewer rain days. Increased dry spell duration is also evident for much of the Free State and Eastern Cape, and decreases in wet spell duration have been observed for parts of the Eastern Cape and the north-eastern parts of SA during 1910–2004 (Kruger, 2006).

Long-term trends in temperature-related indices are generally clearer than trends in rainfall indices. As global mean temperature has been observed to increase over the last century, largely attributable to the warming effects of anthropogenic greenhouse gas emissions (IPCC, 2007), so different regions have experienced changes of varying magnitude. In SA between 1950 and 1993, Easterling et al. (1997) found an increase in annual mean maximum temperature (tmax) and widespread increases – although also some decreases – in annual mean minimum temperature (tmin). Despite a global tendency for a reduction in the diurnal temperature range (dtr, the difference between daily tmax and tmin) the results of Easterling et al. (1997) show much of SA has experienced an increase in dtr. In contrast, however, Hulme et al. (2001) show decreased dtr over SA during the 1950s and 1960s. They also show very strong warming in the central interior of southern Africa and cooling over the coastal regions of SA for the 1901–1995 period. Kruger and Shongwe (2004) examined the period 1960–2003 and found that, with a few exceptions, stations in SA have reported increases in annual mean temperatures, with the strongest warming having occurred in the interior of the country and during the autumn months. The stations showed mixed results with respect to dtr, with no clear regional pattern of change.

New et al. (2006) identified varied results for changes in dtr over a similar time period, but they do show a tendency for the cold extremes of tmin to change more strongly than the cold extremes of tmax. They also reveal a general increase in hot extremes over SA. The most recent published work on South African temperature trends was done by Kruger and Sekele (2013) for the period 1962–2009. They focused on extreme temperature indices for 28 SA stations and found significant changes in the exceedences of the extreme percentile values for tmin and tmax at many of the stations. More specifically, increases in daily measurements in excess of the 90th percentile of tmax and tmin have occurred along with decreases in exceedences of the 10th percentile of tmin and tmax. This is indicative of an overall increased frequency of hot extremes and decreased frequency of cold extremes, with the strongest changes tending to occur in the western and northern interior of the country. There is also a general tendency for stronger increases in the tmax indices than for those related to tmin.

Although some general tendencies are apparent for trends in both rainfall and temperature indices, there is some disagreement between studies. This can largely be attributed to two factors, namely the time period over which the data were analysed and the locations of the stations from which data were obtained. Large, naturally-occurring variations in climate at yearly and decadal timescales can greatly affect the calculation of trends, so it is important to consider the length of record when evaluating any trend analysis. Regional inferences based on individual stations are reliant on how representative a station or group of stations is of that area and should also be treated with caution. Some of the studies also rely on gridded products where station records have been interpolated in space onto a continuous surface. Such products should closely match the raw station data in places where the observational record is good, but in data-sparse regions this information is less reliable, especially where strong environmental gradients exist. Details of the methods used to calculate trends also differ between studies, but these should rarely result in substantially different results.

2.1.2 *Timescales of climate variability and teleconnections*

The climate exhibits numerous modes of variability in global and hemispheric circulation patterns at intraseasonal (of the order of 1 or 2 months) and interannual (year-to-year) timescales (see Figure 5). The El Niño-Southern Oscillation (ENSO) is recognised as the leading mode of interannual variability in the tropics and is driven by variations in sea-surface temperatures (SSTs) in the equatorial Pacific Ocean. Links between ENSO and southern Africa's rainfall have been established such that warm ENSO events (El Niño) are commonly associated with below-average summer rainfall over much of SA and cold events (La Niña) are typified by above-average rainfall in this region. It has been shown that severe summer drought in SA tends to occur under El Niño conditions (Lindesay et al., 1988; Reason et al., 2000), a relationship which seems to have strengthened since the 1970s (Richard et al., 2000, 2001). Furthermore, seasonal prediction of summer rainfall in SA shows more skill during strong ENSO phases (Landman and Beraki, 2012). However, the relationship between ENSO and SA rainfall is far more complex than a simple linear association and many factors influence the region's climate. For example, the frequency of synoptic-scale patterns of convection over SA are modulated by ENSO events, but different synoptic regimes under the same ENSO phase can result in substantially different rainfall responses (Fauchereau et al., 2008). Complexities are also introduced through the influence of other climatic modes, and interactions between these modes.

The second prominent interannual mode relevant for southern Africa is a dipole pattern in SST anomalies between the south-western and south-eastern Indian Ocean. A positive phase of this Indian Ocean Dipole (IOD), characterised by anomalously warm SSTs in the western part of the basin, has been linked to increased summer rainfall over parts of southern Africa (Behera and Yamagata, 2001; Reason, 2001; Hansingo and Reason, 2008). Increased SSTs in the south-west Indian Ocean have also been associated with an enhancement of the El Niño effect over SA (Richard et al., 2000). At an intraseasonal timescale, the Madden-Julian Oscillation (MJO) has a noticeable impact on SA convection and rainfall (Pohl et al., 2007). The MJO is an eastward propagation of large-scale convective clusters in the tropics with a period of 30–60 days. It has been shown that convection over SA tends to be more strongly affected by the MJO during warm phases of ENSO and warm tropical Indian Ocean temperatures, such that intraseasonal variability is higher

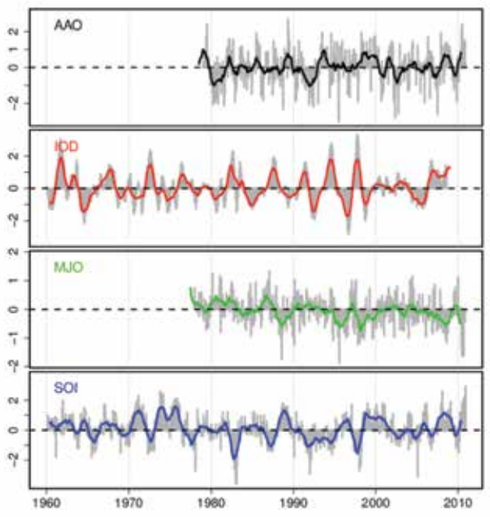

Figure 5. Time series of indices representing four major climate oscillations: Antarctic Oscillation Index (AAO), Indian Ocean Dipole Mode Index (IOD), Madden-Julian Oscillation Index for 20 °E (MJO) and Southern Oscillation Index (SOI). The SOI is a representation of the El Nino-Southern Oscillation. Grey bars show monthly values for each index and the solid curves are a 12-month running mean. Data are provided by the KNMI Climate Explorer (http://climexp.knmi.nl/).

and convection is less active during El Niño events (Pohl et al., 2007). A further low-frequency mode that is present in the mid-latitudes is the Antarctic Oscillation (AAO), which is defined by pressure anomalies between Antarctica and the Southern Hemisphere mid-latitudes. There is some indication of a link between a positive phase of the AAO and enhanced rainfall over central SA, which tends to be stronger during La Niña years (Pohl et al., 2010). It has also been shown for the winter rainfall region of the south-western Cape that particularly wet winters are associated with a negative phase of the AAO and vice versa (Reason and Rouault, 2005).

Beyond the interannual timescale are decadal-scale variations in climate which provide a slowly evolving background around which higher-frequency modes oscillate. For example, an approximately 18 year cycle in southern African rainfall has been identified in instrumental and proxy records extending back as far as 600 years (Tyson et al., 2002). It is not clear what causes this oscillation, but an "ENSO-like" multi-decadal pattern of variation has been identified at multiple periodicities (Reason and Rouault, 2002). It is possible that interaction between phases of the multi-decadal and interannual variations act to enhance or mitigate regional responses (Kruger, 1999; Reason and Rouault, 2002). In the context of the trend analysis presented in this study, it is very important to consider the possible influences of low-frequency variations, especially in rainfall, on the calculation of long-term trends.

2.1.3 *Methodology and data for LTAS observed trends analysis (1960–2010)*

Station observations were obtained through the Climate Information Portal (CIP) hosted by the University of Cape Town's Climate System Analysis Group (http://cip.csag.uct.ac.za). The data originates from two main sources, namely the Computing Centre for Water Resources and the South African Weather Service and has been collated and quality controlled prior to being uploaded to CIP. Stations were selected based on the coverage of monthly data for the period 1960–2010 such that any stations with 20% or more missing values were excluded from the analysis. This constraint resulted in 73, 30 and 27 stations being available for the variables related to rainfall precipitation (ppt), tmax and tmin, respectively. Figure 7 and Figure 8 show the locations of all stations and the completeness of their records. In addition to the three basic variables (ppt, tmax and tmin), a number of climate indices were computed which are summarised in Table 1.

Table 1. Descriptions of rainfall and temperature indices.
* Where seasonal means of these indices are calculated, the percentile value is derived from daily data coinciding with that season only.

Index	*Description*	*Units*
ppt	Total rainfall	mm
rain days	Number of days with ppt above 0.2 mm	days
ppt 90th	Number of days with ppt above 90th percentile of 1960–2010 daily ppt*	days
tmax	Mean of daily maximum temperature	°C
tmin	Mean of daily minimum temperature	°C
hot days	Number of days with tmax above 25°C	days
cold days	Number of days with tmax below 10°C	days
warm nights	Number of days with tmin above 20°C	days
dtr	Difference between tmax and tmin	°C
tmax 90th	Number of days with tmax above 90th percentile of 1960–2010 daily tmax*	days
tmax 10th	Number of days with tmax below 10th percentile of 1960–2010 daily tmax*	days
tmin 90th	Number of days with tmin above 90th percentile of 1960–2010 daily tmin*	days
tmin 10th	Number of days with tmin below 10th percentile of 1960–2010 daily tmin*	days

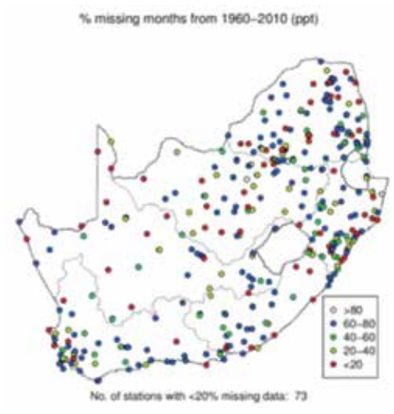

Figure 6. Station coverage for precipitation. Grey lines represent boundaries of the 6 hydrological zones presented in Figure 1.

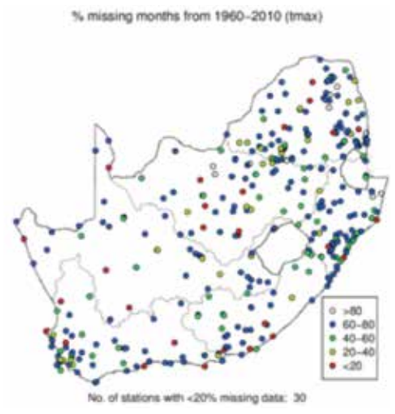

Figure 7. Station coverage for maximum temperature. Grey lines represent boundaries of the 6 hydrological zones presented in Figure 1.

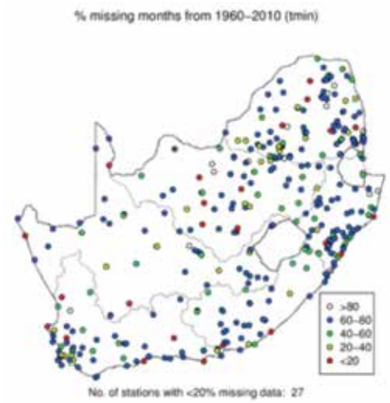

Figure 8. Station coverage for minimum temperature. Grey lines represent boundaries of the 6 hydrological zones presented in Figure 1.

Trends in the indices for the 1960–2010 period were evaluated using a number of approaches. Firstly, the non-parametric Mann-Kendall trend test was applied. This method has the advantages of making no assumptions about the distribution of the underlying data and being relatively insensitive to outliers. The method computes a correlation coefficient called tau, which has a value between -1 and 1 and denotes the relative strength of the trend in a time series. The probability of this trend occurring by chance is also estimated. For statistical significance, we use a 95% level of significance, such that if the probability estimate is less than 0.05, the trend is deemed to be significant. Since the tau statistic does not provide an estimate of the absolute magnitude of the trend, we also calculate the slope of the trend using Sen's slope estimator, which is the median of the slopes calculated between all pairs of data points in the series. Like the Mann-Kendall test, this method is also statistically robust and insensitive to outliers in the data. Lastly, for comparison, we calculate the linear least squares regression line and its associated probability.

The above trend estimates were calculated for seasonal and annual means for all indices. The results are presented as follows. Firstly, annual and seasonal maps of the Mann-Kendall tau for each station and each variable are shown. These depict the relative strength of trends over the historical period at each station and give an indication of any coherent spatial patterns of change. Secondly, annual and seasonal time series plots have been generated for the six water management zones identified in Figure 1. To calculate these regional time series, an anomaly time series is computed for each station falling within the region by subtracting the 1960–2010 station mean from each value in the series. The resulting series are then summed and divided by the number of stations in that region, after which trend statistics are calculated for the regional mean series. A smoothed curve has been added to the figures using a Loess filter with a bandwidth of 0.25. The resulting figures give an indication of the direction and magnitude of long-term trends as well as an illustration of interannual and interdecadal variability in the time series. Two important points should be noted here. Firstly, although the definition of the zones has value in a hydro-climatic context, they do not necessarily coincide with homogenous climates and climatic trends. Opposing trends at stations within the same zone will hence weaken any regional signal. Secondly, the stations falling within a particular zone may not necessarily be a good representation of spatial heterogeneity within that zone. This is particularly true for indices related to rainfall and in zones where station coverage is sparse. Nevertheless, some useful information can be extracted from these regionally-averaged indices.

2.1.4 Results: observed trends for 1960-2010

The results for a selection of the indices described in Table 1 (namely ppt, rain days, ppt 90th, tmax, tmin, dtr, tmax 90th and tmin 10th) are presented in Figures 9 to 32.

The main messages emerging from the analysis are summarised below for each of the 6 hydrological zones.

2.1.4.1 Zone 1 (Limpopo and parts of northern Mpumalanga)

- There is a mixed signal for spatial patterns of rainfall indices in most seasons, but a tendency for reductions in ppt at most stations in MAM (autumn) and fewer rain days in DJF (summer) and MAM. Some stations show reduction in DJF rain days, but increases in ppt 90th, which suggests a possible increase in rainfall intensity at these locations.
- Regional means show large interannual and decadal-scale variability in rainfall indices, but significant reductions in rain days in DJF and MAM.
- All but one station show significant increase in tmax, with the strongest warming signal occurring in SON (spring). Tmin, however, experienced strongest warming in DJF and JJA (winter). Spatial patterns for dtr are mixed and no region-wide trends are evident.
- Extremely hot days (tmax 90th) have increased significantly at all except one station in JJA and SON, but trends in the other months are weak. Extremely cold nights (tmin 10th) show general reductions in all seasons, but not all are significant.

2.1.4.2 Zone 2 (majority of KZN and part of southern Mpumalanga)

- There is large temporal variability and no regional mean trends in rainfall indices, but stations suggest a spatially-coherent reduction in MAM ppt, ppt 90th and rain days.
- A weak, but spatially coherent pattern of increased ppt and ppt 90th in SON and DJF has occurred along with significant increases in rain days in the southern Drakensberg area, which also extends into Zone 5.
- Only three temperature stations are available in this zone. One shows significantly increased annual mean tmax, all three show significant annual mean increases in tmin. All three show increased tmax 90th and decreased tmin 10th for all seasons, but not all are significant.

2.1.4.3 Zone 3 (northern and central interior)

- Opposing signals are shown at individual stations and as a result no clear region-wide trends are evident.
- There have been significant reductions in ppt and rain days at some stations in the east in DJF and MAM and some indication of increases in rainfall indices in the west throughout the wet season from spring to autumn.
- The strongest increases in tmax and tmax 90th are seen in JJA, but significant decreases are shown in tmin, particularly in JJA. This has the effect of significantly increasing the dtr. An increased frequency of extremely cold nights (tmin 10th) is also shown. The reason for the reduction in tmin and tmin 10th has not been rigorously explored in this study, but it is likely to be related to a reduction in nocturnal cloud cover.

2.1.4.4 Zone 4 (Northern Cape, southern Free State and inland parts of Eastern Cape)

- Station coverage is sparse and this region spans a large climatic gradient, so regional means should be interpreted with caution.
- There have been no significant trends in ppt and only one station has experienced a significant decline in ppt 90th in MAM.
- Some significant increases in rain days are apparent in the western part of the region.
- Temperature stations (four for tmax and three for tmin) are limited to the western part of the region and these show strong increases in tmax for all seasons. A large part of this warming can be attributed to persistently above-average temperatures in the last 10 years of the record.
- Tmax 90th has increased significantly at three of the four stations, but the single coastal station has experienced a decline in tmax 90th.
- Increases in tmin are generally weaker than those seen in tmax, resulting in generally increased dtr.

2.1.4.5 Zone 5 (majority of the Eastern Cape and southern part of KZN)

- There are few significant changes in ppt and ppt 90th, but there are some significant increases in rain days across the region (southern Drakensberg and southern coastal areas) in all seasons. A single station on the northern coast, however, shows a significant reduction in rain days.
- Temperature stations are confined to the southern part of the region, where tmax and tmin have increased in all seasons, but with a weaker signal in DJF and SON, respectively.

2.1.4.6 Zone 6 (Western Cape and parts of Northern and Eastern Cape)

- Trends in rainfall variables are generally not significant and show little consistency across the region. Rain days show a fairly consistent decreasing signal along the southern coastal regions, although the stations near the west coast show a tendency for increased rain days.
- Tmax and tmin have increased significantly at most stations in all seasons, accompanied by increases in tmax 90th and decreases in tmin 10th.

2.1.4.7 Patterns overall

Smoothed rainfall variability has an amplitude of about 300 mm, which is about the same as the national average (Figure 17 and Figure 18). Rainfall was above average in the 1970s, the late 1980s, and mid to late 1990s, and below average in the 1960s and in the early 2000s, reverting to average towards 2010. There is a tendency towards an increase in rainfall extreme events, but especially in spring and summer, with a reduction in extremes in autumn (Figure 11). Rainfall trends overall are weak and non-significant, but there is a tendency towards a significant decrease in the number of rain days (Figure 19 and Figure 20). This would support the observed tendency towards an increase in extreme rainfall events.

Maximum and minimum temperatures all show significant increases (Figure 12 and Figure 13) with few exceptions, notably for minimum temperature in the central interior or zone 3 (Vaal). Likewise, high temperature extremes have increased significantly in frequency, and low temperature extremes have decreased significantly in frequency (Figures 15 and 16). Temperature trends show fluctuations in rate, but show their highest rates of increase from the middle 1970s to the early 1980s, and again in the late 1990s to middle 2000s.

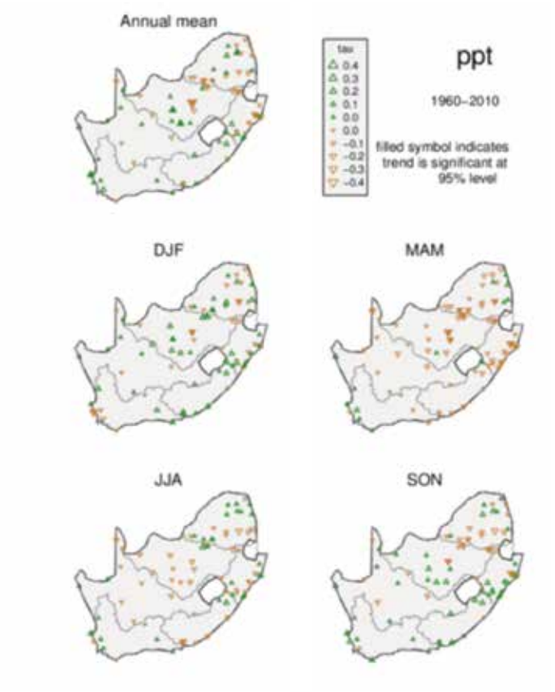

Figure 9. Trends in annual and seasonal mean rainfall for each station according to the Mann-Kendall test. The value of tau represents the direction and relative strength of the trend. Shaded symbols denote trends that are significant at the 95% level. Seasons are summer (DJF), autumn (MAM), winter (JJA) and spring (SON). Grey lines represent boundaries of the 6 hydrological zones presented in Figure 1.

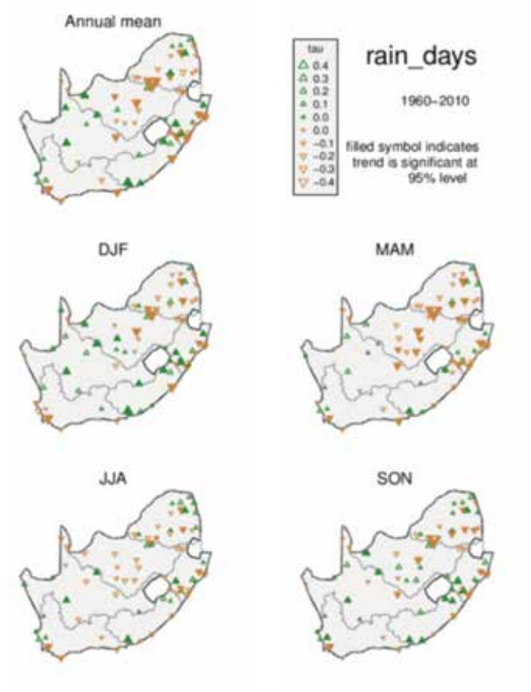

Figure 10. Trends in annual and seasonal number of rain days for each station according to the Mann-Kendall test. The value of tau represents the direction and relative strength of the trend. Shaded symbols denote trends that are significant at the 95% level. Seasons are summer (DJF), autumn (MAM), winter (JJA) and spring (SON). Grey lines represent boundaries of the 6 hydrological zones presented in Figure 1.

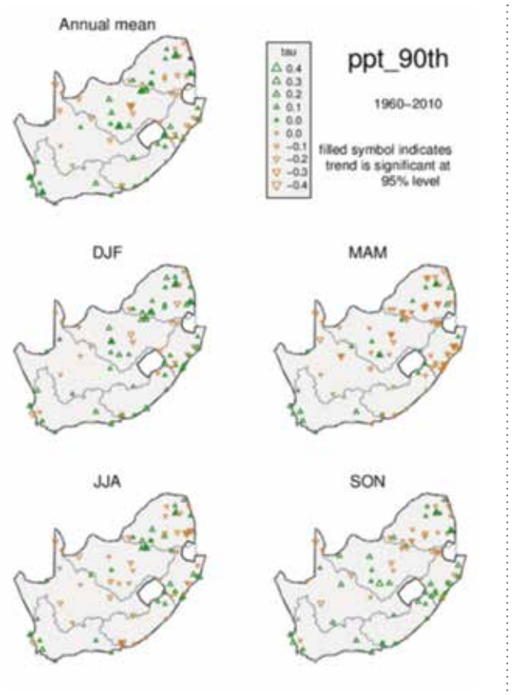

Figure 11. Trends in annual and seasonal number of days above the 90th percentile rainfall for each station according to the Mann-Kendall test. The value of tau represents the direction and relative strength of the trend. Shaded symbols denote trends that are significant at the 95% level. Seasons are summer (DJF), autumn (MAM), winter (JJA) and spring (SON). Grey lines represent boundaries of the 6 hydrological zones presented in Figure 1.

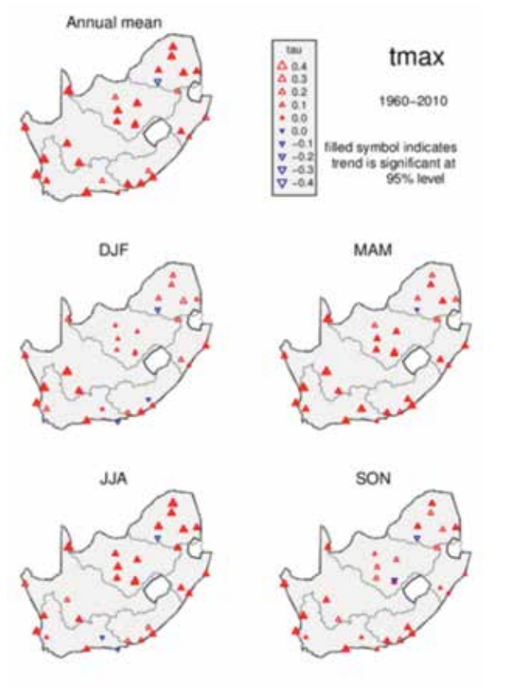

Figure 12. Trends in annual and seasonal maximum temperature for each station according to the Mann-Kendall test. The value of tau represents the direction and relative strength of the trend. Shaded symbols denote trends that are significant at the 95% level. Seasons are summer (DJF), autumn (MAM), winter (JJA) and spring (SON). Grey lines represent boundaries of the 6 hydrological zones presented in Figure 1.

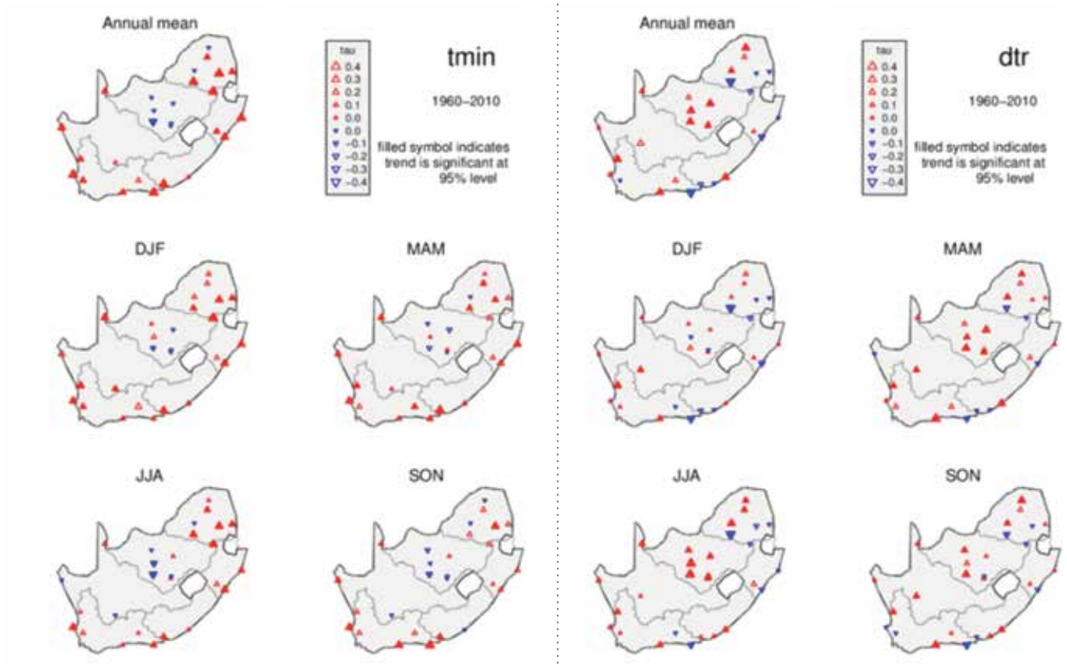

Figure 13. Trends in annual and seasonal minimum temperature for each station according to the Mann-Kendall test. The value of tau represents the direction and relative strength of the trend. Shaded symbols denote trends that are significant at the 95% level. Seasons are summer (DJF), autumn (MAM), winter (JJA) and spring (SON). Grey lines represent boundaries of the 6 hydrological zones presented in Figure 1.

Figure 14. Trends in annual and seasonal daily temperature range for each station according to the Mann-Kendall test. The value of tau represents the direction and relative strength of the trend. Shaded symbols denote trends that are significant at the 95% level. Seasons are summer (DJF), autumn (MAM), winter (JJA) and spring (SON). Grey lines represent boundaries of the 6 hydrological zones presented in Figure 1.

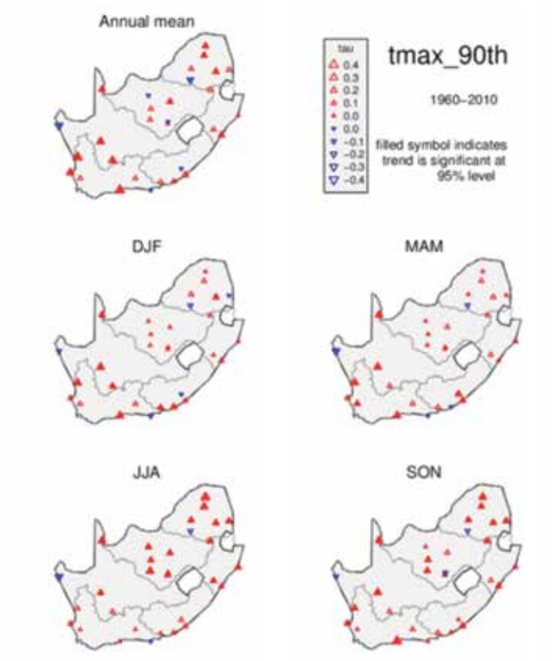

Figure 15. Trends in annual and seasonal number of days above the 90th percentile maximum temperature for each station according to the Mann-Kendall test. The value of tau represents the direction and relative strength of the trend. Shaded symbols denote trends that are significant at the 95% level. Seasons are summer (DJF), autumn (MAM), winter (JJA) and spring (SON). Grey lines represent boundaries of the 6 hydrological zones presented in Figure 1.

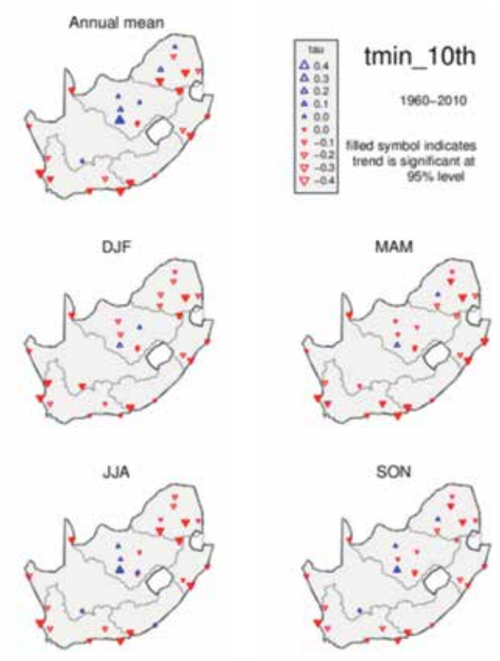

Figure 16. Trends in annual and seasonal number of days below the 10th percentile minimum temperature for each station according to the Mann-Kendall test. The value of tau represents the direction and relative strength of the trend. Shaded symbols denote trends that are significant at the 95% level. Seasons are summer (DJF), autumn (MAM), winter (JJA) and spring (SON). Grey lines represent boundaries of the 6 hydrological zones presented in Figure 1.

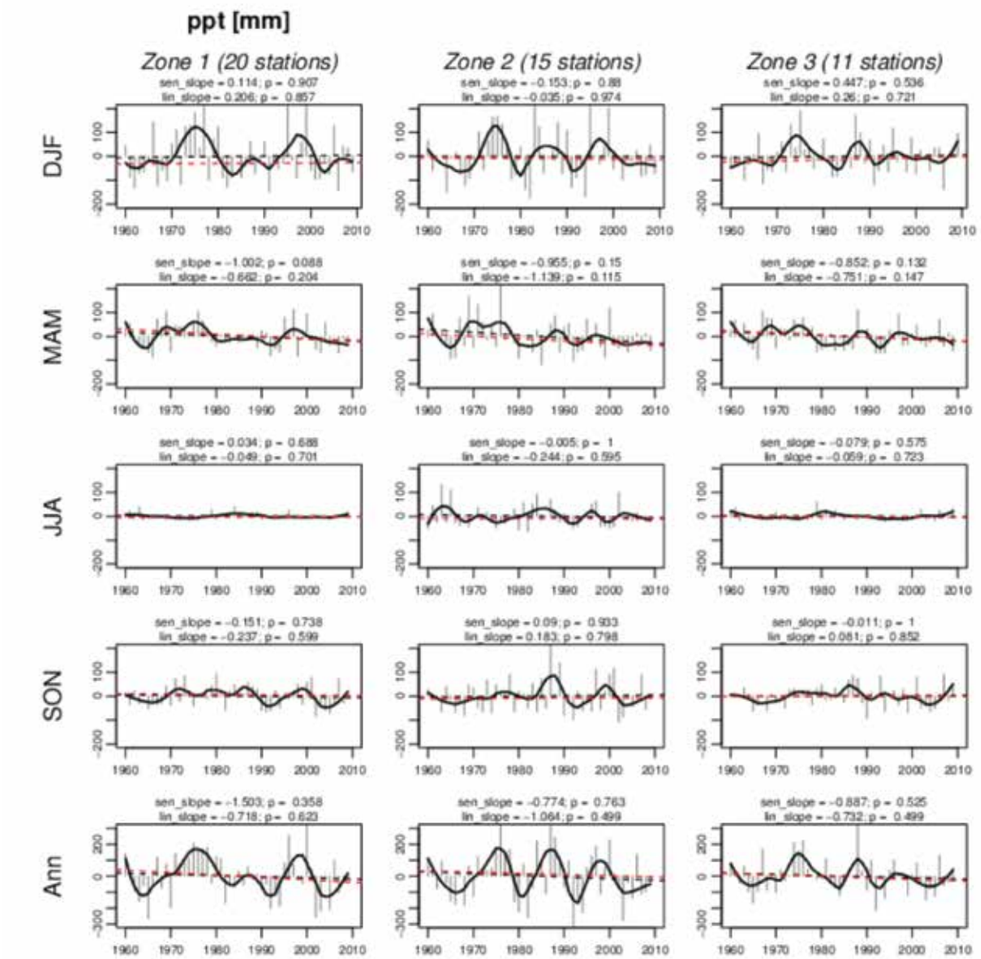

Figure 17. Regional mean time series and trends in total rainfall for stations in zones 1–3 for summer (DJF), autumn (MAM), winter (JJA), spring (SON) and annual (Ann) means. Grey bars represent departures from the 1960–2010 mean for each year. Black curves are a Loess smoothing of the yearly data with a bandwidth of 0.25. Trend lines are shown for the linear least squares fit (black) and Sen's slope estimate (red). Solid trend lines indicate the trend is significant at the 95% level and dashed lines are not significant at this level.

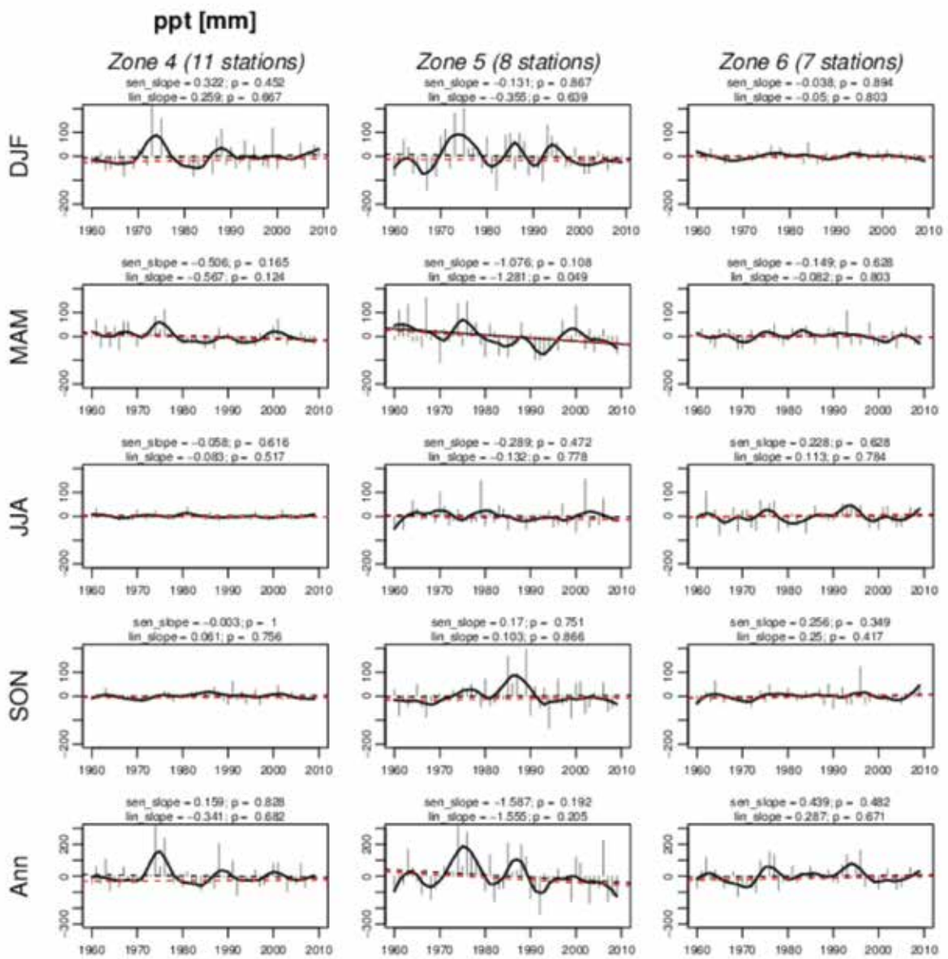

Figure 18. Regional mean time series and trends in total rainfall for stations in zones 4–6 for summer (DJF), autumn (MAM), winter (JJA), spring (SON) and annual (Ann) means. Grey bars represent departures from the 1960–2010 mean for each year. Black curves are a Loess smoothing of the yearly data with a bandwidth of 0.25. Trend lines are shown for the linear least squares fit (black) and Sen's slope estimate (red). Solid trend lines indicate the trend is significant at the 95% level and dashed lines are not significant at this level.

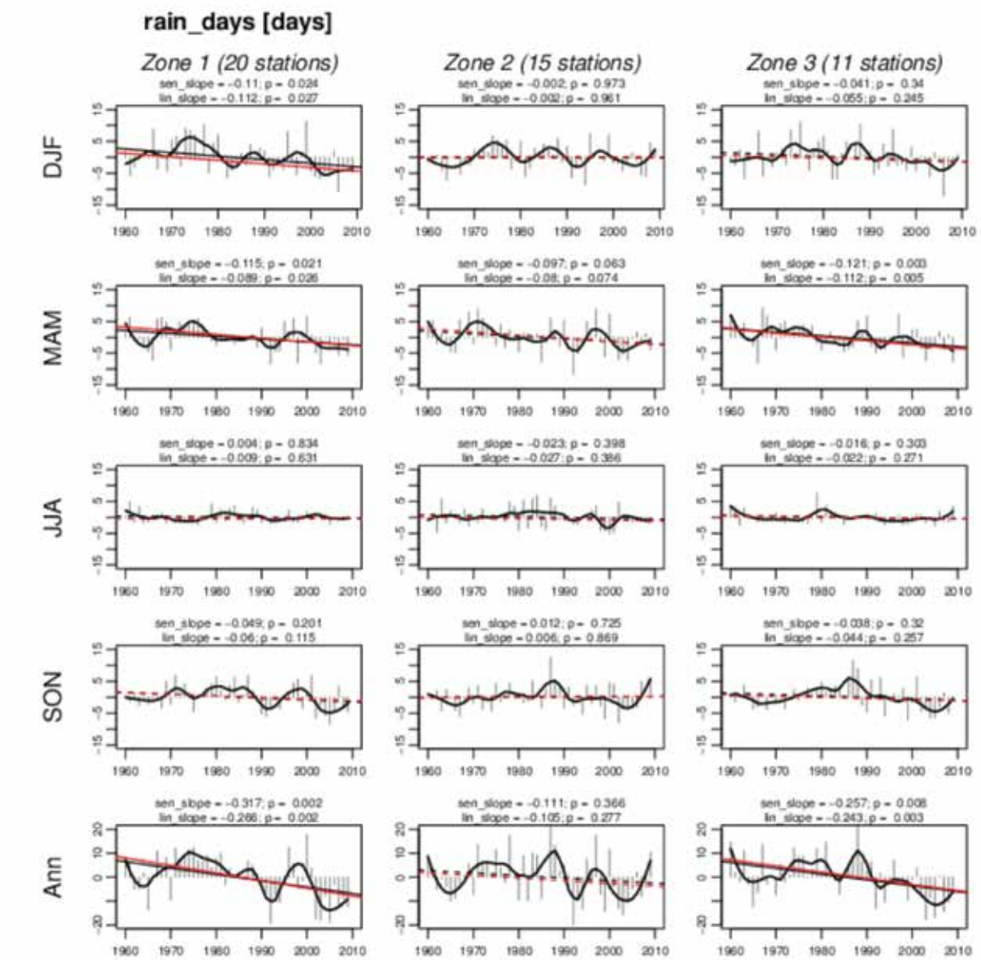

Figure 19. Regional mean time series and trends in number of rain days for stations in zones 1–3 for summer (DJF), autumn (MAM), winter (JJA), spring (SON) and annual (Ann) means. Grey bars represent departures from the 1960–2010 mean for each year. Black curves are a Loess smoothing of the yearly data with a bandwidth of 0.25. Trend lines are shown for the linear least squares fit (black) and Sen's slope estimate (red). Solid trend lines indicate the trend is significant at the 95% level and dashed lines are not significant at this level.

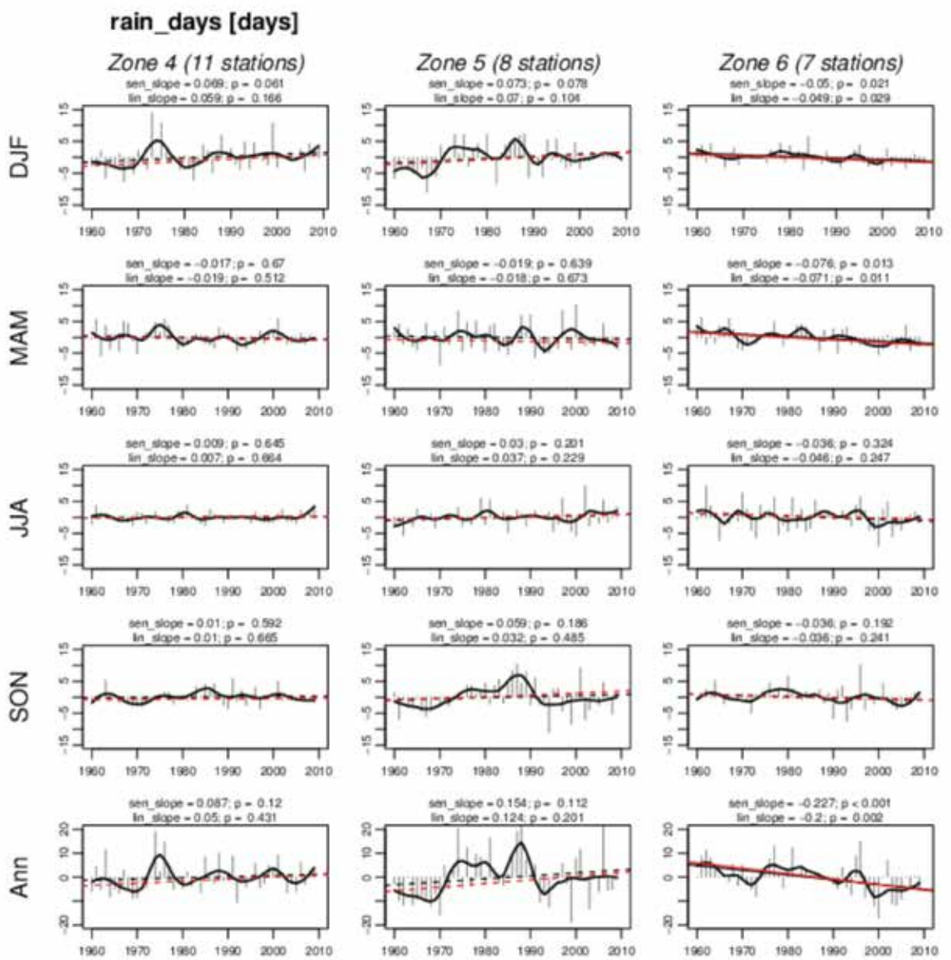

Figure 20. Regional mean time series and trends in number of rain days for stations in zones 4–6 for summer (DJF), autumn (MAM), winter (JJA), spring (SON) and annual (Ann) means. Grey bars represent departures from the 1960–2010 mean for each year. Black curves are a Loess smoothing of the yearly data with a bandwidth of 0.25. Trend lines are shown for the linear least squares fit (black) and Sen's slope estimate (red). Solid trend lines indicate the trend is significant at the 95% level and dashed lines are not significant at this level.

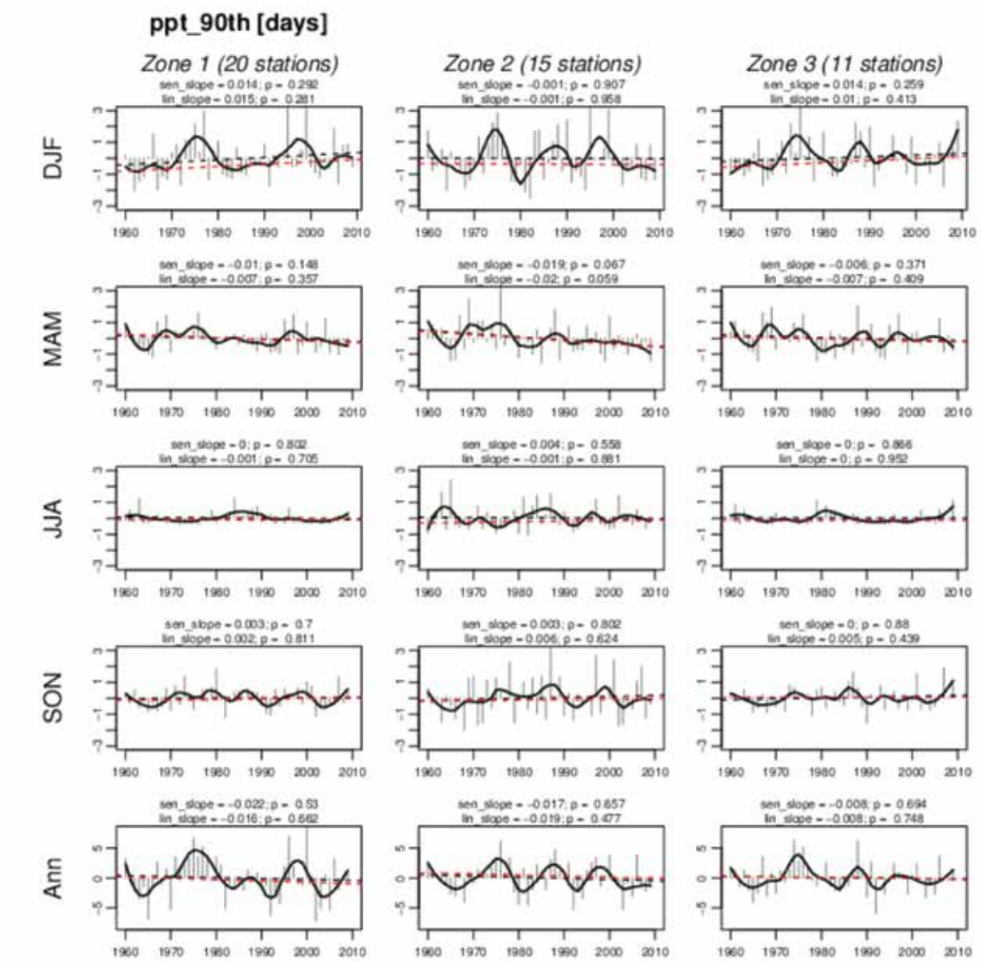

Figure 21. Regional mean time series and trends in number of 90th percentile rainfall days for stations in zones 1–3 for summer (DJF), autumn (MAM), winter (JJA), spring (SON) and annual (Ann) means. Grey bars represent departures from the 1960–2010 mean for each year. Black curves are a Loess smoothing of the yearly data with a bandwidth of 0.25. Trend lines are shown for the linear least squares fit (black) and Sen's slope estimate (red). Solid trend lines indicate the trend is significant at the 95% level and dashed lines are not significant at this level.

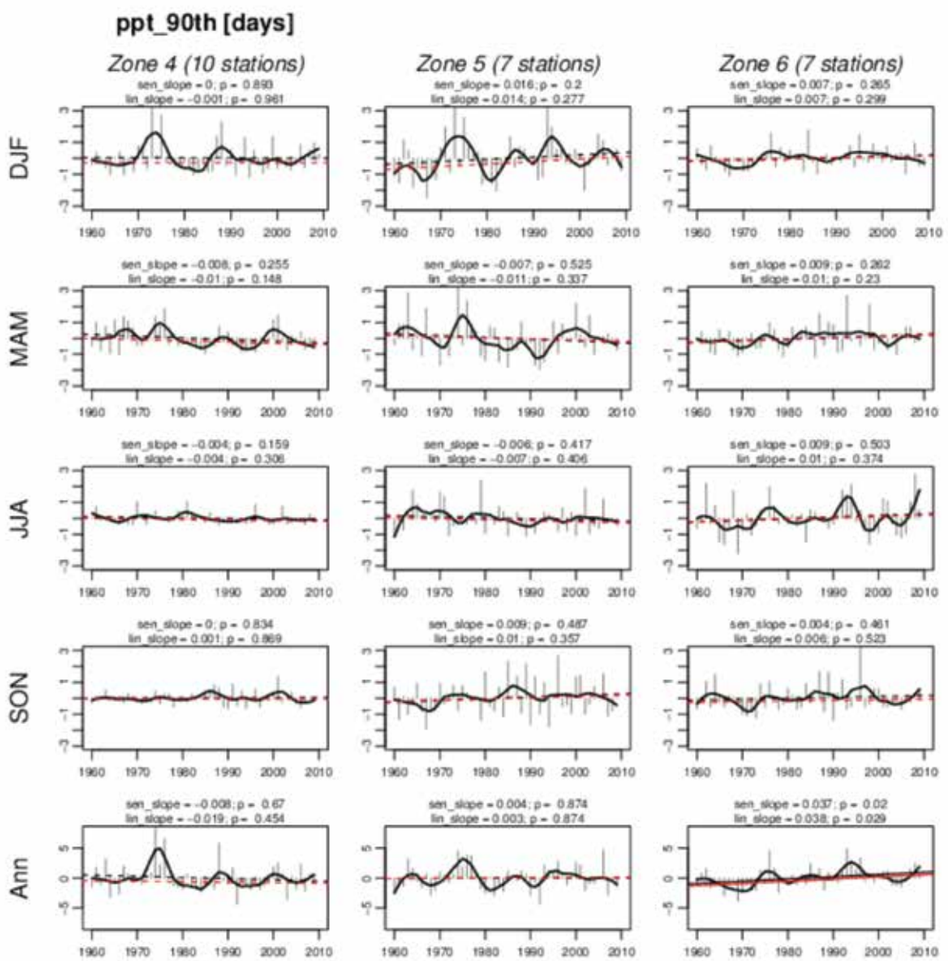

Figure 22. Regional mean time series and trends in number of 90th percentile rainfall days for stations in zones 4–6 for summer (DJF), autumn (MAM), winter (JJA), spring (SON) and annual (Ann) means. Grey bars represent departures from the 1960–2010 mean for each year. Black curves are a Loess smoothing of the yearly data with a bandwidth of 0.25. Trend lines are shown for the linear least squares fit (black) and Sen's slope estimate (red). Solid trend lines indicate the trend is significant at the 95% level and dashed lines are not significant at this level.

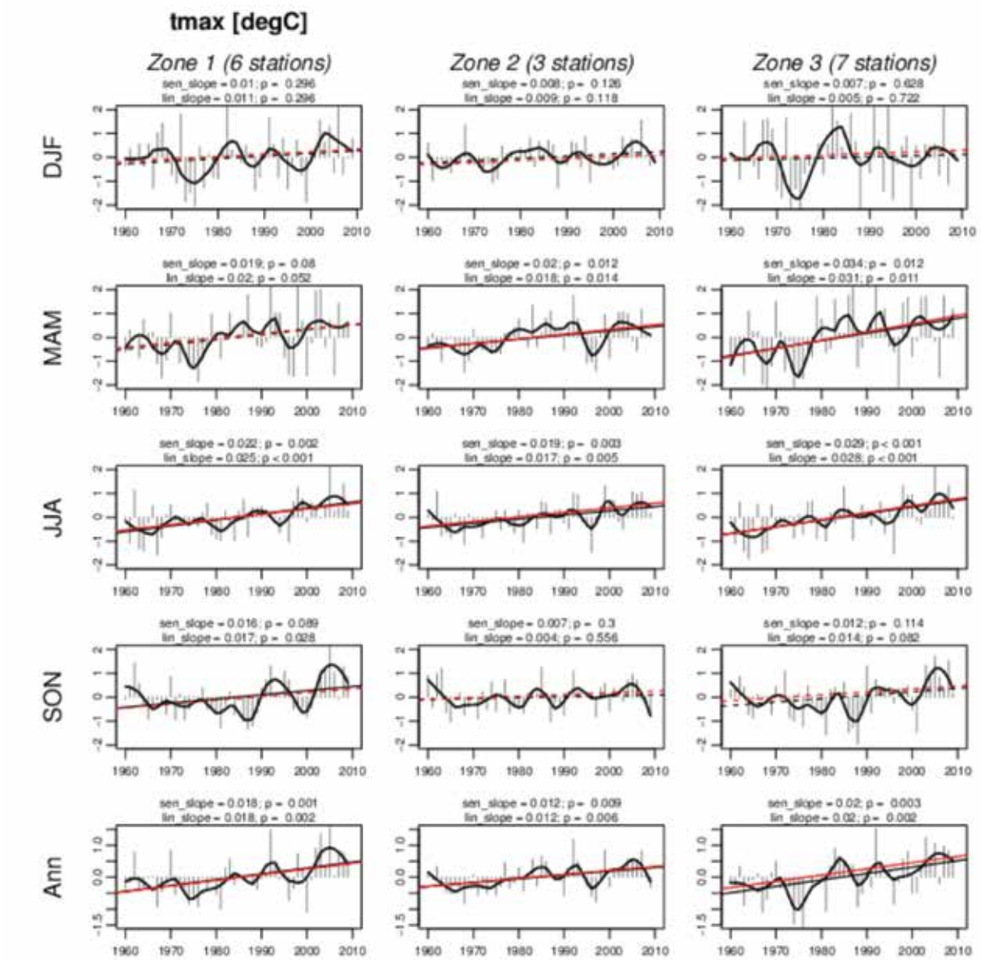

Figure 23. Regional mean time series and trends in maximum temperature for stations in zones 1–3 for summer (DJF), autumn (MAM), winter (JJA), spring (SON) and annual (Ann) means. Grey bars represent departures from the 1960–2010 mean for each year. Black curves are a Loess smoothing of the yearly data with a bandwidth of 0.25. Trend lines are shown for the linear least squares fit (black) and Sen's slope estimate (red). Solid trend lines indicate the trend is significant at the 95% level and dashed lines are not significant at this level.

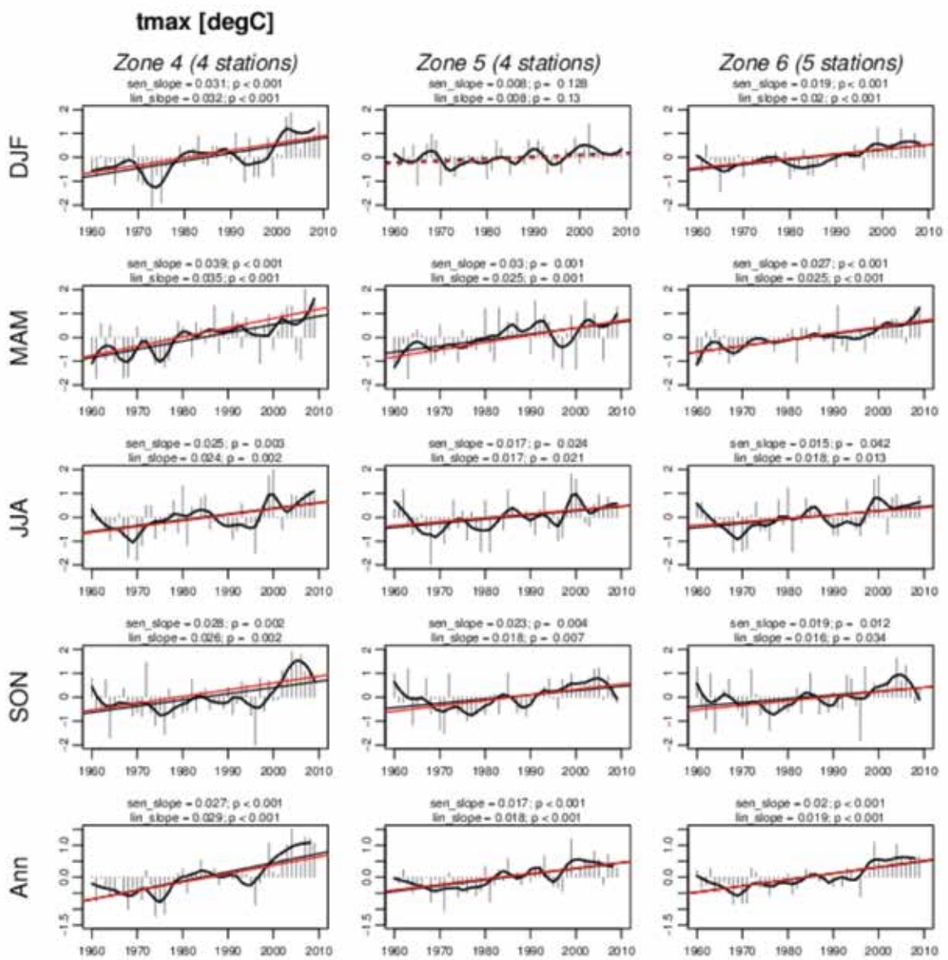

Figure 24. Regional mean time series and trends in maximum temperature for stations in zones 4–6 for summer (DJF), autumn (MAM), winter (JJA), spring (SON) and annual (Ann) means. Grey bars represent departures from the 1960–2010 mean for each year. Black curves are a Loess smoothing of the yearly data with a bandwidth of 0.25. Trend lines are shown for the linear least squares fit (black) and Sen's slope estimate (red). Solid trend lines indicate the trend is significant at the 95% level and dashed lines are not significant at this level.

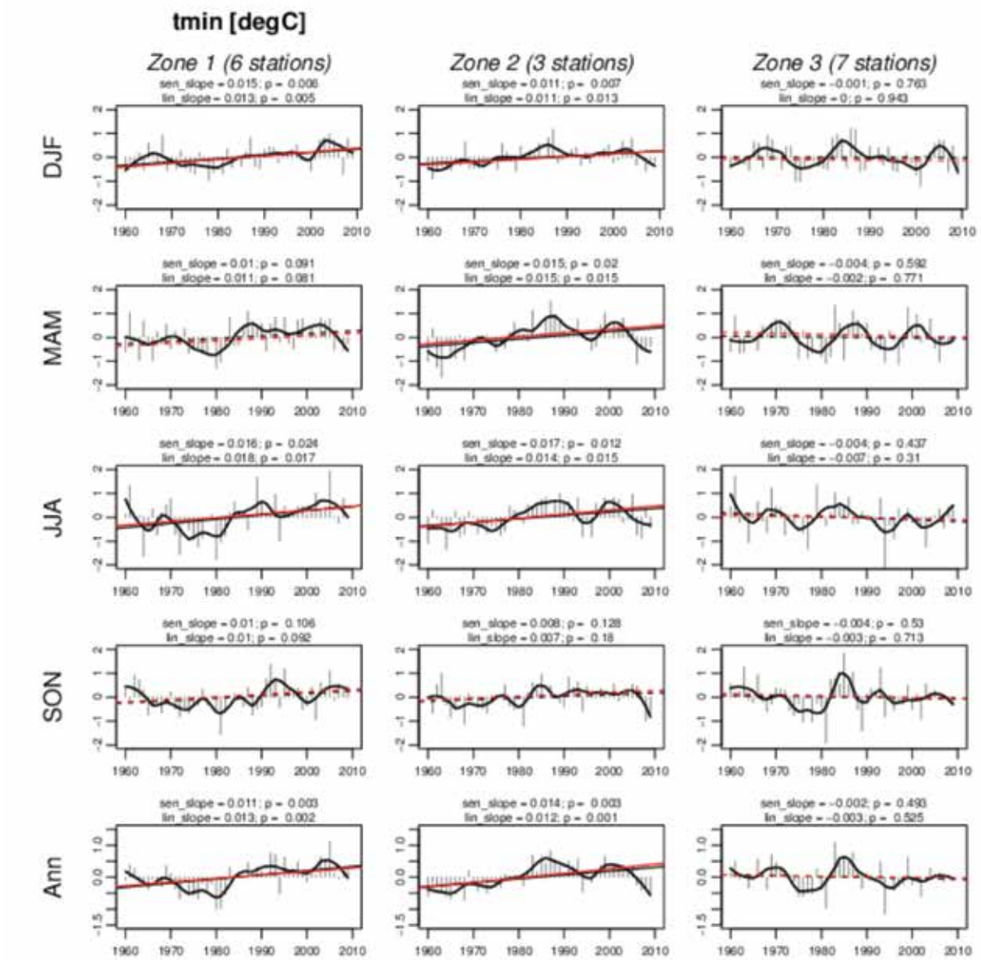

Figure 25. Regional mean time series and trends in minimum temperature for stations in zones 1–3 for summer (DJF), autumn (MAM), winter (JJA), spring (SON) and annual (Ann) means. Grey bars represent departures from the 1960–2010 mean for each year. Black curves are a Loess smoothing of the yearly data with a bandwidth of 0.25. Trend lines are shown for the linear least squares fit (black) and Sen's slope estimate (red). Solid trend lines indicate the trend is significant at the 95% level and dashed lines are not significant at this level.

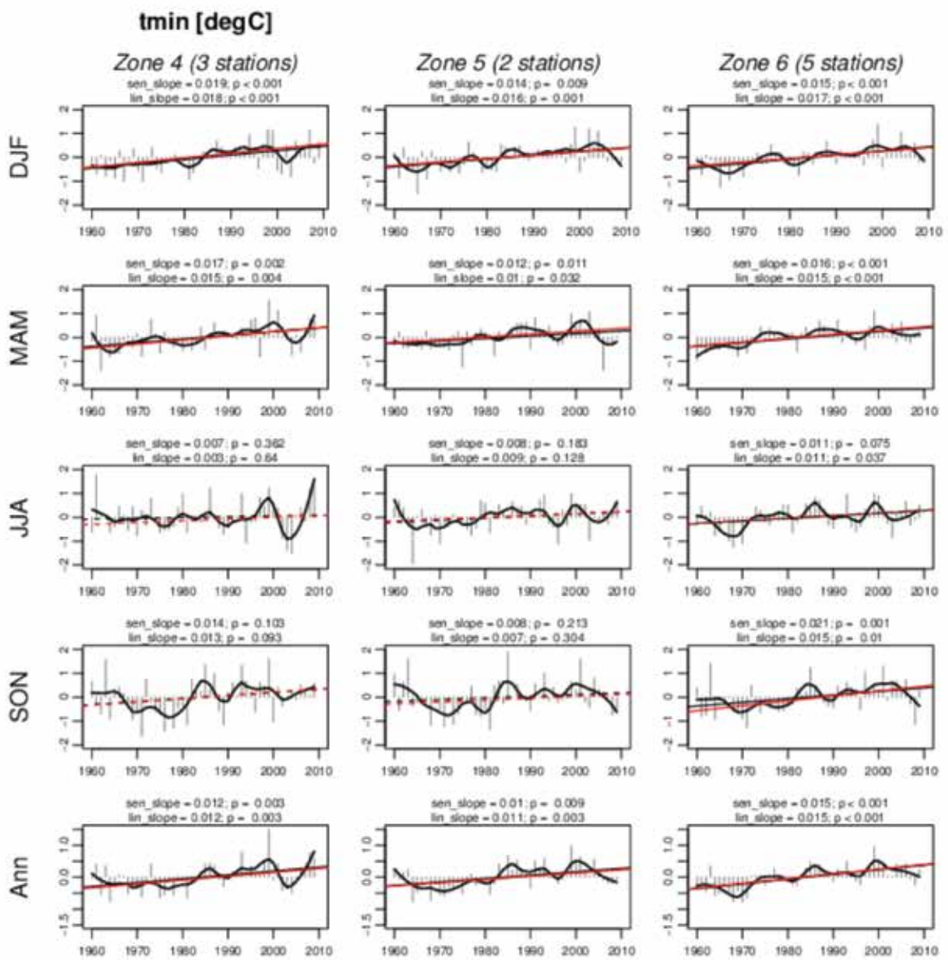

Figure 26. Regional mean time series and trends in minimum temperature for stations in zones 4–6 for summer (DJF), autumn (MAM), winter (JJA), spring (SON) and annual (Ann) means. Grey bars represent departures from the 1960–2010 mean for each year. Black curves are a Loess smoothing of the yearly data with a bandwidth of 0.25. Trend lines are shown for the linear least squares fit (black) and Sen's slope estimate (red). Solid trend lines indicate the trend is significant at the 95% level and dashed lines are not significant at this level.

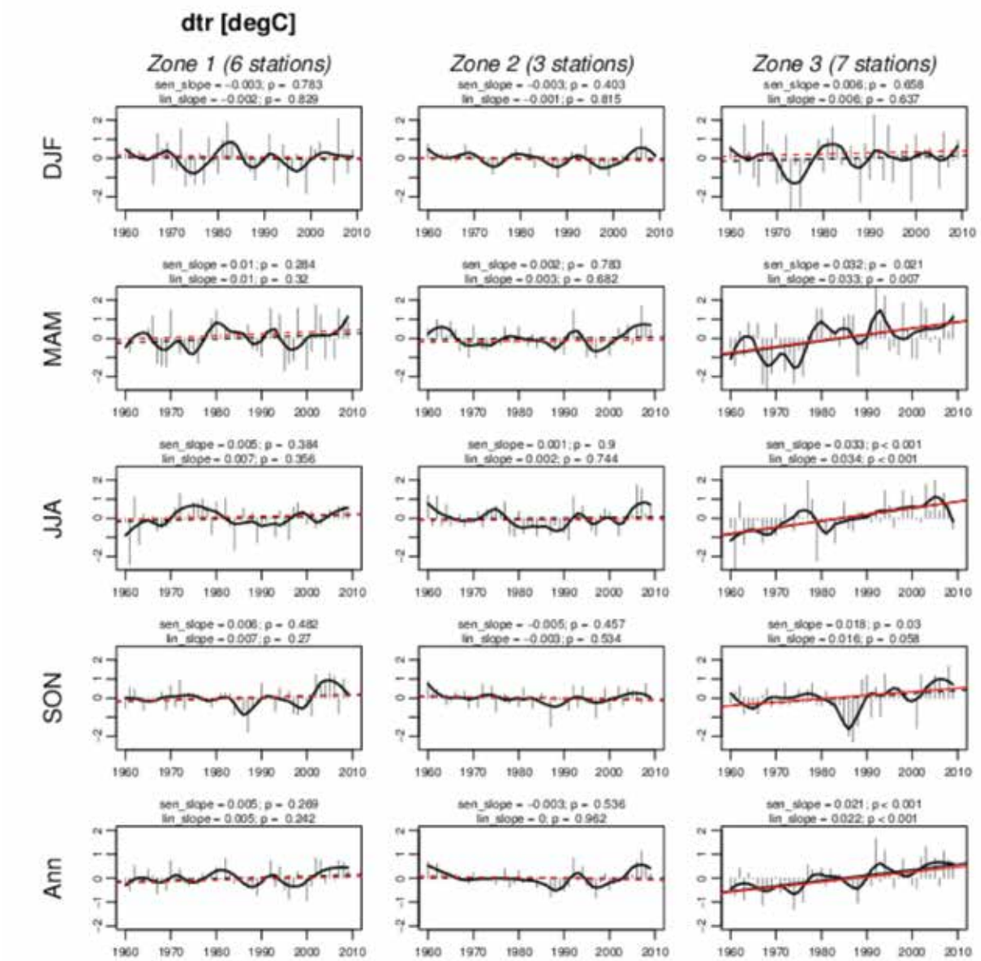

Figure 27. Regional mean time series and trends in diurnal temperature range for stations in zones 1–3 for summer (DJF), autumn (MAM), winter (JJA), spring (SON) and annual (Ann) means. Grey bars represent departures from the 1960–2010 mean for each year. Black curves are a Loess smoothing of the yearly data with a bandwidth of 0.25. Trend lines are shown for the linear least squares fit (black) and Sen's slope estimate (red). Solid trend lines indicate the trend is significant at the 95% level and dashed lines are not significant at this level.

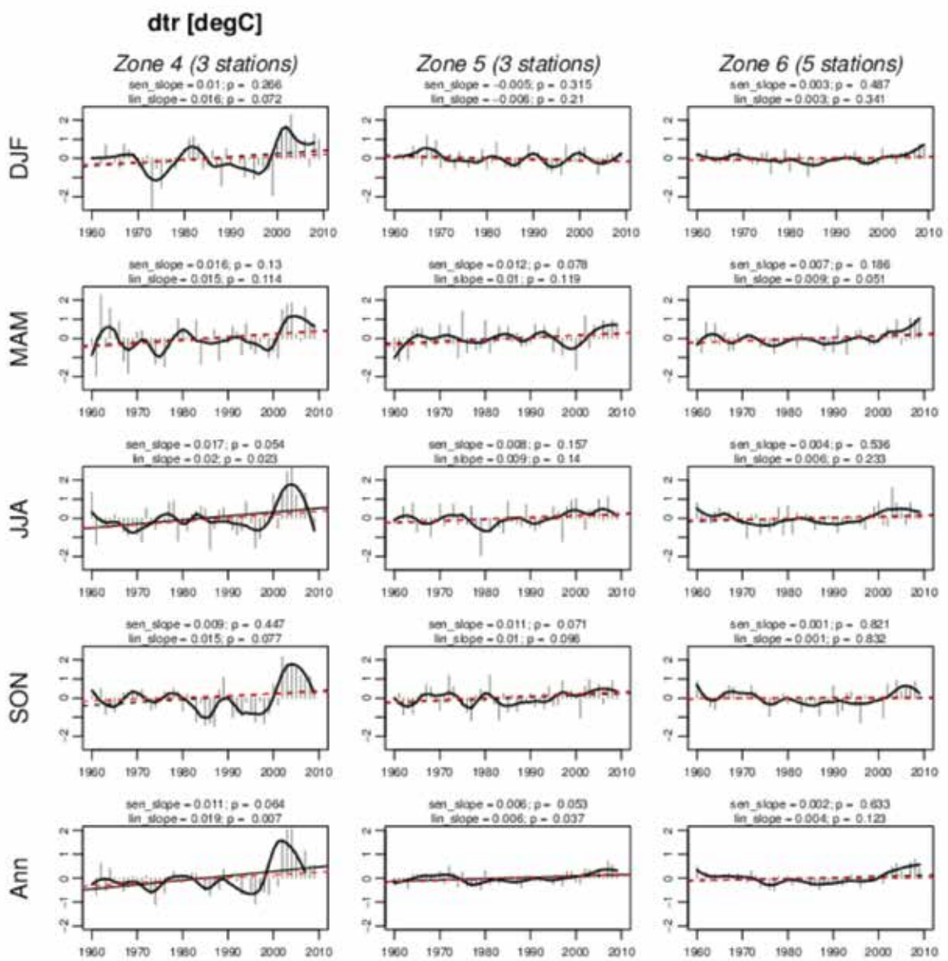

Figure 28. Regional mean time series and trends in diurnal temperature range for stations in zones 4–6 for summer (DJF), autumn (MAM), winter (JJA), spring (SON) and annual (Ann) means. Grey bars represent departures from the 1960–2010 mean for each year. Black curves are a Loess smoothing of the yearly data with a bandwidth of 0.25. Trend lines are shown for the linear least squares fit (black) and Sen's slope estimate (red). Solid trend lines indicate the trend is significant at the 95% level and dashed lines are not significant at this level.

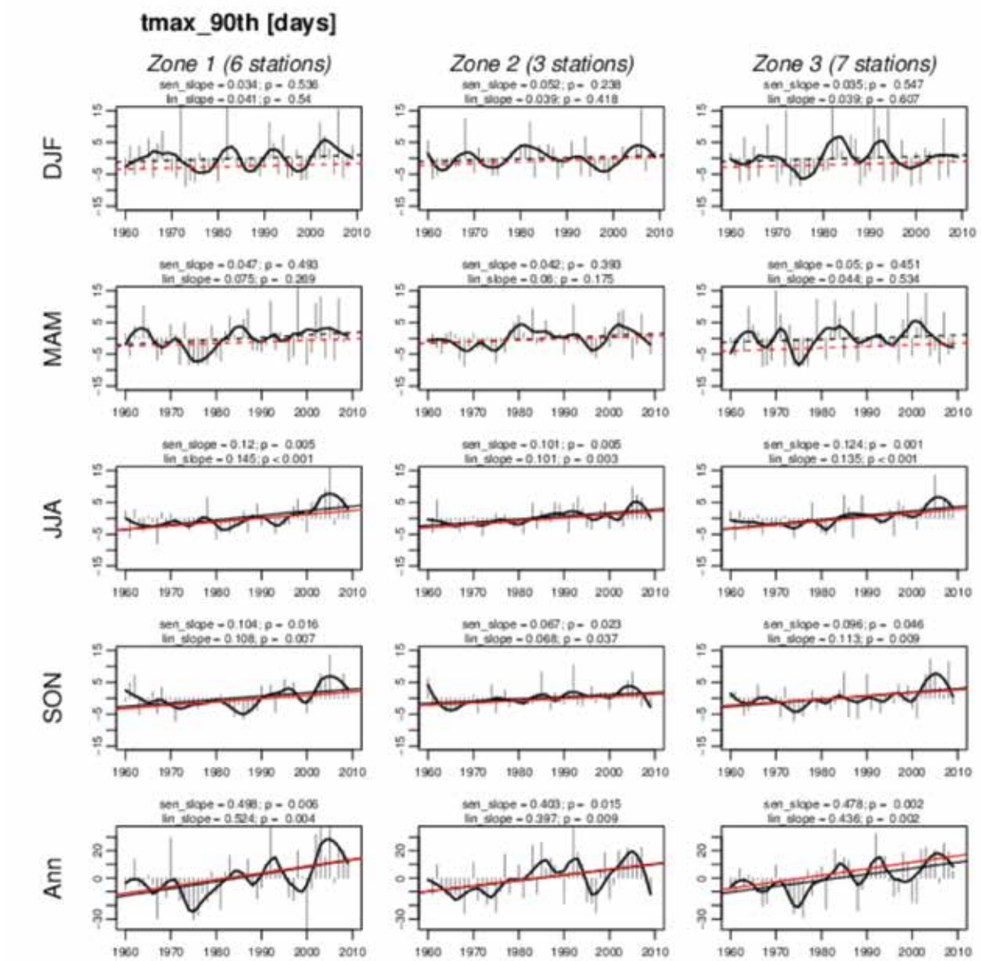

Figure 29. Regional mean time series and trends in number of days above the 90th percentile of maximum for stations in zones 1–3 for summer (DJF), autumn (MAM), winter (JJA), spring (SON) and annual (Ann) means. Grey bars represent departures from the 1960–2010 mean for each year. Black curves are a Loess smoothing of the yearly data with a bandwidth of 0.25. Trend lines are shown for the linear least squares fit (black) and Sen's slope estimate (red). Solid trend lines indicate the trend is significant at the 95% level and dashed lines are not significant at this level.

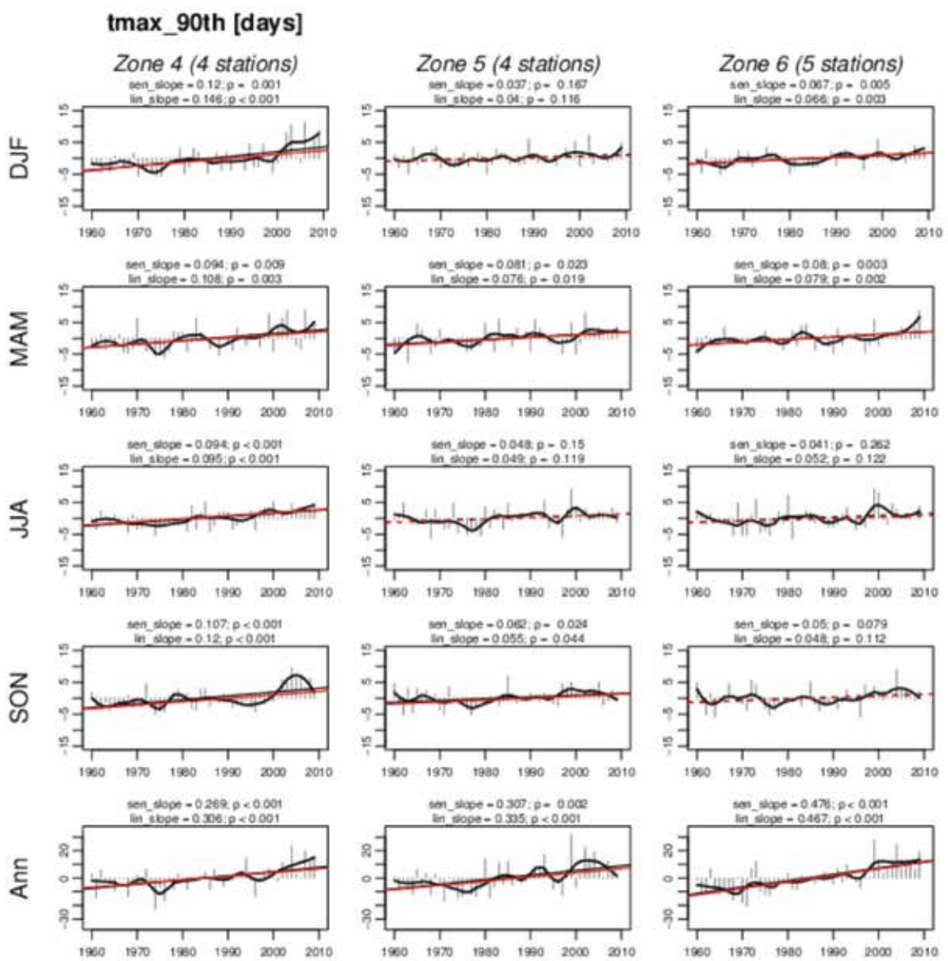

Figure 30. Regional mean time series and trends in number of days above the 90th percentile of maximum for stations in zones 4–6 for summer (DJF), autumn (MAM), winter (JJA), spring (SON) and annual (Ann) means. Grey bars represent departures from the 1960–2010 mean for each year. Black curves are a Loess smoothing of the yearly data with a bandwidth of 0.25. Trend lines are shown for the linear least squares fit (black) and Sen's slope estimate (red). Solid trend lines indicate the trend is significant at the 95% level and dashed lines are not significant at this level.

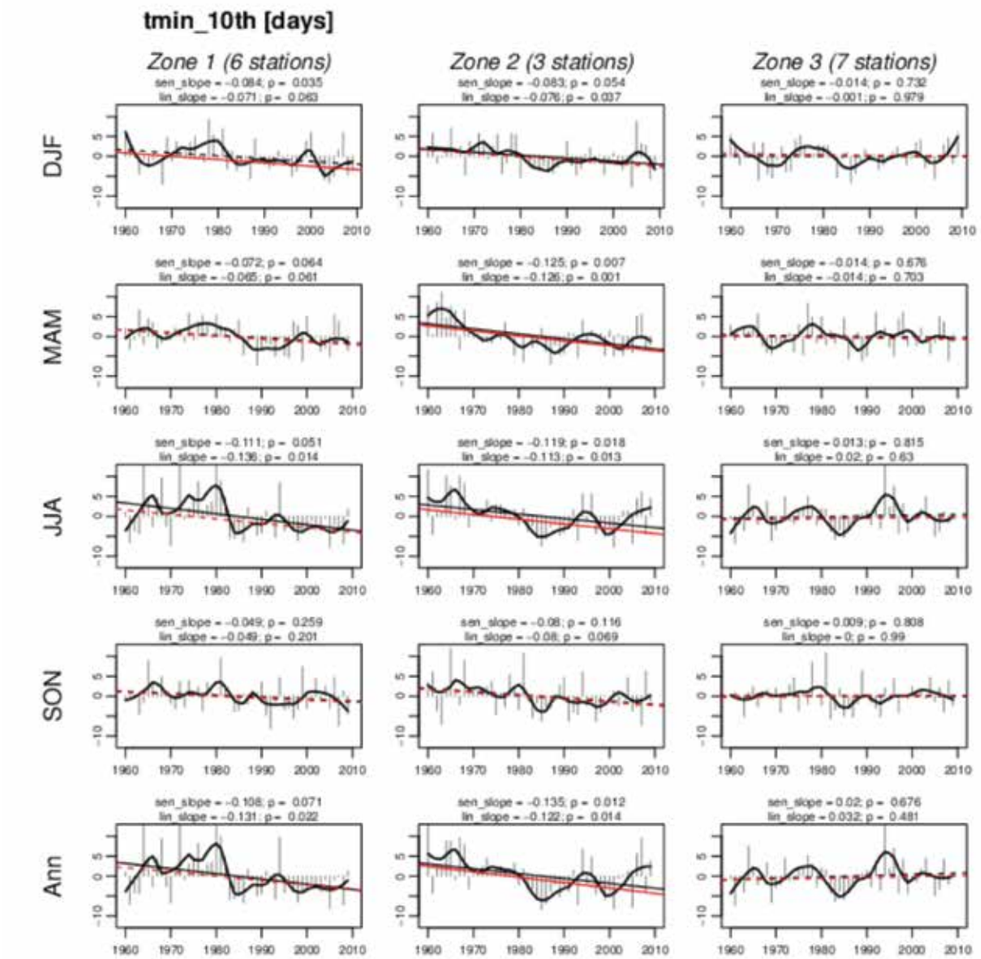

Figure 31. Regional mean time series and trends in number of days below the 10th percentile of minimum for stations in zones 1–3 for summer (DJF), autumn (MAM), winter (JJA), spring (SON) and annual (Ann) means. Grey bars represent departures from the 1960–2010 mean for each year. Black curves are a Loess smoothing of the yearly data with a bandwidth of 0.25. Trend lines are shown for the linear least squares fit (black) and Sen's slope estimate (red). Solid trend lines indicate the trend is significant at the 95% level and dashed lines are not significant at this level.

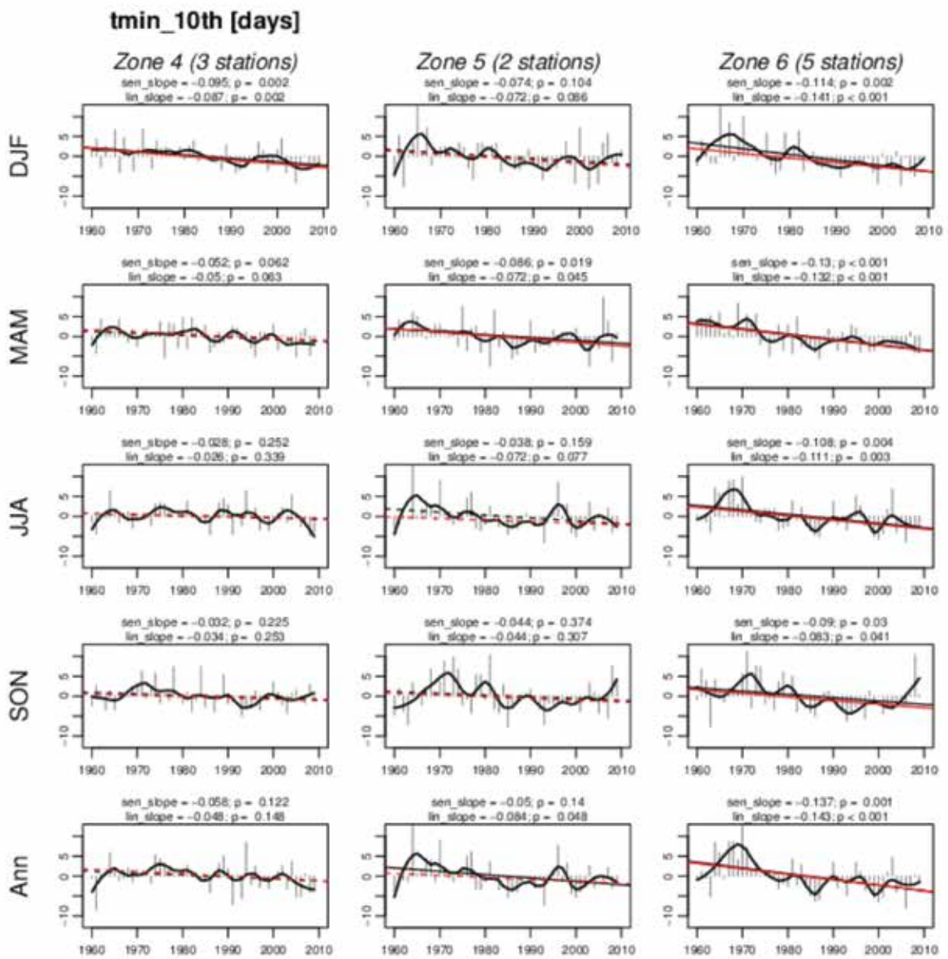

Figure 32. Regional mean time series and trends in number of days below the 10th percentile of minimum for stations in zones 4–6 for summer (DJF), autumn (MAM), winter (JJA), spring (SON) and annual (Ann) means. Grey bars represent departures from the 1960–2010 mean for each year. Black curves are a Loess smoothing of the yearly data with a bandwidth of 0.25. Trend lines are shown for the linear least squares fit (black) and Sen's slope estimate (red). Solid trend lines indicate the trend is significant at the 95% level and dashed lines are not significant at this level.

3. COMPARISON OF MODEL AND OBSERVED TRENDS FOR 1960–2010

Figure 33 shows a comparison of observed trends to trends calculated for multiple GCM simulations downscaled to the same stations, for the same historical period. This gives an indication of whether or not the models have captured the long-term trends that have emerged from the analysis of observations. A selection of four variables is presented (ppt, tmin, tmax and dtr) and a number of observations can be made. Firstly, it is shown that the reductions in MAM ppt that are evident in the observed trends for most regions are not captured by the models. In fact, the models tend to show an opposite trend. Similarly in SON, where observed trends are weak, the models show a tendency for reduced ppt in all regions. Observed temperature trends are more closely matched by the models, with the notable exception of tmin in zone 3. This is the region where decreases in tmin have been observed, but none of the models simulate this. If the reason for the tmin reduction is indeed a reduction in nocturnal cloud cover, as speculated above, then this result suggests that the models do not adequately represent the processes causing this. In general the changes in dtr are much larger in the observations than in the model simulations.

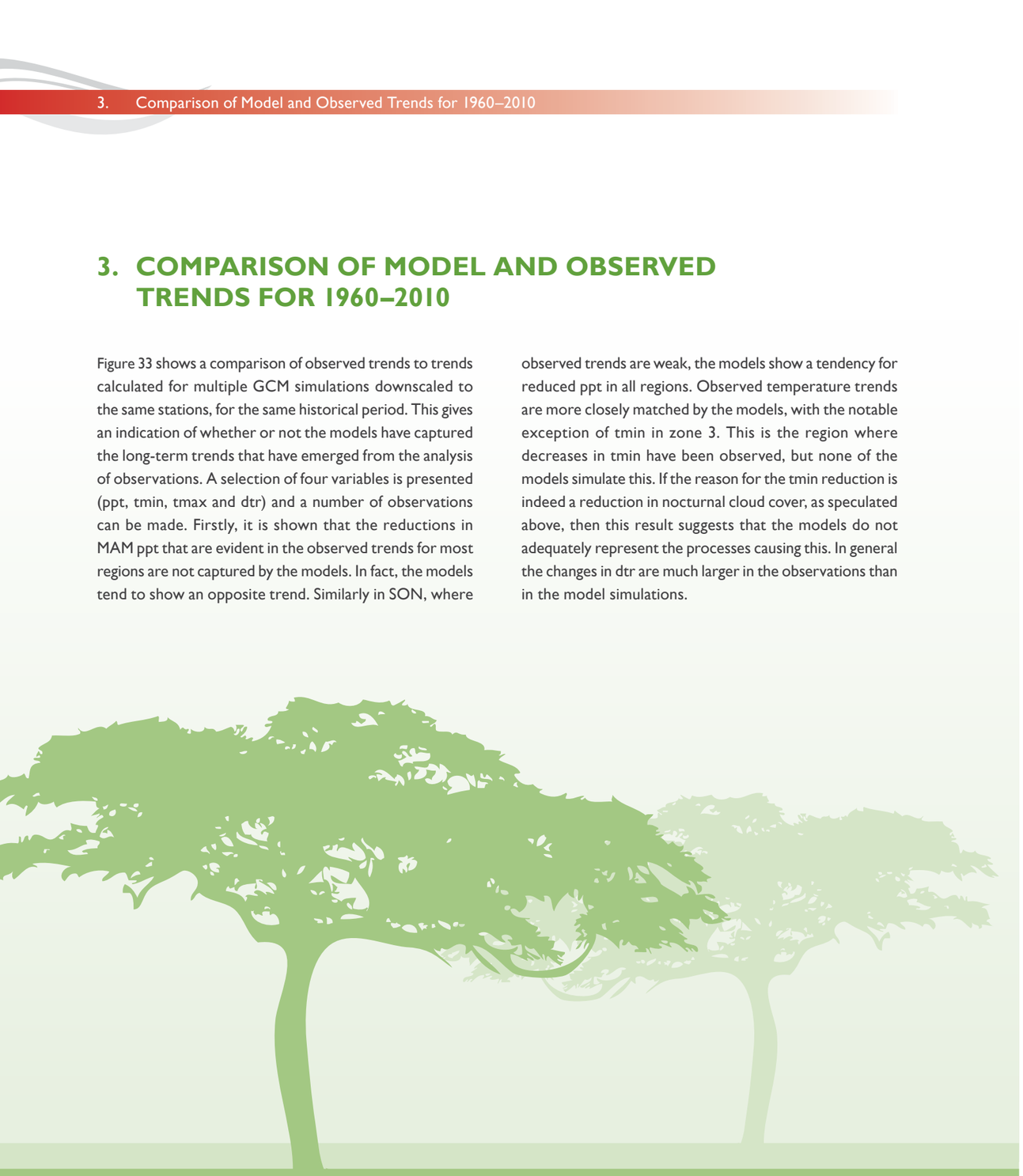

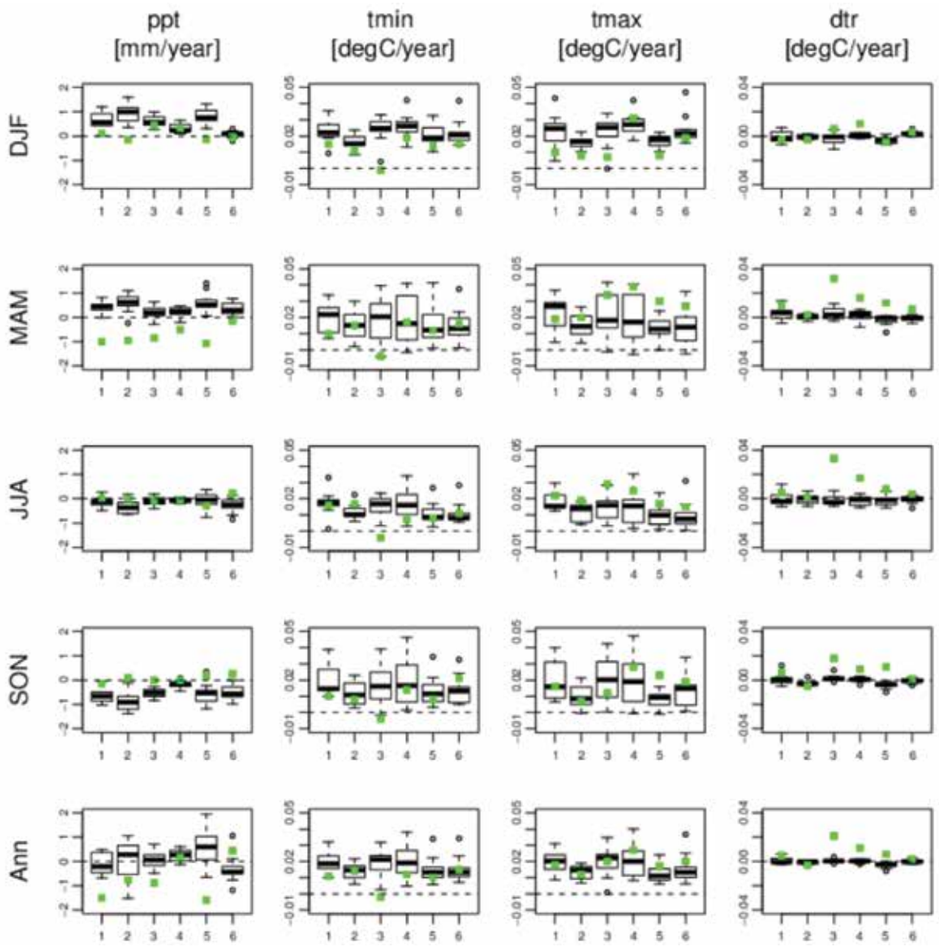

Figure 33. Correspondence between observed trends and downscaled GCM trends for 1960–2010. Trends are averages for stations in each of the 6 hydrological zones(x axis). Green symbols show observed trend (Sen's slope estimate) and box and whisker plots represent the 11 downscaled model trends. Black circles show models lying outside 1.5 times the interquartile range.

4. STATISTICALLY DOWNSCALED PROJECTIONS

A statistical downscaling technique (Hewitson and Crane 2006) has been applied to obtain downscalings of daily precipitation and temperature fields over South Africa, for various time periods within the 1961–2100 period, and for various Special Report on Emissions Scenarios (SRES) and RCP scenarios, and for different CGCMs. The results are presented below.

4.1 CSAG statistical projections for SRES B1

4.1.1 Temperature

The median of the ensemble of statistical downscalings indicate moderate temperature increases over the South African interior under the B1 SRES scenario, of about 2 to 2.5°C for 2040–2060, reaching about 3°C by the far-future. Similar changes are projected for both minimum (Figure 34 and Figure 35) and maximum temperatures (Figure 36 and Figure 37).

4.1.2 Rainfall

Projected changes in the average seasonal rainfall (mm) over South Africa for DJF, MAM, SON and JJA, for the periods 2040–2060 and 2080–2100, relative to 1971–2005, are displayed in Figure 38 and Figure 39. The 90th percentile (upper panels), median (middle panels) and 10th percentile (lower panels) are shown for an ensemble of downscalings of ten coupled general circulation model (CGCM) projections, for each of the seasons and each of the time periods.

For the summer months of the mid-future (2040–2060), the downscalings indicate a range of different rainfall futures, ranging from a much wetter eastern South Africa (projected increases of more than 20 mm/month over Limpopo – 90th percentile) to a drier future in the east (rainfall decreases of more than 20 mm/month – 10th percentile). The median of downscalings indicate a mixed signal with small rainfall anomalies. Most ensemble members project a drier autumn for South Africa, with decreases of more than 20 mm/month projected for eastern South Africa by some ensemble members. However, most ensemble members project slight to moderate increases in autumn rainfall over the south-western Cape. Most downscalings are also indicative of moderate to strong increases in winter precipitation over the south-western Cape, although significant drying is also plausible. Uncertainty surrounds the projections of changes in winter rain over the summer rainfall region of South Africa, with projected changes varying from increases of more than 20 mm/month, to decreases of more than 20 mm/month. For spring, most of the downscalings are indicative of rainfall increases over eastern South Africa, as well as the south-western Cape, although decreases are also plausible.

For the far-future (2075–2095), most ensemble members projected drier summers over eastern South Africa, although significantly wetter summers (more than 20 mm/month) are also plausible. The projected far-future changes for autumn are very similar to those projected for the mid-future, with most (but not all) ensemble members indicating generally drier conditions for eastern South Africa. A mixed signal, ranging from significant drying to significant wetting, is projected for the south-western Cape. The projected rainfall signal for winter also shows close correspondence between the near-future and far-future time periods. Most ensemble members project significant rainfall increases for the south-western Cape, with no consensus among the ensemble members regarding the rainfall signal over eastern South Africa. The projected far-future changes in spring rainfall similarly show close correspondence to the near-future signal – most ensemble members project rainfall increases over the south-western Cape and also over eastern South Africa.

4.1.3 Key messages from the CSAG SRES B1 scenarios

Reasonably modest temperature increases, of about 2 to 2.5°C by the mid-future, reaching about 3°C in the far-future, are projected by the ensemble mean.

Most ensemble members project moderate to significant rainfall increases over the winter rainfall region of the south-western Cape, extending to the Cape south coast, for the seasons autumn to spring, and for both the mid- and far-futures. However, a smaller number of ensemble members indicate that a significantly drier future is also plausible over these regions.

Some ensemble members project significantly wetter futures over the summer rainfall region, however, for the far-future, when the climate change signal is best developed, most ensemble members project modest to significant drying for this region, for both summer and autumn.

It is noteworthy that rather strong patterns of drying or wetting are projected to occur for the B1 scenario, which is regarded as one of the more positive scenarios with relatively slow growth and eventual stabilisation of emissions.

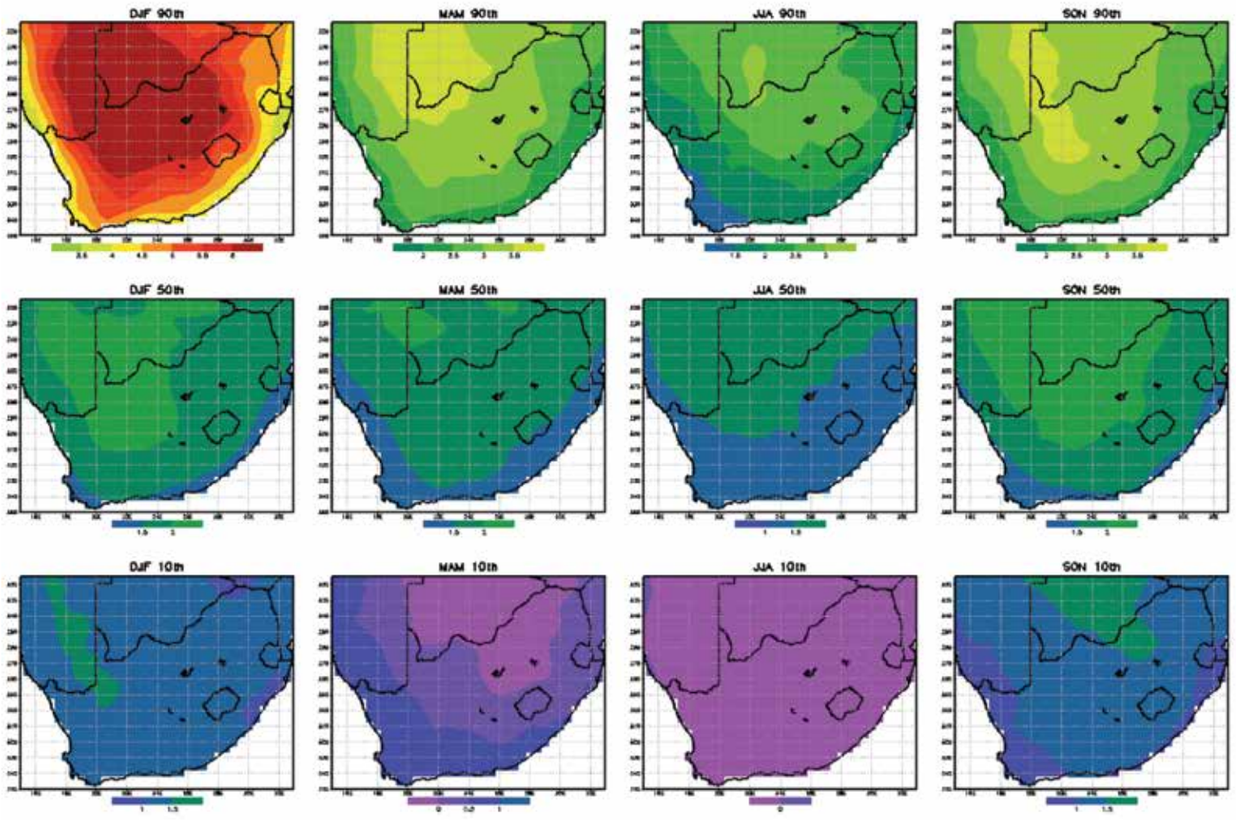

Figure 34. Projected change in the average seasonal minimum temperatures (°C) over South Africa for JJA, SON, DJF and MAM, for the period 2040–2060 relative to 1971–2005. The 90th percentile (upper panels), median (middle panels) and 10th percentile (lower panels) are shown for an ensemble of downscalings of ten CGCM projections, for each of the seasons. The downscalings were generated using the CSAG statistical downscaling procedure. All the CGCM projections contributed to CMIP3 and AR4 of the IPCC, and are for the B1 SRES scenario.

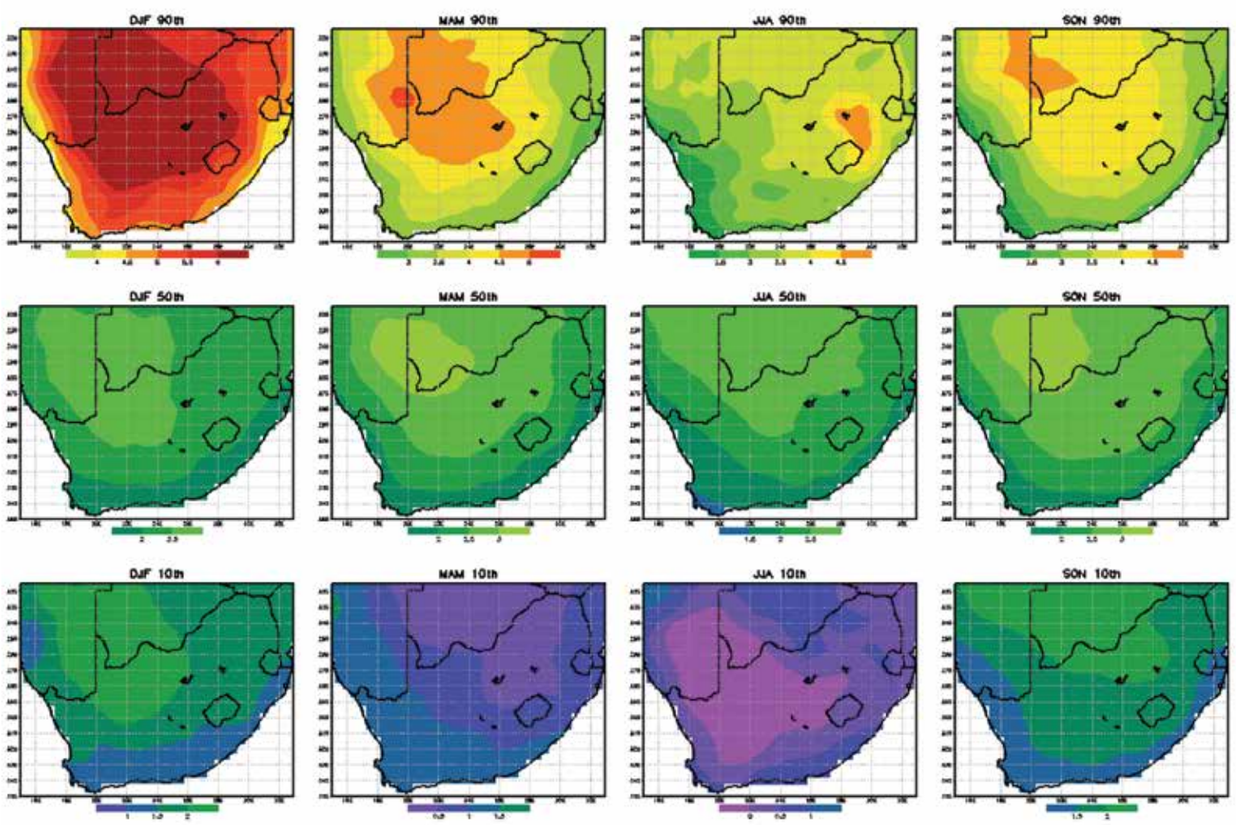

Figure 35. Projected change in the average seasonal minimum temperatures (°C) over South Africa for JJA, SON, DJF and MAM, for the period 2075–2095 relative to 1971–2005. The 90th percentile (upper panels), median (middle panels) and 10th percentile (lower panels) are shown for an ensemble of downscalings of ten CGCM projections, for each of the seasons. The downscalings were generated using the CSAG statistical downscaling procedure. All the CGCM projections contributed to CMIP3 and AR4 of the IPCC, and are for the B1 SRES scenario.

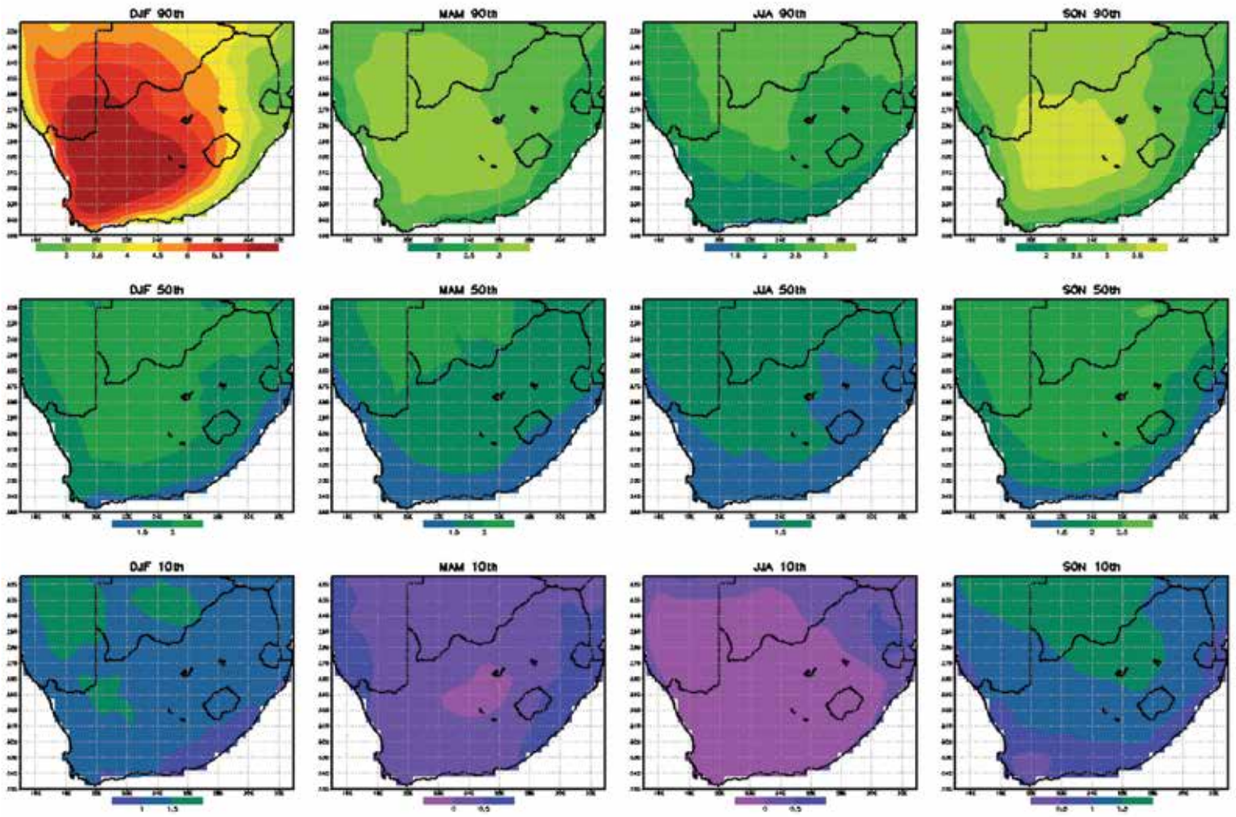

Figure 36. Projected change in the average seasonal maximum temperatures (°C) over South Africa for JJA, SON, DJF and MAM, for the period 2040–2060 relative to 1971–2005. The 90th percentile (upper panels), median (middle panels) and 10th percentile (lower panels) are shown for an ensemble of downscalings of ten CGCM projections, for each of the seasons. The downscalings were generated using the CSAG statistical downscaling procedure. All the CGCM projections contributed to CMIP3 and AR4 of the IPCC, and are for the B1 SRES scenario.

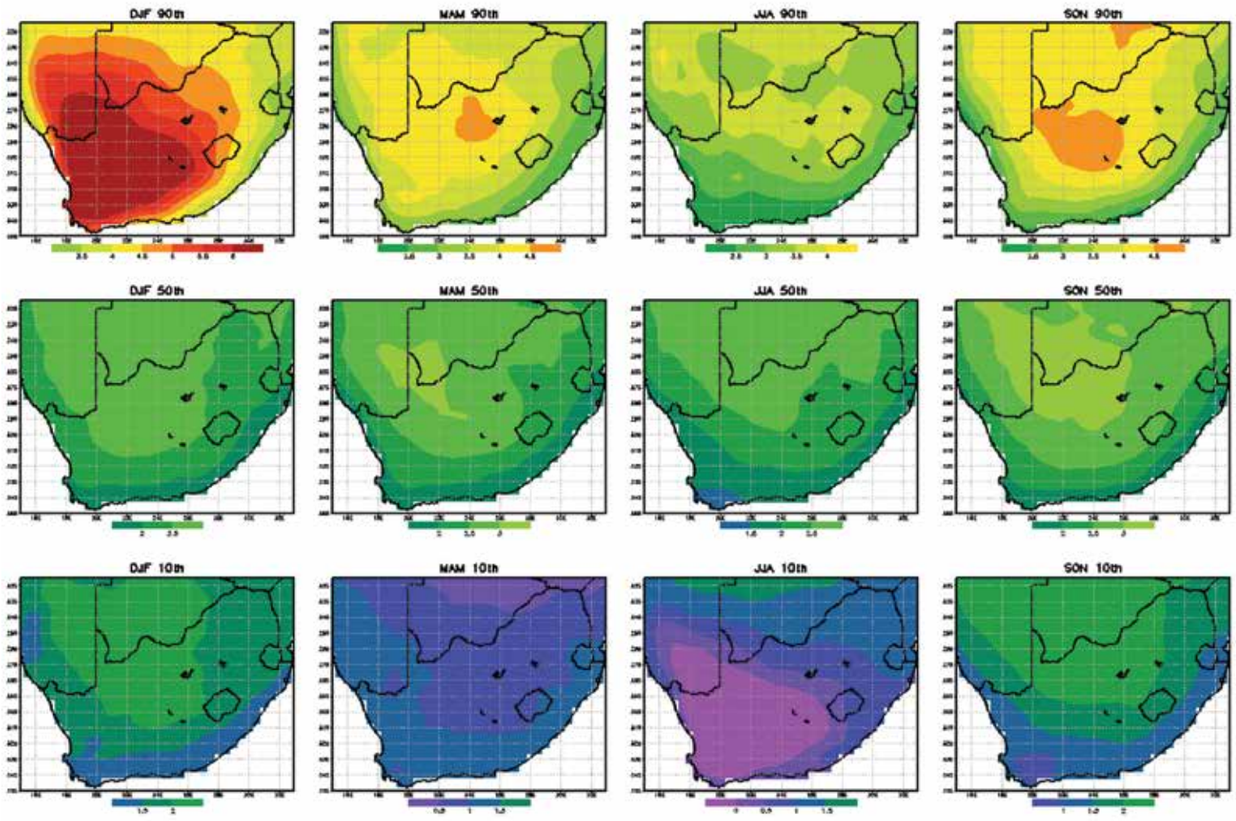

Figure 37. Projected change in the average seasonal maximum temperatures (°C) over South Africa for JJA, SON, DJF and MAM, for the period 2075–2095 relative to 1971–2005. The 90th percentile (upper panels), median (middle panels) and 10th percentile (lower panels) are shown for an ensemble of downscalings of ten CGCM projections, for each of the seasons. The downscalings were generated using the CSAG statistical downscaling procedure. All the CGCM projections contributed to CMIP3 and AR4 of the IPCC, and are for the B1 SRES scenario.

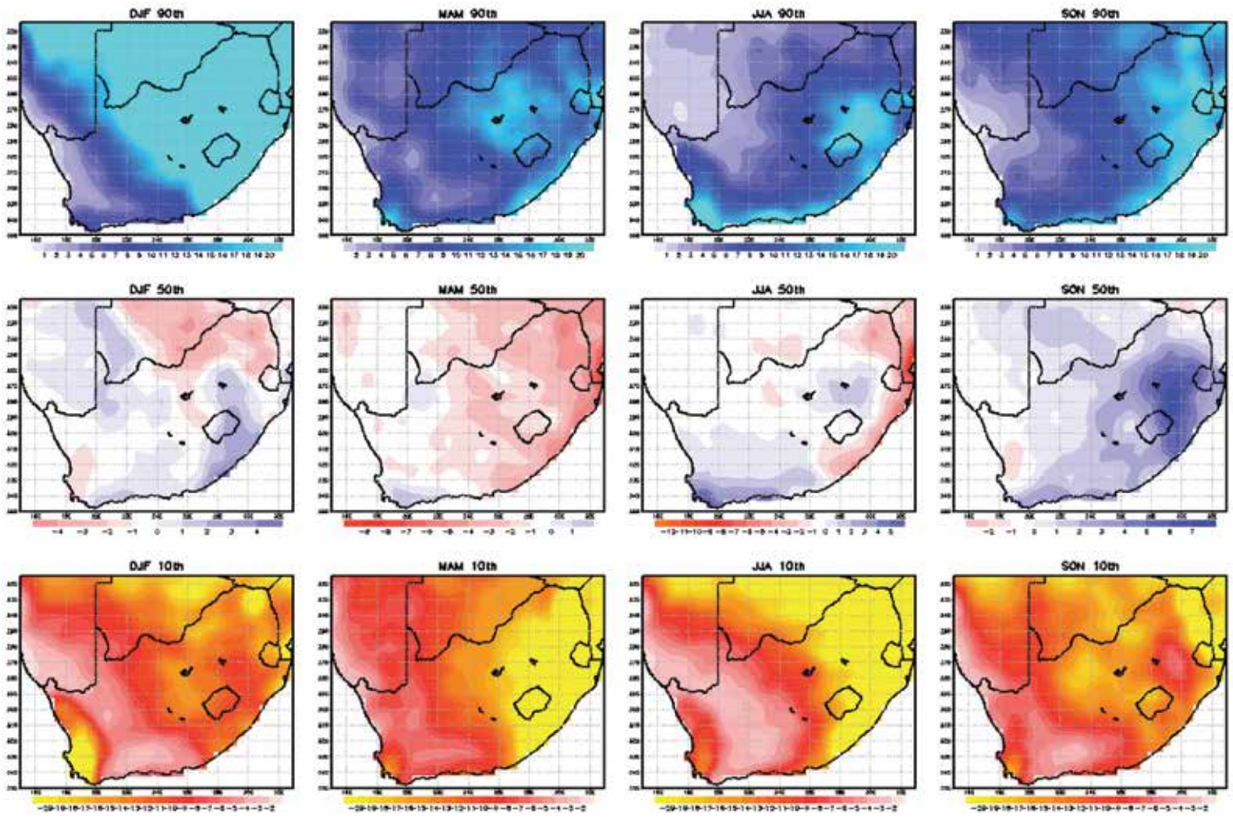

Figure 38. Projected change in the average seasonal rainfall (mm) over South Africa for DJF, MAM, JJA and SON, for the period 2040–2060 relative to 1971–2005. The 90th percentile (upper panels), median (middle panels) and 10th percentile (lower panels) are shown for an ensemble of downscalings of ten CGCM projections, for each of the seasons. The downscalings were generated using the CSAG statistical downscaling procedure. All the CGCM projections contributed to CMIP3 and AR4 of the IPCC, and are for the B1 SRES scenario.

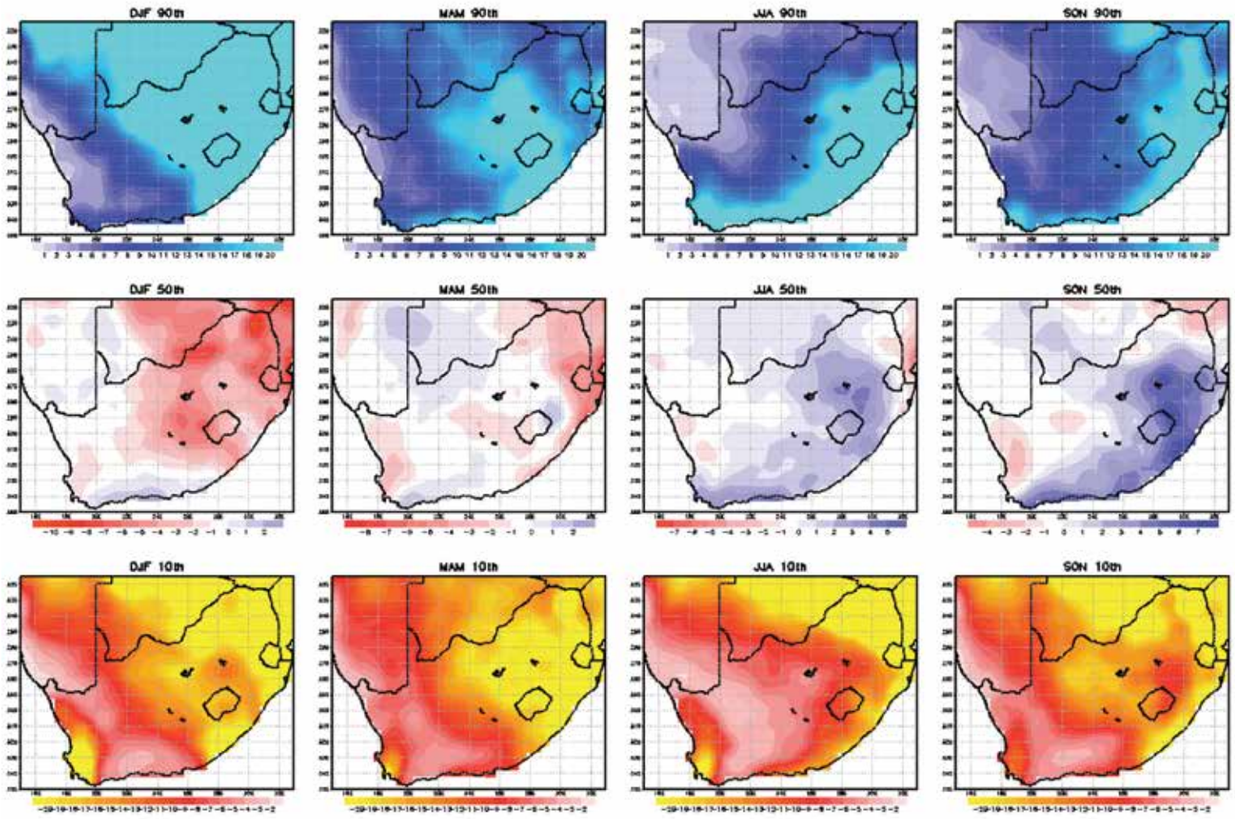

Figure 39. Projected change in the average seasonal rainfall (mm) over South Africa for DJF, MAM, JJA and SON, for the period 2075–2095 relative to 1971–2005. The 90th percentile (upper panels), median (middle panels) and 10th percentile (lower panels) are shown for an ensemble of downscalings of ten CGCM projections, for each of the seasons. The downscalings were generated using the CSAG statistical downscaling procedure. All the CGCM projections contributed to CMIP3 and AR4 of the IPCC, and are for the B1 SRES scenario.

4.2 CSAG statistical projections for SRES A2

4.2.1 Temperature

The ensemble mean indicates that both minimum (Figure 40 and Figure 41) and maximum (Figure 42 and Figure 43) temperatures are to rise by 2 to 3°C over the interior, by 2040–2060, under the A2 scenario. Significant increases, of more than 4°C, are projected for the far-future period of 2075–2095.

4.2.2 Rainfall

Projected changes in the average seasonal rainfall (mm) over South Africa for DJF, MAM, SON and JJA, for the periods 2040–2060 and 2080–2100, relative to 1971–2005, are displayed in (Figure 44 and Figure 45). The 90th percentile (upper panels), median (middle panels) and 10th percentile (lower panels) are shown for an ensemble of downscalings of ten CGCM projections, for each of the seasons and each of the time periods. For the summer and autumn months of the mid-future (2040–2060), most ensemble members indicate slight to extreme (more than 20 mm/month) drying over eastern South Africa. However, significant increases in rainfall (more than 20 mm per month) are projected by some ensemble members for eastern South Africa, for both summer and autumn, indicating the vast range of different projected climate futures for the summer rainfall region. For winter and spring, most ensemble members project wetting over the south-western Cape, extending to the Cape south coast, although a significantly drier future is also plausible. A mixed rainfall signal is projected for the summer rainfall region for winter and spring, ranging from significant drying (decreases of more than 20 mm/month) to significant wetting (rainfall increases of more than 20 mm/month). For the far-future (2075–2095), very similar patterns are projected as for the 2040–2060 time period. Most ensemble members indicate drier, or significantly drier, rainfall futures over the summer rainfall region. Wetter conditions are projected for the Cape south coast by most ensemble members, however. A pronounced pattern of wetter conditions, extending from the Cape south coast to the east coast and eastern escarpment areas, is projected by most ensemble members for winter and spring. However, significantly drier futures are also plausible over these regions.

4.2.3 Key messages from the CSAG SRES A2 scenarios

The ensemble mean indicates that under the A2 scenario both minimum and maximum temperatures will rise by 2 to 3°C over the interior, by 2040–2060. Significant increases, of more than 4°C, are projected for the far-future period of 2075–2095.

The CSAG statistical projections of rainfall changes under the B1 and A2 scenarios are qualitatively similar. This is a somewhat surprising result, taking into account that the enhanced greenhouse effect is considerably stronger for the far-future in the A2 scenario, compared to the B1 scenario. This may reflect the outcome of the statistical downscaling method which may constrain the extent of future rainfall change due to its empirical method that is based on current day relationships between synoptic conditions and rainfall.

Most ensemble members project moderate to significant rainfall increases over the winter rainfall region of the south-western Cape, extending to the Cape south coast, for the seasons autumn to spring, and for both the mid- and far-futures. However, a smaller number of ensemble members indicate that a significantly drier future is also plausible over these regions.

Significantly wetter futures are projected over the summer rainfall region by some ensemble members, however, for the far-future, when the climate change signal is best developed, most ensemble members project modest to significant drying for this region, for both summer and autumn.

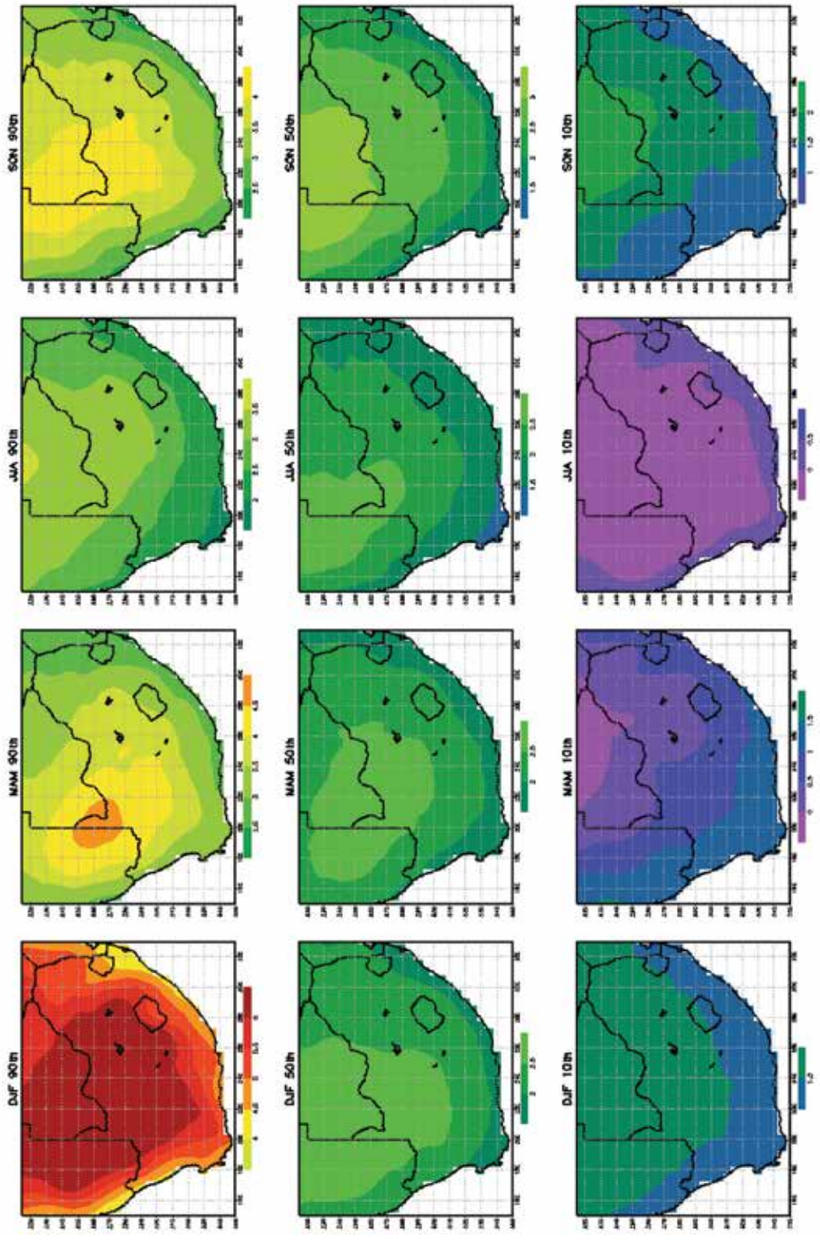

Figure 40. Projected change in the average seasonal minimum temperatures (°C) over South Africa for JJA, SON, DJF and MAM, for the period 2040–2060 relative to 1971–2005. The 90th percentile (upper panels), median (middle panels) and 10th percentile (lower panels) are shown for an ensemble of downscalings of ten CGCM projections, for each of the seasons. The downscalings were generated using the CSAG statistical downscaling procedure. All the CGCM projections contributed to CMIP3 and AR4 of the IPCC, and are for the A2 SRES scenario.

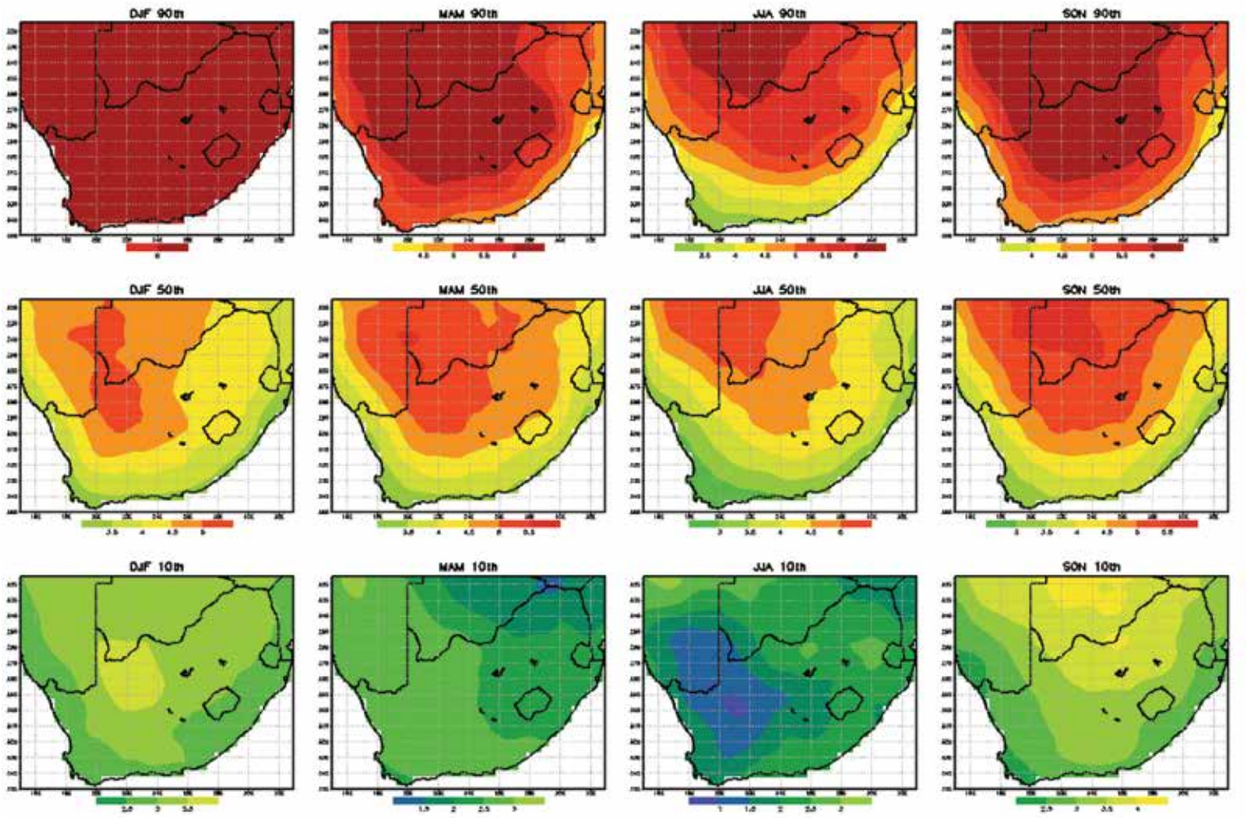

Figure 41. Projected change in the average seasonal minimum temperatures (°C) over South Africa for JJA, SON, DJF and MAM, for the period 2075–2095 relative to 1971–2005. The 90th percentile (upper panels), median (middle panels) and 10th percentile (lower panels) are shown for an ensemble of downscalings of ten CGCM projections, for each of the seasons. The downscalings were generated using the CSAG statistical downscaling procedure. All the CGCM projections contributed to CMIP3 and AR4 of the IPCC, and are for the A2 SRES scenario.

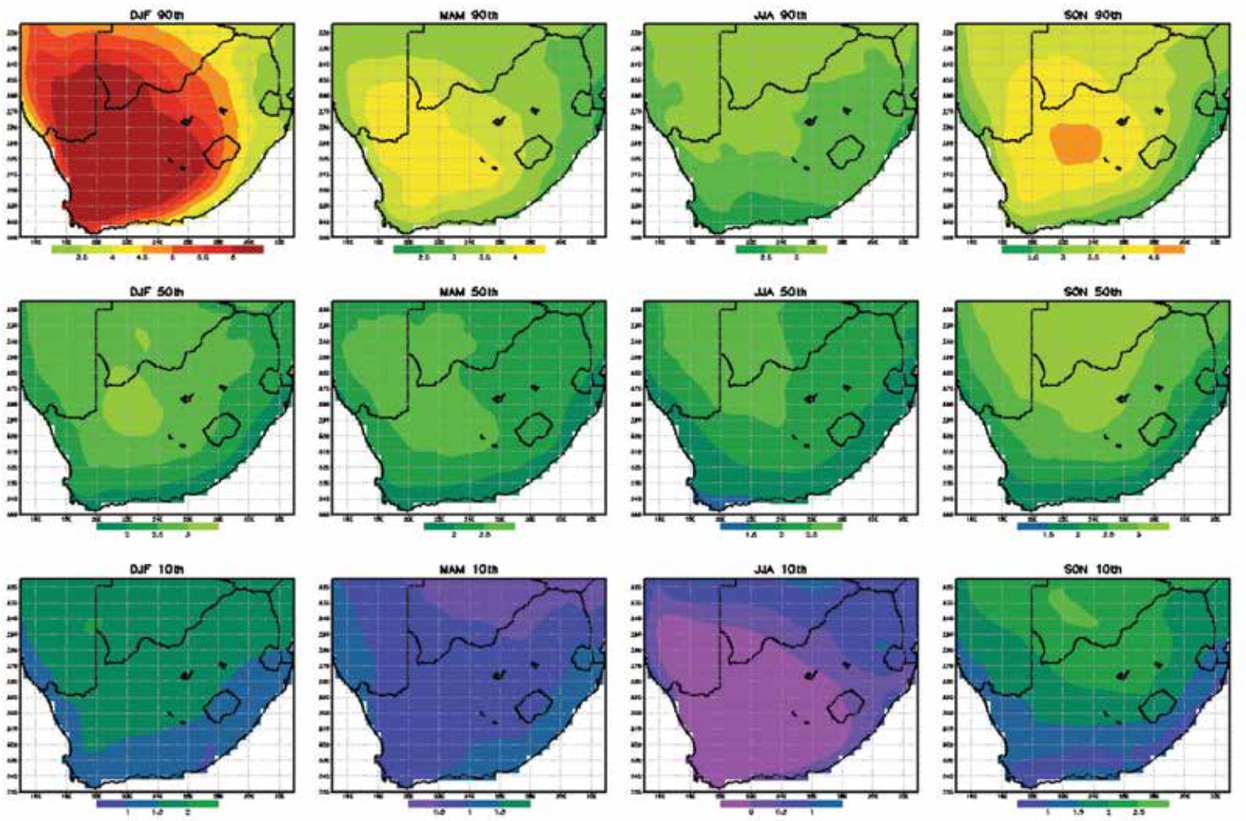

Figure 42. Projected change in the average seasonal maximum temperatures (°C) over South Africa for JJA, SON, DJF and MAM, for the period 2040–2060 relative to 1971–2005. The 90th percentile (upper panels), median (middle panels) and 10th percentile (lower panels) are shown for an ensemble of downscalings of ten CGCM projections, for each of the seasons. The downscalings were generated using the CSAG statistical downscaling procedure. All the CGCM projections contributed to CMIP3 and AR4 of the IPCC, and are for the A2 SRES scenario.

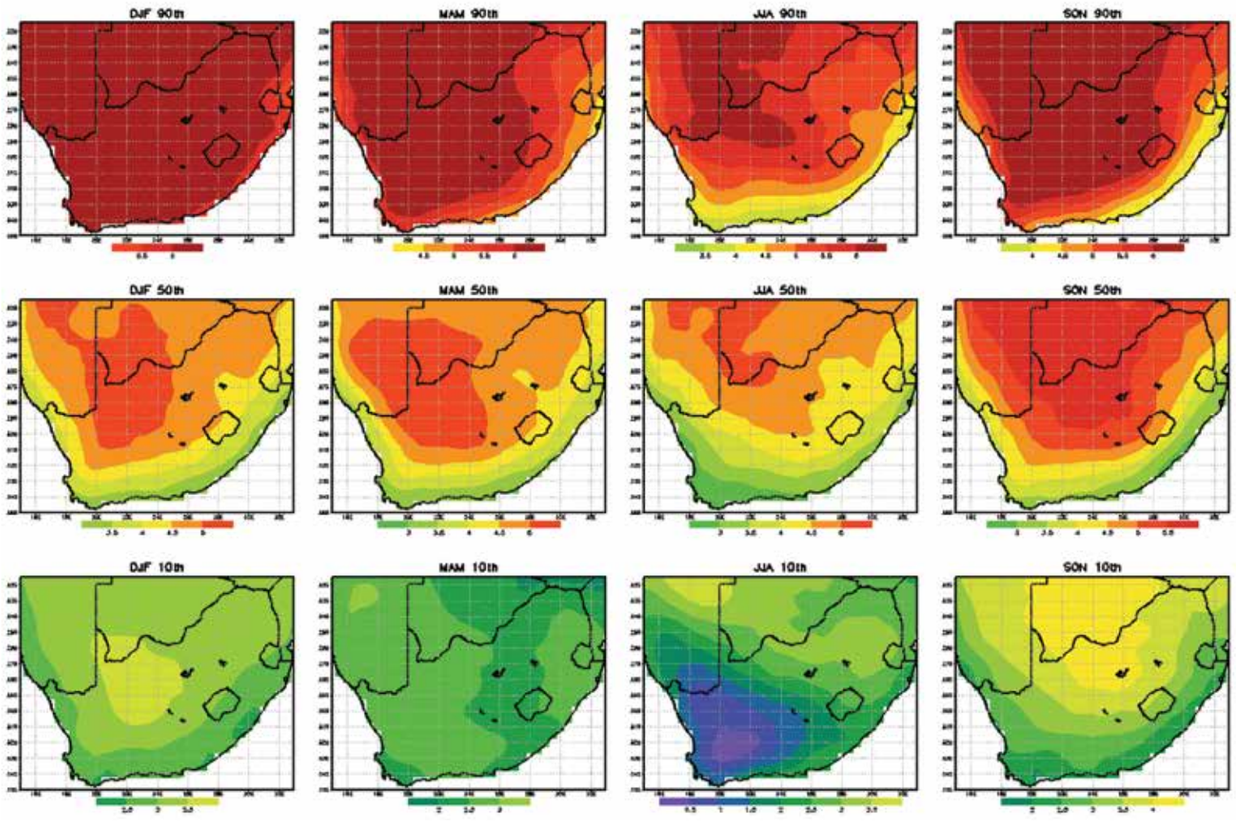

Figure 43. Projected change in the average seasonal maximum temperatures (°C) over South Africa for JJA, SON, DJF and MAM, for the period 2075–2095 relative to 1971–2005. The 90th percentile (upper panels), median (middle panels) and 10th percentile (lower panels) are shown for an ensemble of downscalings of ten CGCM projections, for each of the seasons. The downscalings were generated using the CSAG statistical downscaling procedure. All the CGCM projections contributed to CMIP3 and AR4 of the IPCC, and are for the A2 SRES scenario.

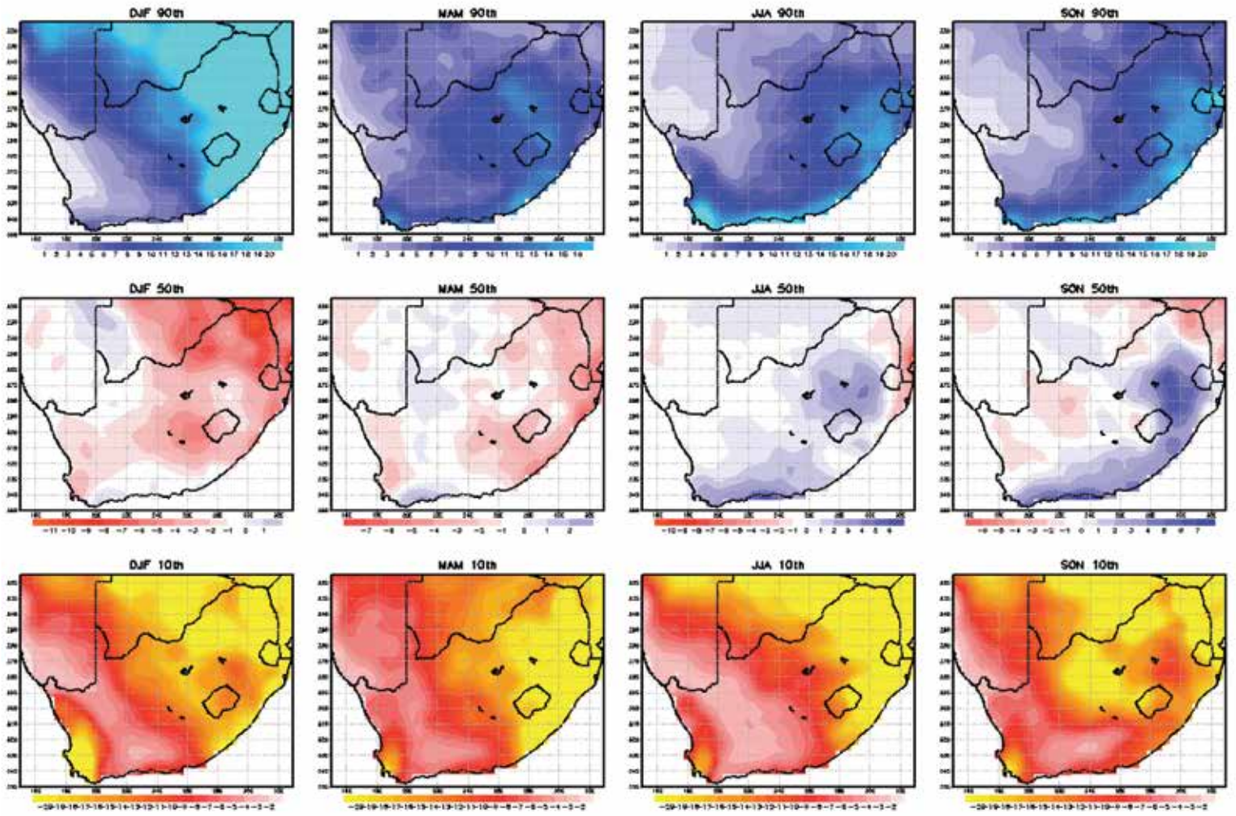

Figure 44. Projected change in the average seasonal rainfall (mm) over South Africa for DJF, MAM, JJA and SON, for the period 2040–2060 relative to 1971–2005. The 90th percentile (upper panels), median (middle panels) and 10th percentile (lower panels) are shown for an ensemble of downscalings of ten CGCM projections, for each of the seasons. The downscalings were generated using the CSAG statistical downscaling procedure. All the CGCM projections contributed to CMIP3 and AR4 of the IPCC, and are for the A2 SRES scenario.

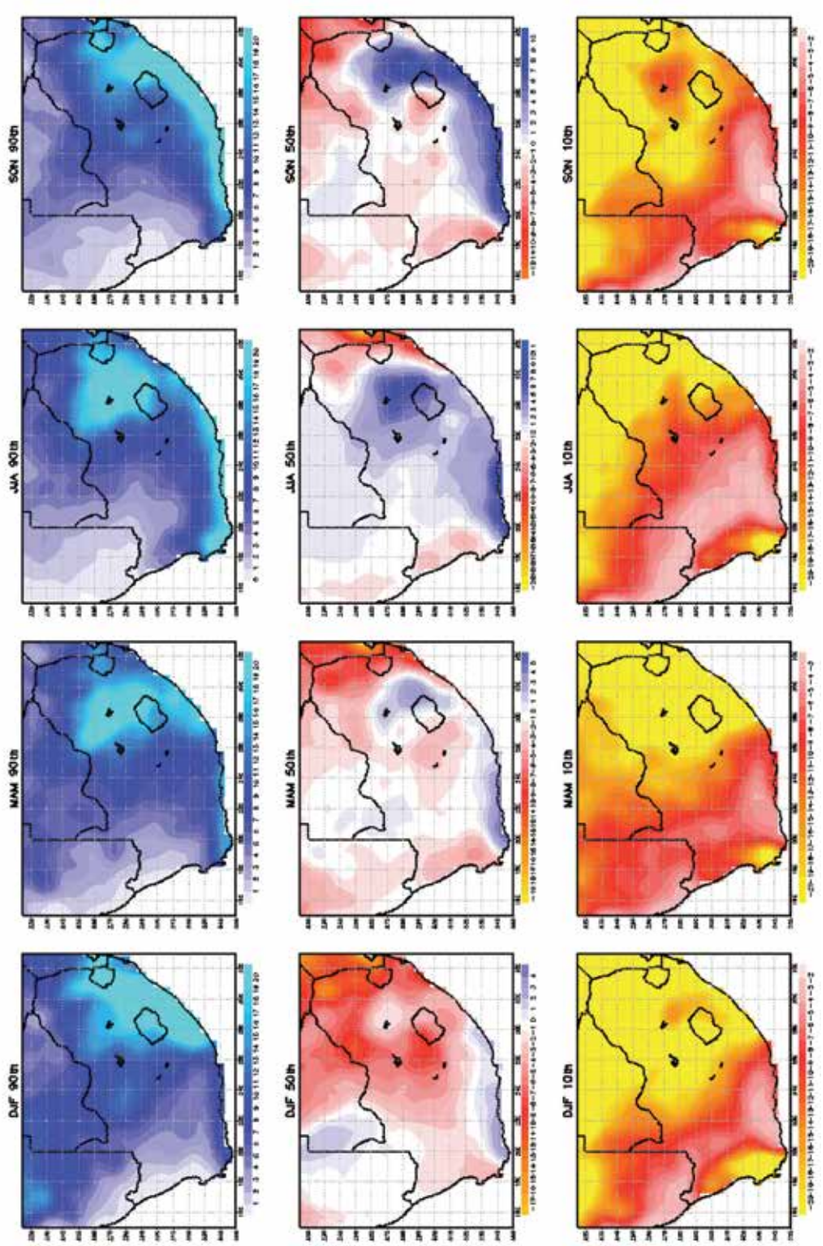

Figure 45: Projected change in the average seasonal rainfall (mm) over South Africa for DJF, MAM, JJA and SON, for the period 2075–2095 relative to 1971–2005. The 90th percentile (upper panels), median (middle panels) and 10th percentile (lower panels) are shown for an ensemble of downscalings of ten CGCM projections, for each of the seasons. The downscalings were generated using the CSAG statistical downscaling procedure. All the CGCM projections contributed to CMIP3 and AR4 of the IPCC, and are for the A2 SRES scenario.

4.3 CSAG statistical projections for RCP4.5

4.3.1 Temperature

The ensemble mean indicates that both minimum (Figure 46, Figure 47 and Figure 48) and maximum (Figure 49, Figure 50 and Figure 51) temperatures could plausibly increase by less than 1°C over the coastal areas, and by 1 to 2°C over the interior regions, for all seasons, by 2015–2035. The median of projected changes is less than 2.5°C for 2040–2060, and less than 3°C for 2075–2095.

4.3.2 Rainfall

Projected changes in the average seasonal rainfall (mm) over South Africa for DJF, MAM, SON and JJA, for the periods 2015–2035 2040–2060 and 2075–2095 relative to 1971–2005, are displayed in (Figure 52, Figure 53, and Figure 54).

The 90th percentile (upper panels), median (middle panels) and 10th percentile (lower panels) are shown for an ensemble of downscalings of ten CGCM projections, for each of the seasons and each of the time periods. The ensemble of projections is qualitatively similar for the three different future time periods. A largely mixed signal is projected for summer and autumn over the summer rainfall region, with rainfall decreases of more than 20 mm/month projected for these regions by some downscalings, whilst others project rainfall increases of the same magnitude. For the far-future, the projected rainfall signal seems to become somewhat better established, with the majority of ensemble members indicating rainfall increases during summer over the summer rainfall region, with decreases projected by most members for autumn. Most ensemble members indicate slight to significant increases in winter rainfall over the south-western Cape, although drying is also plausible. Increases in winter rainfall are also projected by most ensemble members over the east coast areas and the eastern escarpment. A largely mixed rainfall signal is projected for spring, ranging from significant increases to significant decreases.

4.3.3 Key messages from the CSAG RCP4.5 projections

The ensemble mean indicates that both minimum and maximum temperatures are plausible to rise by less than 1°C over the coastal areas, and by 1 to 2°C over the interior regions, for all seasons, by 2015–2035 (Figure 46 and Figure 49). The median of projected changes is less than 2.5°C for 2040–2060 (Figure 47 and Figure 50), and less than 3°C for 2075–2095 (Figure 48 and Figure 51).

Most ensemble members project moderate to significant rainfall increases for winter and spring of the far-future over the south-western Cape, extending to the Cape south coast. This signal is not present in the median of projections for the near- and mid-futures, when projections range from very dry to very wet for these regions. Even for the far-future, a smaller number of ensemble members indicate that a significantly drier future is also plausible over the south-western Cape and Cape south coast.

For winter, spring and summer, most ensemble members project rainfall increases over eastern South Africa for the far-future. This signal is particularly strong for summer. However, significant drying is also indicated to be plausible in the east, for these three seasons. Autumn in the far-future is projected to become drier by most ensemble members. For the near- and mid-futures, these patterns are not so well developed, and the projections indicate in general a mixed signal of wetter or drier conditions.

Key differences between the CSAG downscalings for RCP 4.5, and those for the B1 and A2 scenarios, is that the signal of most ensemble members indicating a wetter south-western Cape and Cape south coast is weaker in amplitude, and limited to the seasons of winter and spring. Whereas both summer and autumn are projected to become drier by most ensemble members in the B1 and A2 scenarios, summer is projected to become wetter in the far-future, in the RCP4.5 scenarios.

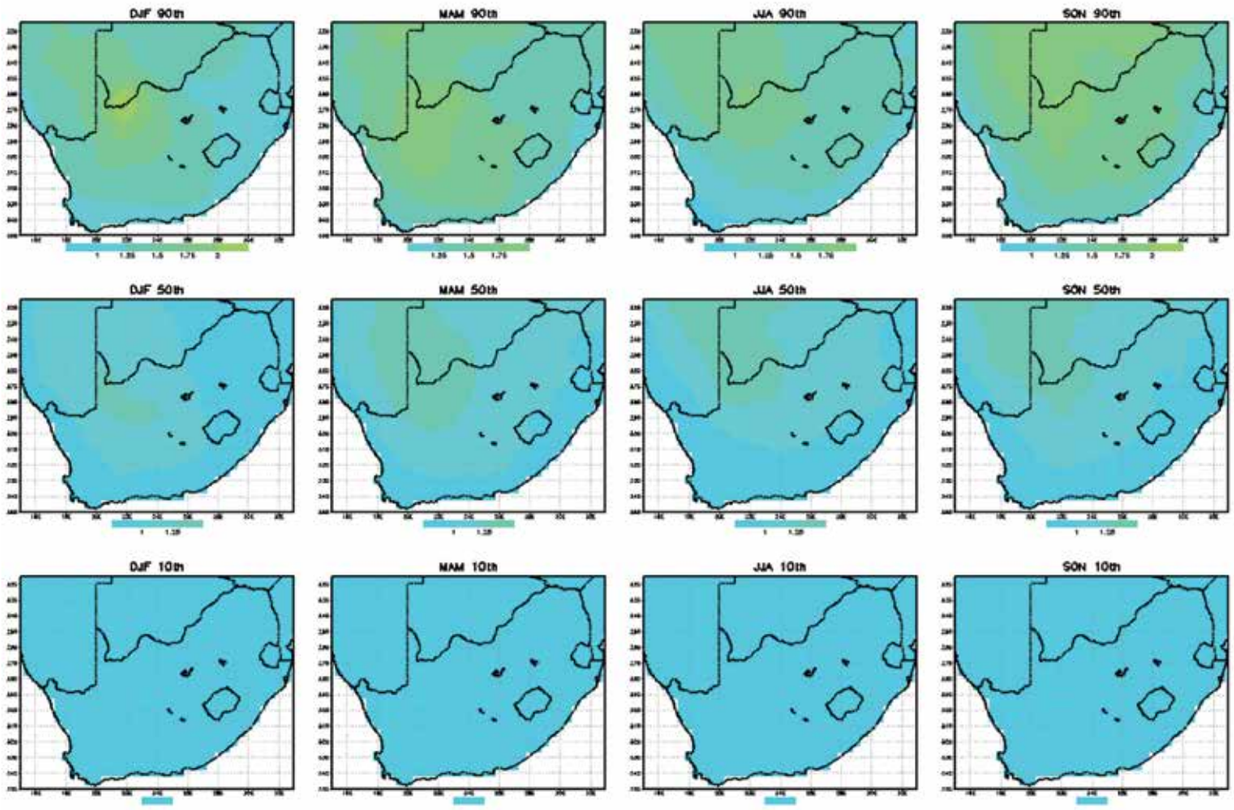

Figure 46. Projected change in the average seasonal minimum temperatures (°C) over South Africa for JJA, SON, DJF and MAM, for the period 2015–2035 relative to 1971–2005. The 90th percentile (upper panels), median (middle panels) and 10th percentile (lower panels) are shown for an ensemble of downscalings of ten CGCM projections, for each of the seasons. The downscalings were generated using the CSAG statistical downscaling procedure. All the CGCM projections contributed to CMIP5 and AR5 of the IPCC, and are for RCP4.5.

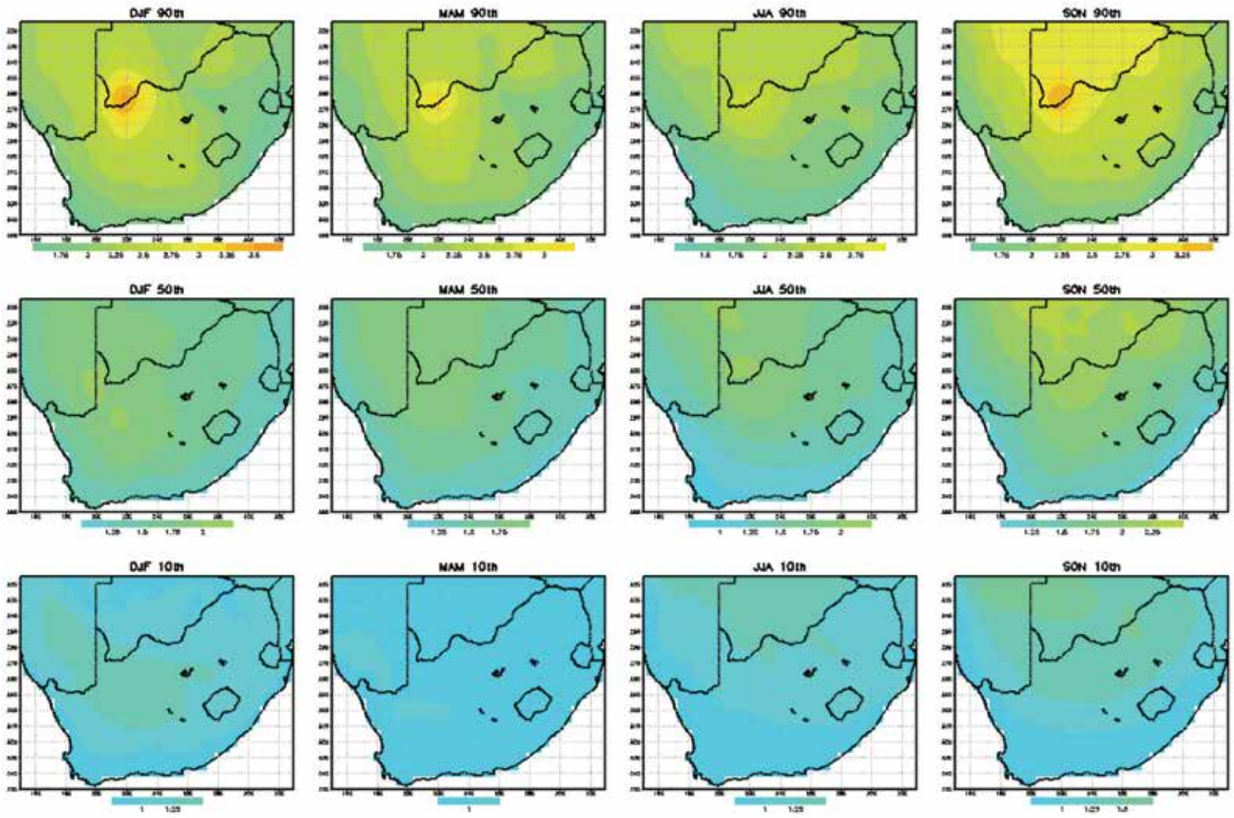

Figure 47. Projected change in the average seasonal minimum temperatures (°C) over South Africa for JJA, SON, DJF and MAM, for the period 2040–2060 relative to 1971–2005. The 90th percentile (upper panels), median (middle panels) and 10th percentile (lower panels) are shown for an ensemble of downscalings of ten CGCM projections, for each of the seasons. The downscalings were generated using the CSAG statistical downscaling procedure. All the CGCM projections contributed to CMIP5 and AR5 of the IPCC, and are for RCP4.5.

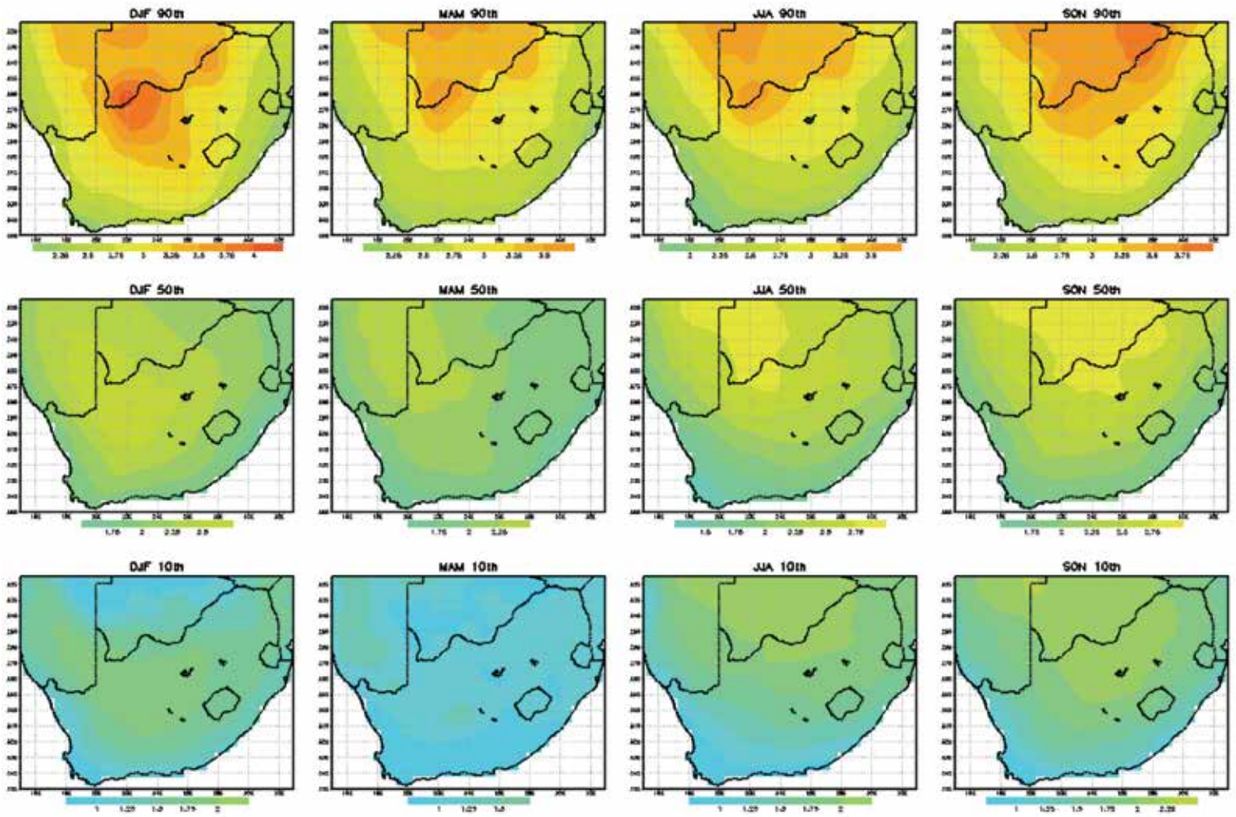

Figure 48. Projected change in the average seasonal minimum temperatures (°C) over South Africa for JJA, SON, DJF and MAM, for the period 2075–2095 relative to 1971–2005. The 90th percentile (upper panels), median (middle panels) and 10th percentile (lower panels) are shown for an ensemble of downscalings of ten CGCM projections, for each of the seasons. The downscalings were generated using the CSAG statistical downscaling procedure. All the CGCM projections contributed to CMIP5 and AR5 of the IPCC, and are for RCP4.5.

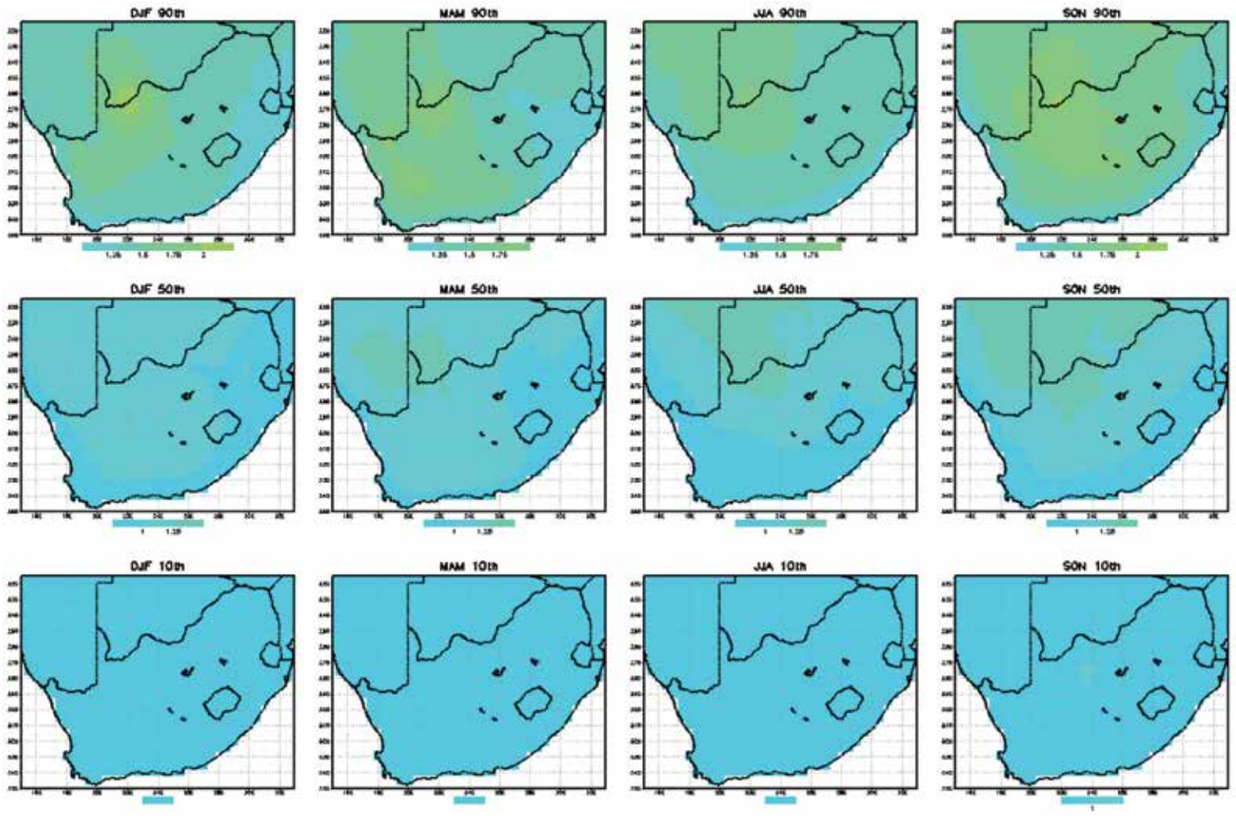

Figure 49. Projected change in the average seasonal maximum temperatures (°C) over South Africa for JJA, SON, DJF and MAM, for the period 2015–2035 relative to 1971–2005. The 90th percentile (upper panels), median (middle panels) and 10th percentile (lower panels) are shown for an ensemble of downscalings of ten CGCM projections, for each of the seasons. The downscalings were generated using the CSAG statistical downscaling procedure. All the CGCM projections contributed to CMIP5 and AR5 of the IPCC, and are for RCP4.5.

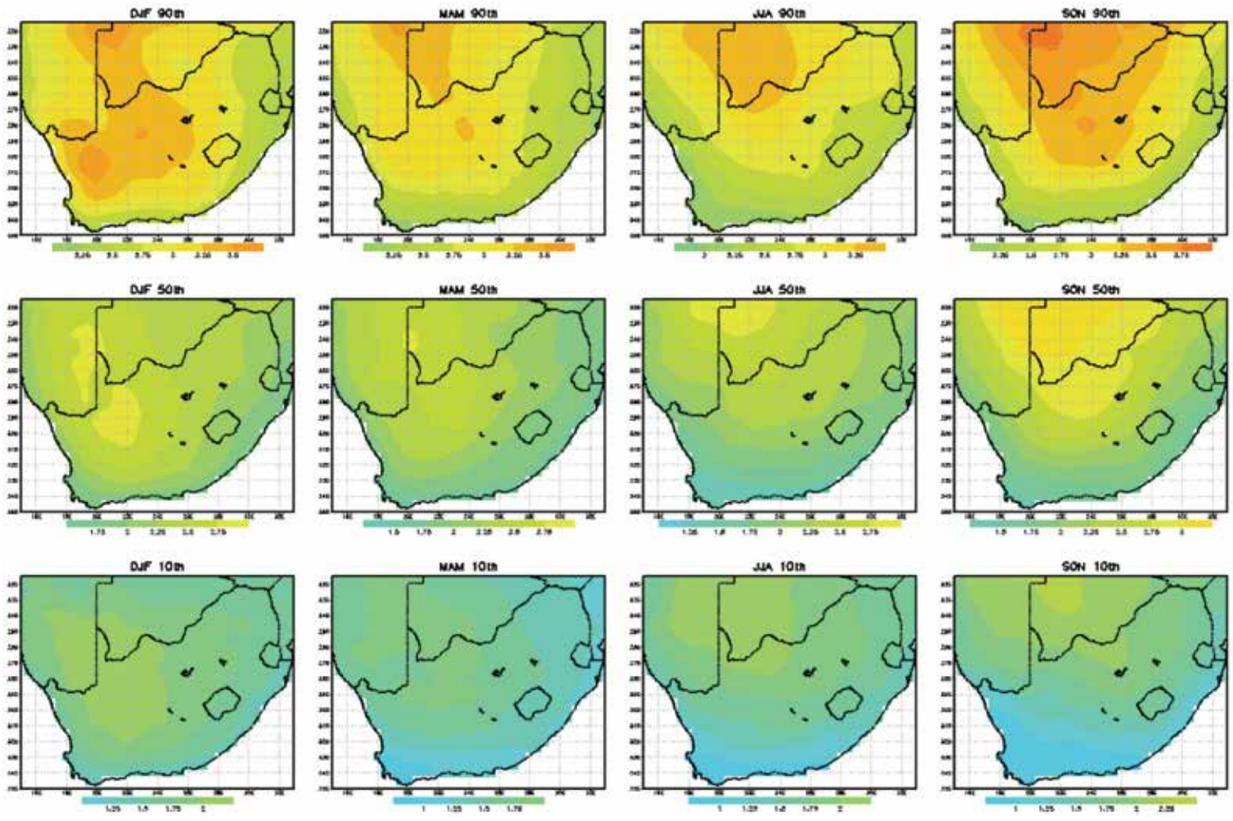

Figure 50. Projected change in the average seasonal maximum temperatures (°C) over South Africa for JJA, SON, DJF and MAM, for the period 2040–2060 relative to 1971–2005. The 90th percentile (upper panels), median (middle panels) and 10th percentile (lower panels) are shown for an ensemble of downscalings of ten CGCM projections, for each of the seasons. The downscalings were generated using the CSAG statistical downscaling procedure. All the CGCM projections contributed to CMIP5 and AR5 of the IPCC, and are for RCP4.5.

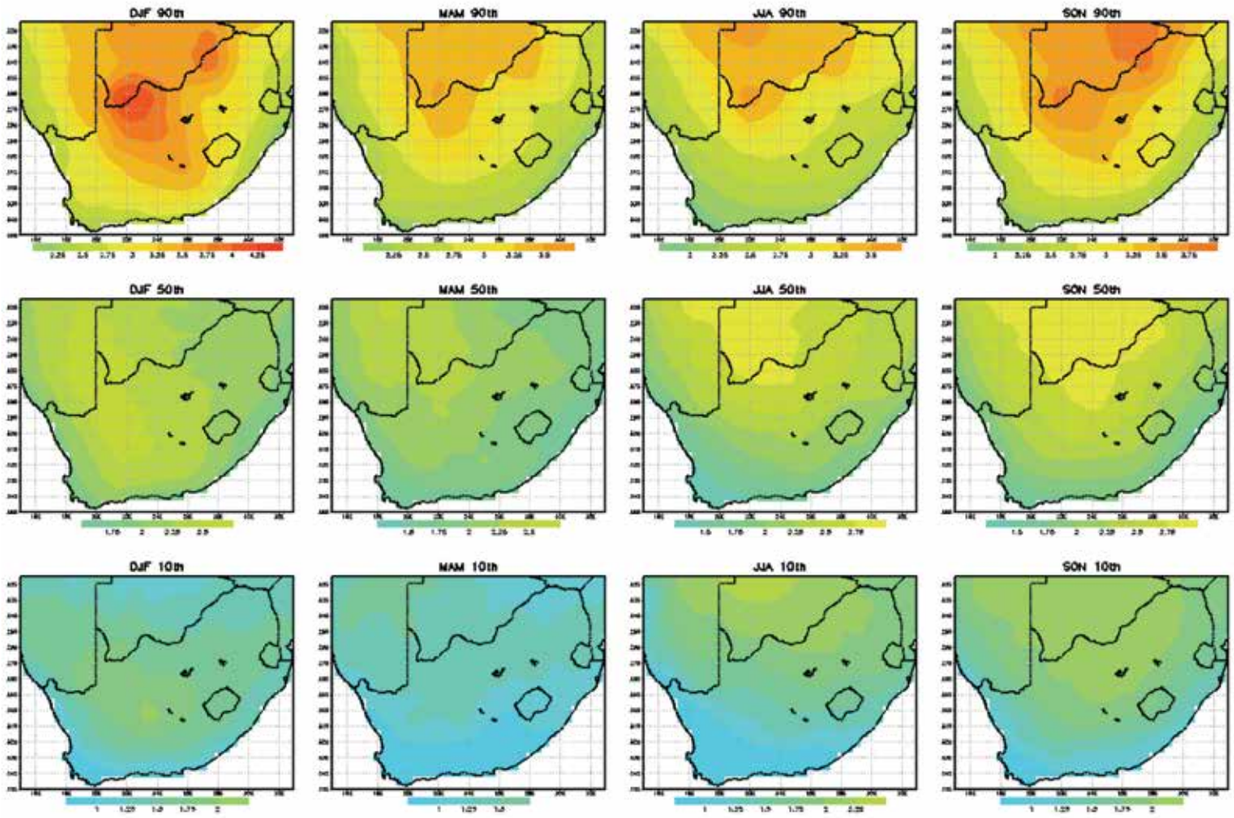

Figure 51. Projected change in the average seasonal maximum temperatures (°C) over South Africa for JJA, SON, DJF and MAM, for the period 2075–2095 relative to 1971–2005. The 90th percentile (upper panels), median (middle panels) and 10th percentile (lower panels) are shown for an ensemble of downscalings of ten CGCM projections, for each of the seasons. The downscalings were generated using the CSAG statistical downscaling procedure. All the CGCM projections contributed to CMIP5 and AR5 of the IPCC, and are for RCP4.5.

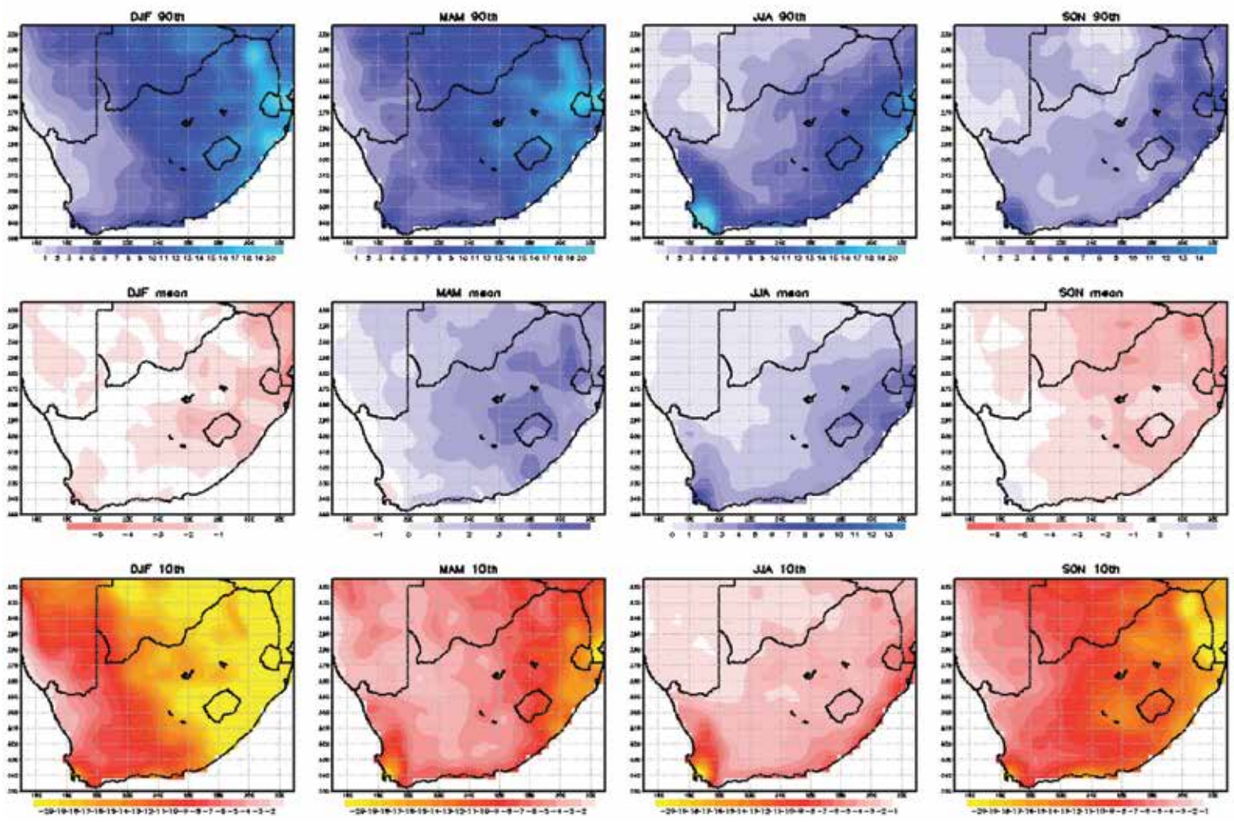

Figure 52. Projected change in the average seasonal rainfall (mm) over South Africa for DJF, MAM, JJA and SON, for the period 2015–2035 relative to 1971–2005. The 90th percentile (upper panels), median (middle panels) and 10th percentile (lower panels) are shown for an ensemble of downscalings of ten CGCM projections, for each of the seasons. The downscalings were generated using the CSAG statistical downscaling procedure. All the CGCM projections contributed to CMIP5 and AR5 of the IPCC, and are for RCP4.5.

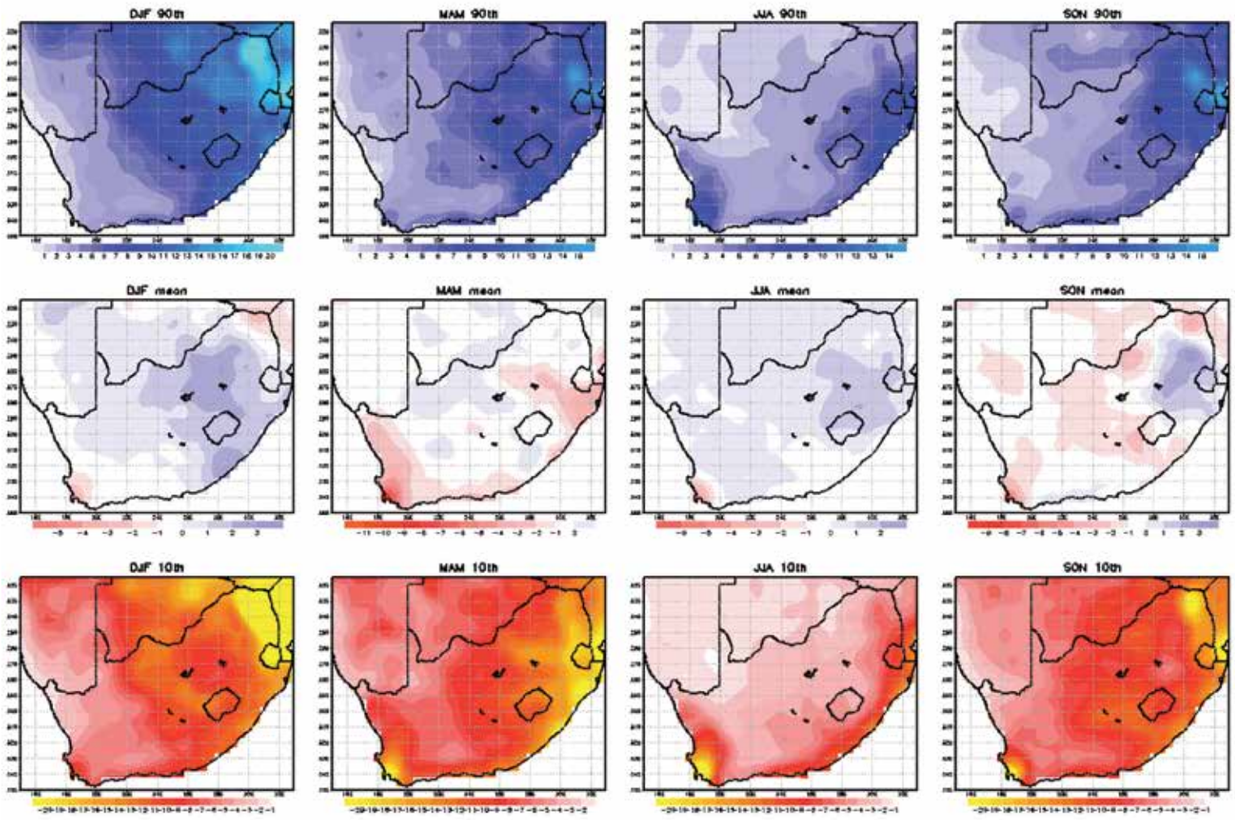

Figure 53. Projected change in the average seasonal rainfall (mm) over South Africa for DJF, MAM, JJA and SON, for the period 2040–2060 relative to 1971–2005. The 90th percentile (upper panels), median (middle panels) and 10th percentile (lower panels) are shown for an ensemble of downscalings of ten CGCM projections, for each of the seasons. The downscalings were generated using the CSAG statistical downscaling procedure. All the CGCM projections contributed to CMIP5 and AR5 of the IPCC, and are for RCP4.5.

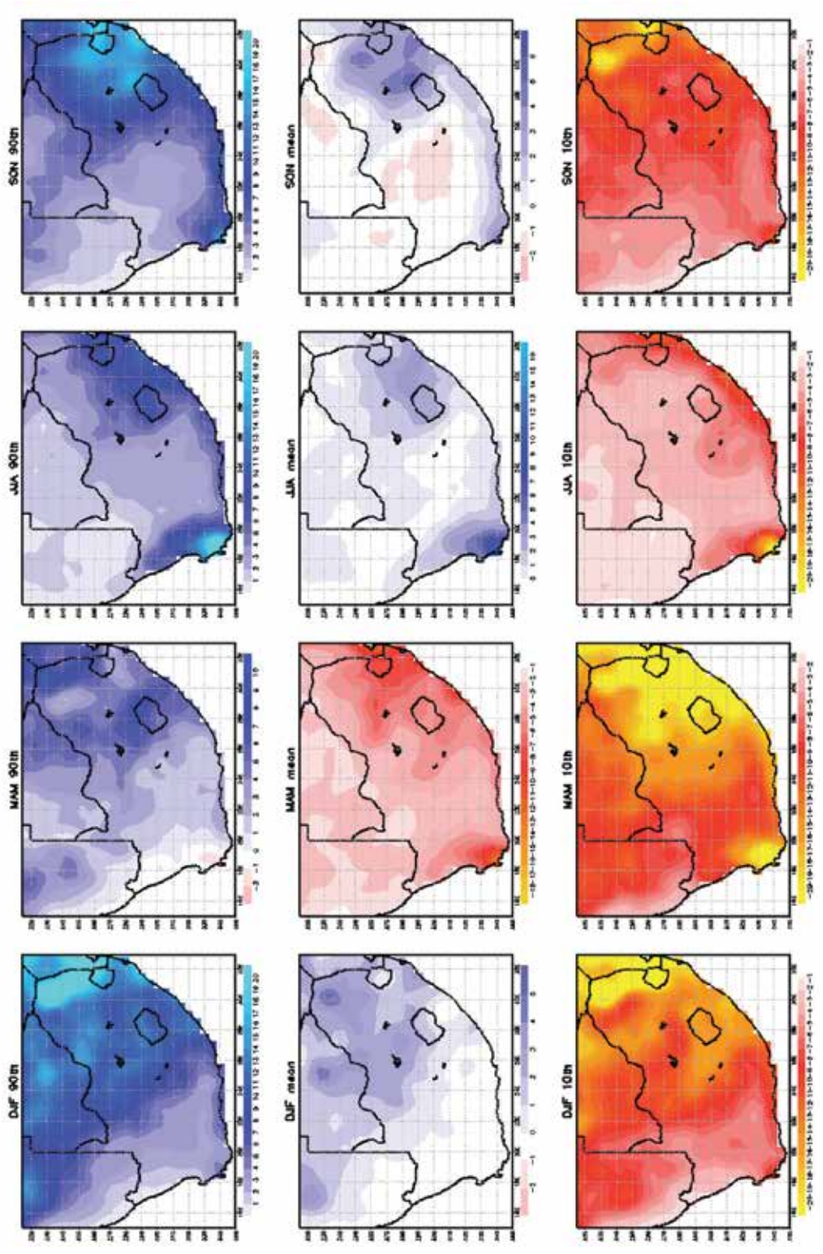

Figure 54. Projected change in the average seasonal rainfall (mm) over South Africa for DJF, MAM, JJA and SON, for the period 2075–2095 relative to 1971–2005. The 90th percentile (upper panels), median (middle panels) and 10th percentile (lower panels) are shown for an ensemble of downscalings of ten CGCM projections, for each of the seasons. The downscalings were generated using the CSAG statistical downscaling procedure. All the CGCM projections contributed to CMIP5 and AR5 of the IPCC, and are for RCP4.5.

4.4 CSAG statistical projections for RCP8.5

4.4.1 Temperature

The ensemble mean indicates that both minimum (Figure 55, Figure 56 and Figure 57) and maximum (Figure 58, Figure 59 and Figure 60) temperatures are plausible to rise by less than 1°C over the coastal areas, and by 1 to 2°C over the interior regions, for all seasons, by 2015–2035. The median of projected changes is less than 2.5°C for 2040–2060 over the interior, but exceeds 4°C for 2075–2095.

4.4.2 Rainfall

Projected changes in the average seasonal rainfall (mm) over South Africa for DJF, MAM, SON and JJA, for the periods 2015–2035, 2040–2060 and 2075–2095, relative to 1971–2005, are displayed in Figure 61, Figure 62 and Figure 63. The 90th percentile (upper panels), median (middle panels) and 10th percentile (lower panels) are shown for an ensemble of downscalings of ten CGCM projections, for each of the seasons and each of the time periods. The ensemble of projections is qualitatively similar for the three different future time periods. A largely mixed signal is projected for summer and autumn over the summer rainfall region, with rainfall decreases of more than 20 mm/month projected for these regions by some downscalings, whilst others project rainfall increases of the same magnitude. For the far-future, the projected rainfall signal seems to become somewhat better established, with the majority of ensemble members indicating rainfall increases during summer over the summer rainfall region, with decreases projected by most members for autumn. Most ensemble members indicate slight to significant increases in winter rainfall over the south-western Cape, although drying is also plausible. Increases in winter rainfall are also projected by most ensemble members over the east coast areas and the eastern escarpment. A largely mixed rainfall signal is projected for spring, ranging from significant increases to significant decreases, except for the far-future, when most ensemble members indicate increases in rainfall.

4.4.3 Key messages from the CSAG RCP8.5 projections

The ensemble mean indicates that both minimum and maximum temperatures could plausibly rise by less than 1°C over the coastal areas, and by 1 to 2°C over the interior regions, for all seasons, by 2015–2035 (Figure 55 and Figure 58). The median of projected changes is less than 2.5°C for 2040–2060 (Figure 56 and Figure 59) over the interior, but exceeds 4°C for 2075–2095 (Figure 60 and Figure 61).

For far-future rainfall, the RCP8.5 projections are qualitatively the same as the RCP4.5 projections:

Most ensemble members project moderate to significant rainfall increases for winter and spring of the far-future over the south-western Cape, extending to the Cape south coast. This signal is not present in the median of projections for the near- and mid-futures, when projections range from very dry to very wet for these regions. Even for the far-future, a smaller number of ensemble members indicate that a significantly drier future is also plausible over the south-western Cape and Cape south coast.

For winter, spring and summer, most ensemble members project rainfall increases over eastern south Africa for the far-future. This signal is particularly strong for summer. However, significant drying is also indicated to be plausible in the east, for all three seasons. Autumn in the far-future is projected to become drier by most ensemble members. For the near- and mid-futures, these patterns are not so well developed, and the projections indicate in general a mixed signal of wetter or drier conditions.

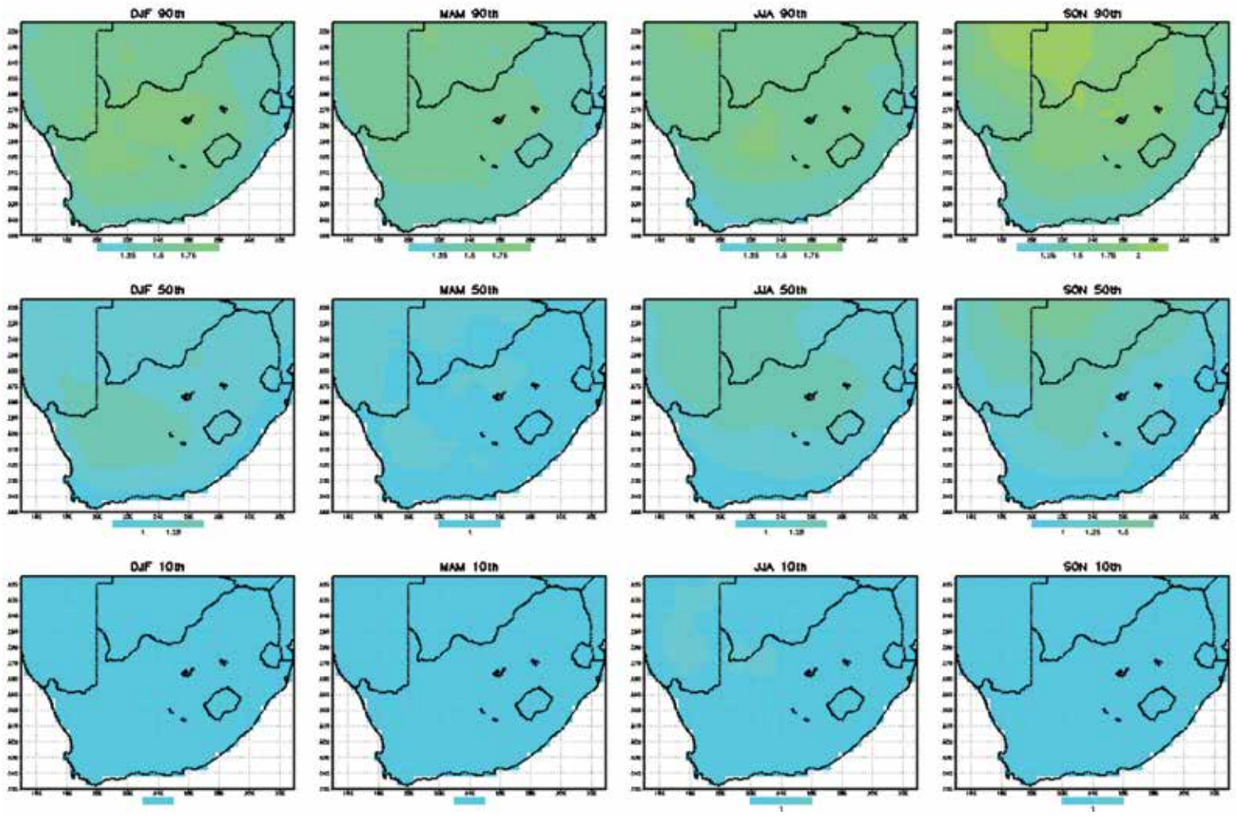

Figure 55. Projected change in the average seasonal minimum temperatures (°C) over South Africa for JJA, SON, DJF and MAM, for the period 2015–2035 relative to 1971–2005. The 90th percentile (upper panels), median (middle panels) and 10th percentile (lower panels) are shown for an ensemble of downscalings of ten CGCM projections, for each of the seasons. The downscalings were generated using the CSAG statistical downscaling procedure. All the CGCM projections contributed to CMIP5 and AR5 of the IPCC, and are for RCP8.5.

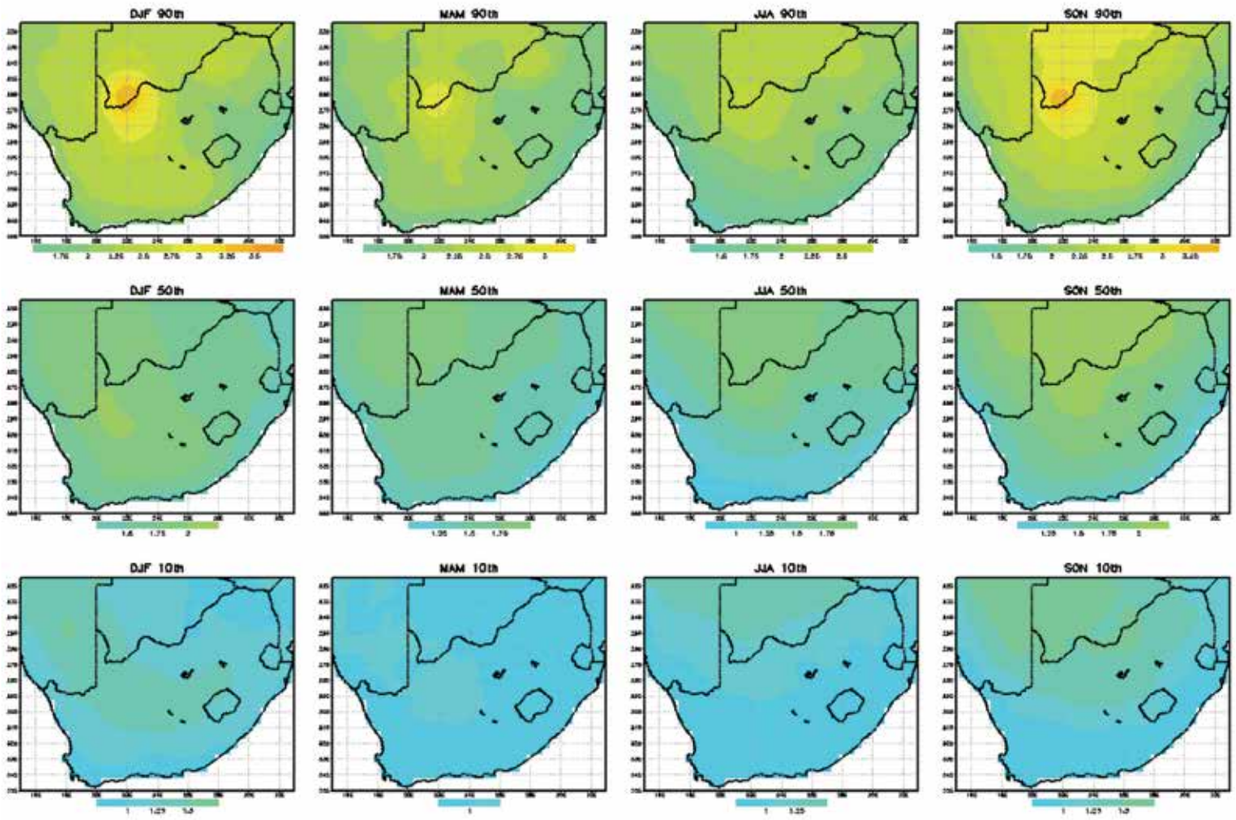

Figure 56. Projected change in the average seasonal minimum temperatures (°C) over South Africa for JJA, SON, DJF and MAM, for the period 2040–2060 relative to 1971–2005. The 90th percentile (upper panels), median (middle panels) and 10th percentile (lower panels) are shown for an ensemble of downscalings of ten CGCM projections, for each of the seasons. The downscalings were generated using the CSAG statistical downscaling procedure. All the CGCM projections contributed to CMIP5 and AR5 of the IPCC, and are for RCP8.5.

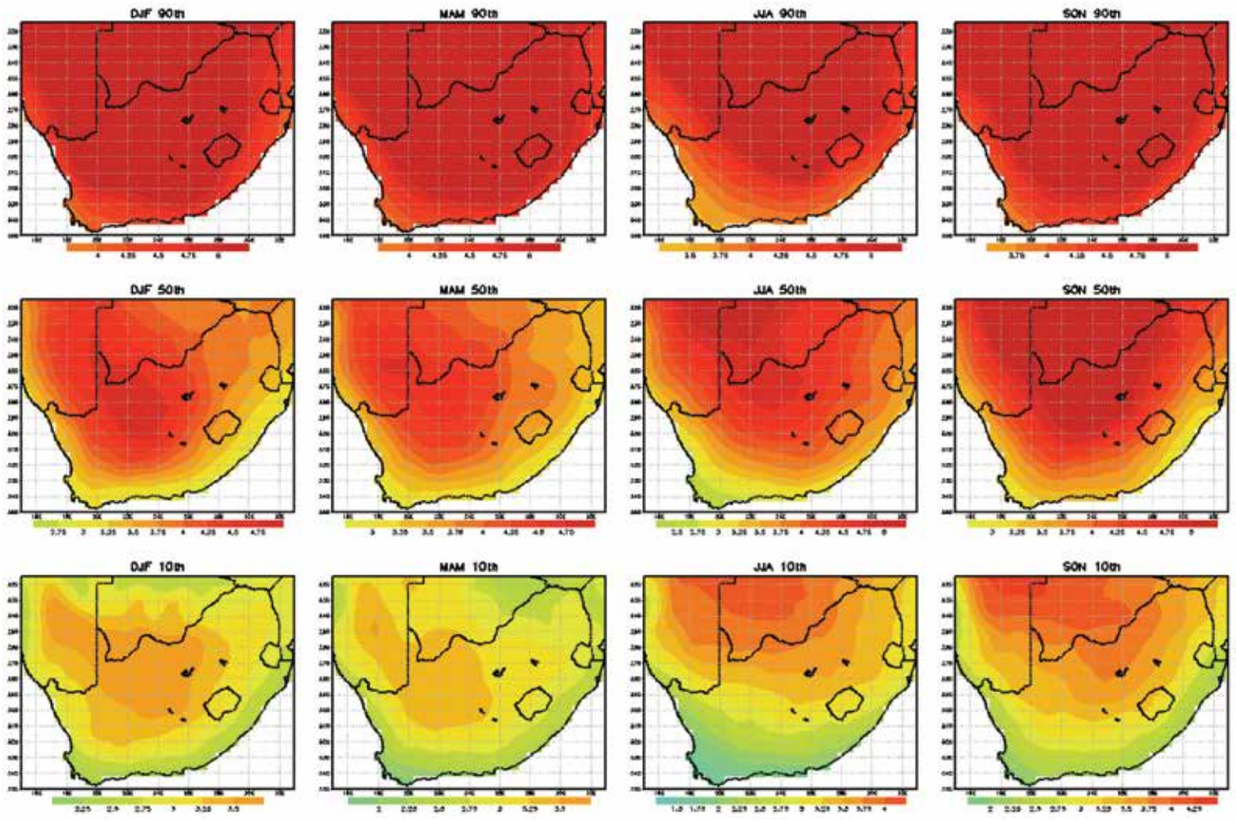

Figure 57. Projected change in the average seasonal minimum temperatures (°C) over South Africa for JJA, SON, DJF and MAM, for the period 2075–2095 relative to 1971–2005. The 90th percentile (upper panels), median (middle panels) and 10th percentile (lower panels) are shown for an ensemble of downscalings of ten CGCM projections, for each of the seasons. The downscalings were generated using the CSAG statistical downscaling procedure. All the CGCM projections contributed to CMIP5 and AR5 of the IPCC, and are for RCP8.5.

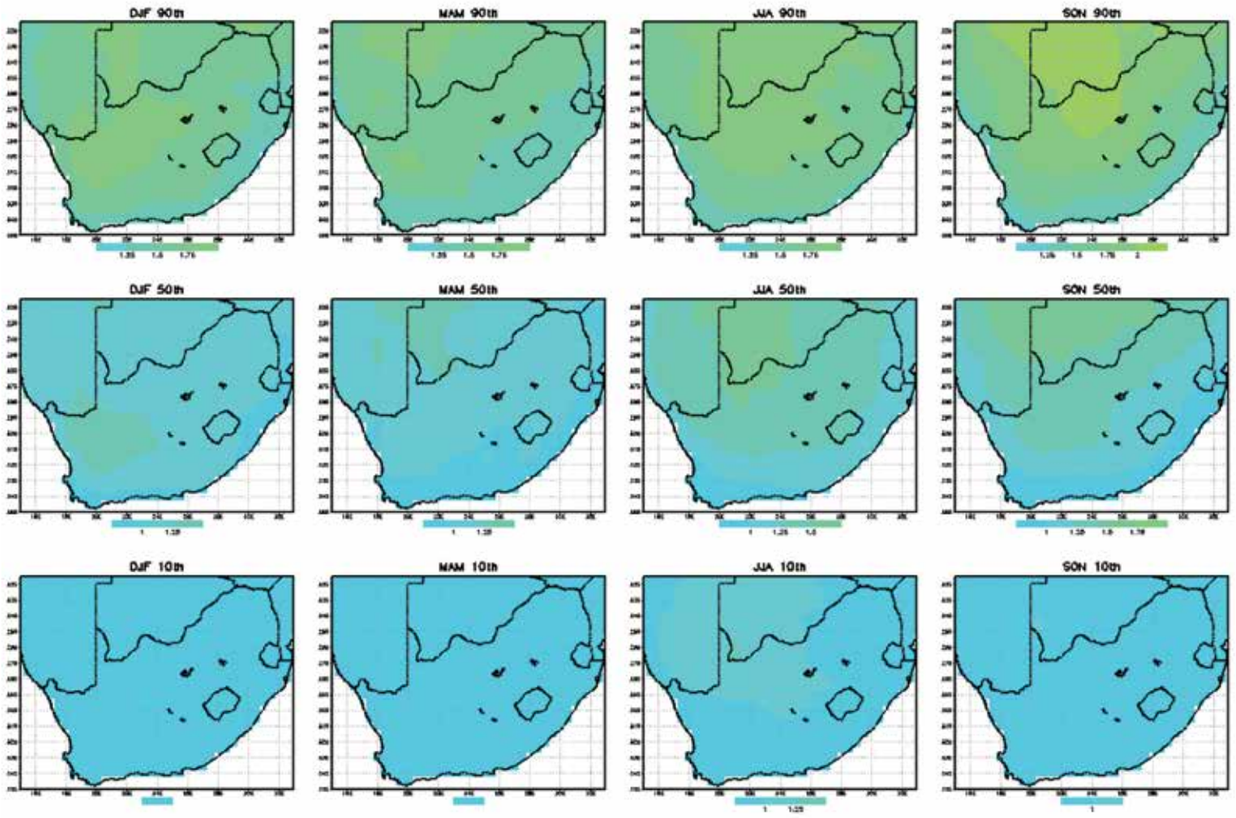

Figure 58. Projected change in the average seasonal maximum temperatures (°C) over South Africa for JJA, SON, DJF and MAM, for the period 2015–2035 relative to 1971–2005. The 90th percentile (upper panels), median (middle panels) and 10th percentile (lower panels) are shown for an ensemble of downscalings of ten CGCM projections, for each of the seasons. The downscalings were generated using the CSAG statistical downscaling procedure. All the CGCM projections contributed to CMIP5 and AR5 of the IPCC, and are for RCP8.5.

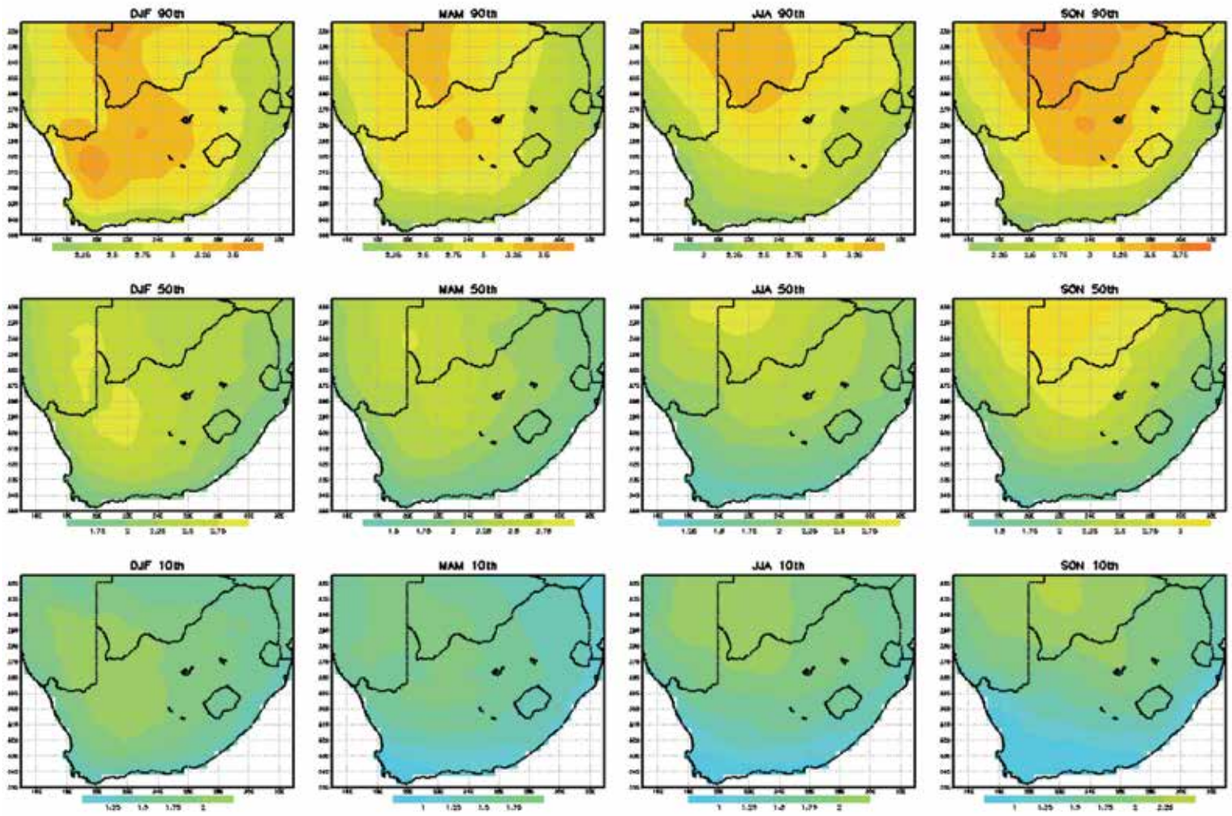

Figure 59. Projected change in the average seasonal maximum temperatures (°C) over South Africa for JJA, SON, DJF and MAM, for the period 2040–2060 relative to 1971–2005. The 90th percentile (upper panels), median (middle panels) and 10th percentile (lower panels) are shown for an ensemble of downscalings of ten CGCM projections, for each of the seasons. The downscalings were generated using the CSAG statistical downscaling procedure. All the CGCM projections contributed to CMIP5 and AR5 of the IPCC, and are for RCP8.5.

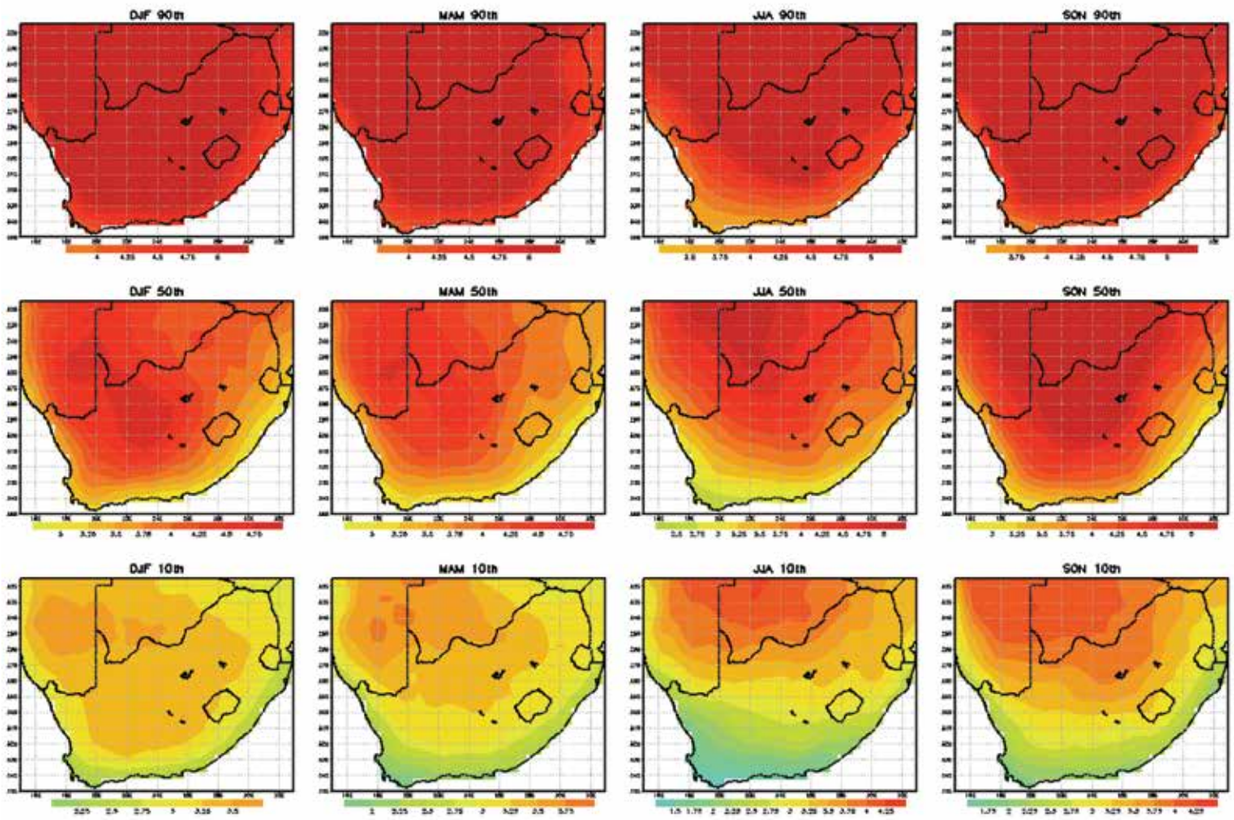

Figure 60. Projected change in the average seasonal maximum temperatures (°C) over South Africa for JJA, SON, DJF and MAM, for the period 2075–2095 relative to 1971–2005. The 90th percentile (upper panels), median (middle panels) and 10th percentile (lower panels) are shown for an ensemble of downscalings of ten CGCM projections, for each of the seasons. The downscalings were generated using the CSAG statistical downscaling procedure. All the CGCM projections contributed to CMIP5 and AR5 of the IPCC, and are for RCP8.5.

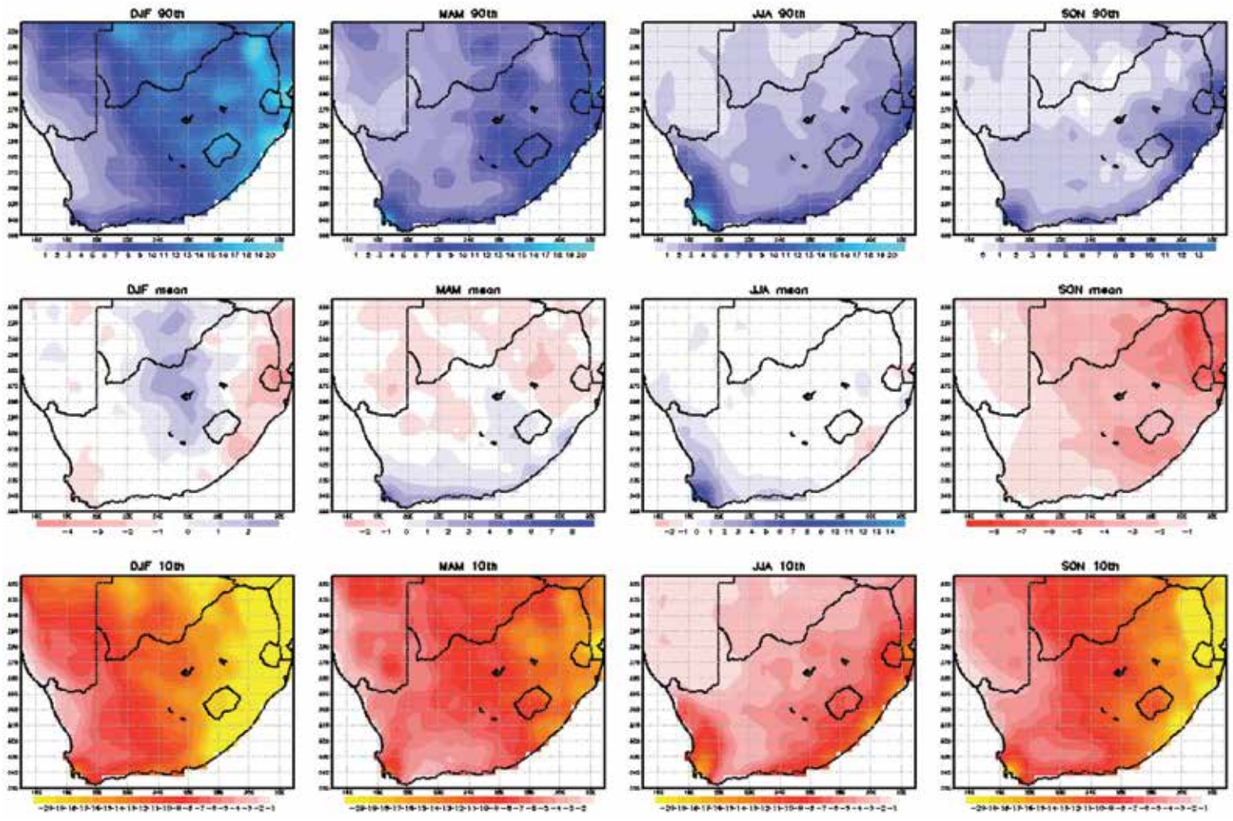

Figure 61. Projected change in the average seasonal rainfall (mm) over South Africa for DJF, MAM, JJA and SON, for the period 2015–2035 relative to 1971–2005. The 90th percentile (upper panels), median (middle panels) and 10th percentile (lower panels) are shown for an ensemble of downscalings of ten CGCM projections, for each of the seasons. The downscalings were generated using the CSAG statistical downscaling procedure. All the CGCM projections contributed to CMIP5 and AR5 of the IPCC, and are for RCP8.5.

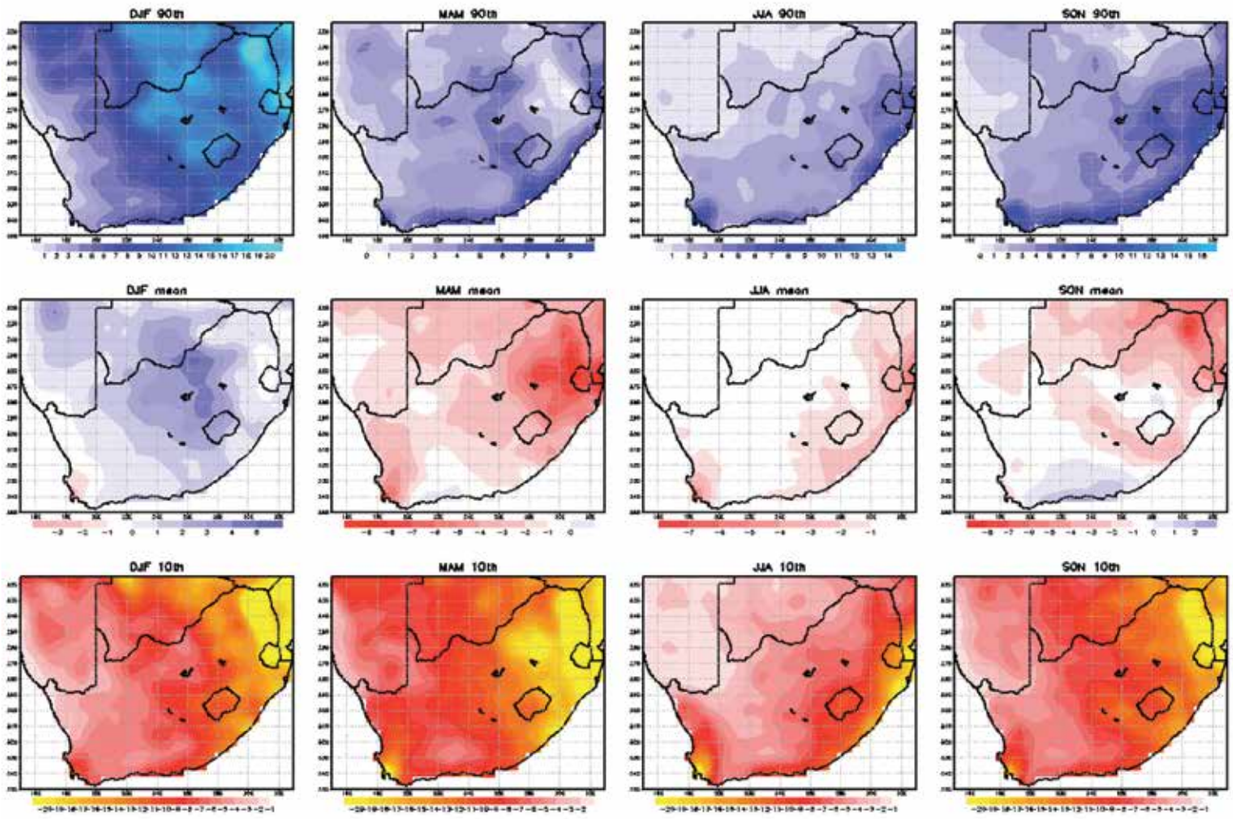

Figure 62. Projected change in the average seasonal rainfall (mm) over South Africa for DJF, MAM, JJA and SON, for the period 2040–2060 relative to 1971–2005. The 90th percentile (upper panels), median (middle panels) and 10th percentile (lower panels) are shown for an ensemble of downscalings of ten CGCM projections, for each of the seasons. The downscalings were generated using the CSAG statistical downscaling procedure. All the CGCM projections contributed to CMIP5 and AR5 of the IPCC, and are for RCP8.5.

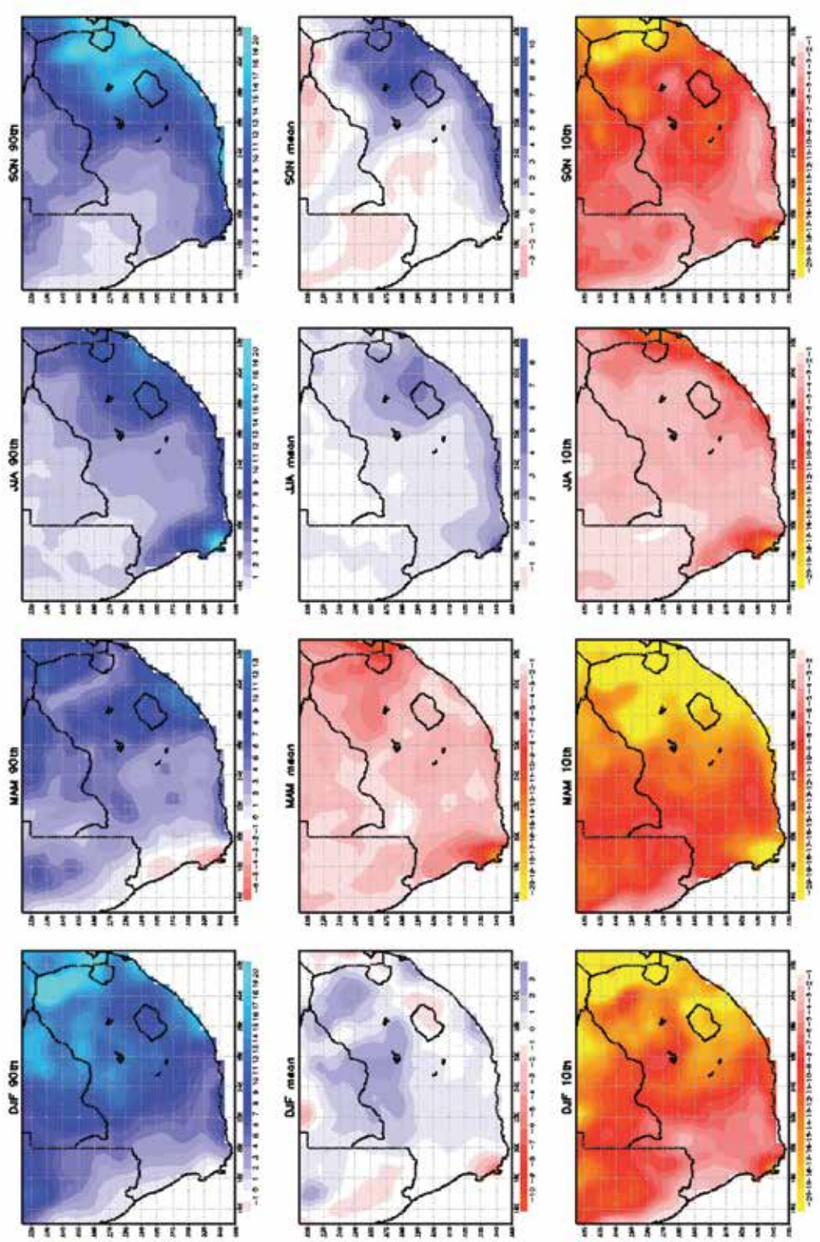

Figure 63. Projected change in the average seasonal rainfall (mm) over South Africa for DJF, MAM, JJA and SON, for the period 2075–2095 relative to 1971–2005. The 90th percentile (upper panels), median (middle panels) and 10th percentile (lower panels) are shown for an ensemble of downscalings of ten CGCM projections, for each of the seasons. The downscalings were generated using the CSAG statistical downscaling procedure. All the CGCM projections contributed to CMIP5 and AR5 of the IPCC, and are for RCP8.5.

5. DYNAMICALLY DOWNSCALED PROJECTIONS

The dynamic regional climate model applied within LTAS for projecting southern Africa's climate futures is a variable-resolution global atmospheric model, the conformal-cubic atmospheric model (CCAM) (McGregor, 2005). It has been shown that CCAM may be used to obtain plausible projections of future climate change, as well as skilful forecasts at the seasonal and short-range timescales, over the southern African region (Engelbrecht et al. 2009, Engelbrecht et al. 2011; Malherbe et al., 2013). It also realistically simulates observed daily climate statistics over the region, such as the number frequency of extreme precipitation events and the tracks of cut-off lows and tropical cyclones (Engelbrecht et al., 2012; Malherbe et al., 2013). The model has also been applied for simulations of current climatic conditions at spatial scales from global to very small scale at high (1 km) resolution (Engelbrecht et al., 2011). Application of the simulation model at the shorter timescales has allowed testing of its capability to represent fundamental forcing mechanisms (including drivers of decadal variability such as the ENSO). The performance of this modelling approach across "verifiable" timescales, and across multiple spatial scales, enhances the confidence in its ability to produce credible model projections of future climate change. The major drawback of this approach is, however, technical – compared to the statistical downscaling methods it requires considerably more computing power to perform simulations, and these take several weeks to months in some cases to complete. For this reason, the LTAS approach has been making use of collaborative work between the Council for Scientific and Industrial Research (CSIR) in South Africa and the Commonwealth Scientific and Industrial Research Organisation (CSIRO) in Australia, in order to provide the latest simulations using RCP4.5 and 8.5 Wm^{-2} emissions scenarios. It is expected that an ensemble of RCP downscalings of increasing size will become available over the next few months as an outcome of this collaboration. All the CSIR simulations described here have been performed on the computer clusters of the Centre for High Performance Computing (CHPC) in South Africa.

The LTAS is currently able to report on the scenarios generated by this approach using the SRES A2 emissions scenario, which is a relatively high end emissions scenario developed under the AR4, and the 8.5 Wm^{-2} RCP of AR5 – an even more negative scenario of continued strong growth in emissions. For the A2 scenario the Geophysical Fluid Dynamics Laboratory Coupled Model, version 2.0 (GFDL-CM2.0); the GFDL-CM2.1; the Max Planck Institute for Meteorology ECHAM5/MPI-Ocean coupled climate model; the United Kingdom Met Office, Hadley Centre coupled model, version 3 (UKMO-HadCM3); the Model for Interdisciplinary Research on Climate, medium resolution (MIROC3.2-medres); and the CSIRO Mark3.5 CGCMs were downscaled (see Engelbecht et al. (2011) and Malherbe et al. (2013) for more details). A multiple nudging procedure was followed, using the sea-ice and bias-corrected sea-surface temperatures (SSTs) of the CGCMs to first drive 200 km quasi-uniform resolution global simulations of CCAM, followed by subsequent downscaling of the simulations to 50 km resolution over southern Africa (Engelbrecht et al., 2011).

The CGCMs downscaled from the Coupled Model Intercomparison Project Phase 5 (CMIP5) (AR5) include the Australian Community Climate and Earth System Simulator (ACCESS1-0); the Geophysical Fluid Dynamics Laboratory Coupled Model (GFDL-CM3); the National Centre for Meteorological Research Coupled Global Climate Model, version 5 (CNRM-CM5); the Max Planck Institute Coupled Earth System Model (MPI-ESM-LR); the Model for Interdisciplinary Research on Climate (MIROC4h); the Norwegian Earth System Model (NorESM1-M); the Community Climate System Model (CCSM4); the Meteorological Research Institute Global Climate Model (MRI-GCM3); and the Institute Piere Simon Laplace Climate Modelling Centre Coupled Model (IPSL-CM5A-MR). Results from the downscaling of the first three of these CGCMs are presented here. For the RCP CGCMs, the downscaling involves using the sea-ice concentrations and bias-corrected sea-surface temperatures of the CGCMs, to force very high resolution

CCAM simulations performed globally, at a quasi-uniform resolution of approximately 50 km. The integrations use RCPs 4.5 and 8.5 of the IPCC AR5 and will contribute to the Coordinated Regional Downscaling Experiment (CORDEX). In these simulations, CCAM is integrated /coupled to the CSIRO Atmosphere Biosphere Land Exchange (CABLE) model, a dynamic land-surface model with the capability to interactively simulate the carbon flux between the land-surface and atmosphere. The monthly simulated climatologies for rainfall and temperature, of the CCAM A2 scenarios performed at the CSIR for the period 1961–1990, were bias-corrected using observed climatologies of the CRU TS3.1 data set of the Climatic Research Unit (CRU), before the projected climate-change signals were calculated.

5.1 CCAM projections for the A2 emission scenario

5.1.1 Temperature

Rapid rises in the annual average near-surface temperature are projected to occur over southern Africa during the 21st century, in the CCAM downscalings. The projected changes are shown in Figure 64 for the future time-periods 2015–2035 (near-future), 2040–2060 (mid-future) and 2080–2100 (far-future), relative to the baseline period 1971–2005. For each time period, the 10th, 50th (median) and 90th percentiles are shown, for the ensemble of projected changes. For the near-future, temperature increases of less than 1°C are projected by most ensemble members, with the 90th percentile of the projected changes indicating temperature increases of more than 1°C, but less than 2°C. For the period 2040–2060, annual average temperatures are projected to rise by 2.5 to 3.5°C over most of the interior, relative to the baseline period. Over the southern interior and coastal areas, temperature increases of less than 2.5°C are projected. Drastic increases in average annual temperatures are projected for the far-future period. Increases of more than 3.5°C are projected for all interior regions across the ensemble, with most ensemble members projecting increases of more than 4°C over the central and northern interior. More moderate increases, of between 2.5 and 3.5°C, are projected by most ensemble members for the coastal areas. Generally, the pattern and amplitude of projected temperature increases shows close correspondence across the different ensemble members, indicating that the projected signal is robust.

Average temperatures for the projected changes in winter (June to August, JJA), spring (September to November, SON), summer (December to February, DJF) and autumn (March to May, MAM) are displayed for the various time periods in Figure 65, Figure 66 and Figure 67. For each season within each time period, the 10th, 50th (median) and 90th percentiles of the projected changes are shown. For the near-future period of 2015–2035, the projected temperature signal is similar across the different seasons (Figure 65). Most ensemble members project increases of less than 1°C for all seasons, with the 90th percentile indicating increases of more than 1 but less than 2°C. Winter and spring is projected to warm somewhat less than summer and autumn. For all seasons, warming of between 2.5 and 3.5°C are projected for the northern interior regions, for the period 2040–2060. The southern interior and coastal regions are projected to warm by less than 2.5°C for this period, relative to the baseline. Winter is projected to warm somewhat more than the other seasons. The majority of ensemble members indicate warming of more than 4.5°C over the northern interior, for autumn and winter of 2080–2100 (Figure 67), relative to the baseline. Warming of more than 4°C is projected for the central interior, with somewhat smaller rises projected for the southern interior and coastal areas. Autumn and winter are the seasons that are projected to warm most.

5.1.2 Rainfall

The CCAM ensemble projects a diversity of plausible 21st century rainfall futures for South Africa. These are displayed in Figure 68 which shows the projected change in the average annual rainfall (mm) for the time periods 2015–2035, 2040–2060 and 2080–2100, relative to 1970–2005. The 10th percentile (left), median (middle) and 90th percentile (right) are shown for the ensemble of downscalings of six CGCM projections, for each of the time periods. Most ensemble members project the southern African region to become generally drier during the 21st century (Engelbrecht et al., 2011; Malherbe et al., 2013), in response to a general strengthening of the subtropical high-pressure belt over the region (Engelbrecht et al., 2009; Malherbe et al., 2013). The pattern of drying projected for Limpopo and southern Mozambique is also related to the northward displacement of tropical lows and cyclones in the simulations (Malherbe et al., 2013). For the ensemble members that do project general drying, the biggest rainfall reductions (for South Africa) are projected to occur over the south-western Cape and Limpopo province. The amplitude of the projected drying increases over time, and for the 2080–2100 time period rainfall decreases of more than 40 mm/year are projected for Limpopo and the south-western Cape. Despite the general pattern of drying, most ensemble members project increases in average annual rainfall over the central interior and south-eastern parts of more than 40 mm/year for the far-future in the median of projections. This pattern is related dynamically to the strengthening of the heat low over the western interior (e.g. Engelbrecht et al., 2009), which is conducive to thunderstorm formation to the east of the trough axis.

Projected changes in the average seasonal rainfall (mm) over South Africa for JJA, SON, DJF and MAM, for the periods 2015–2035, 2040–2060 and 2080–2100, relative to 1971–2005, are displayed in Figure 69, Figure 70 and Figure 71. The 10th percentile (left), median (middle) and 90th percentile (right) are shown for an ensemble of downscalings of six CGCM projections, for each of the seasons and each of the time periods. For the near-future, only slight and physically insignificant changes in rainfall are projected for the winter months over the summer rainfall region. For the winter rainfall region of the south-western Cape, most downscalings indicate drier conditions for the near-future, although slight increases in rainfall are also plausible. The seasons spring to autumn are projected to become generally drier in the near-future by most ensemble members, although slight to moderate increases in rainfall are also plausible over the central interior. Physically significant decreases, of more than 30 mm/season, are plausible to occur in the near-future over Limpopo, for all of the seasons spring to autumn. Also noteworthy, are the physically significant rainfall decreases that are projected for the south-western Cape in spring and in autumn, in addition to the plausible rainfall decreases that are projected over this region for winter.

For the mid-future period, the patterns of projected rainfall changes are very similar to those of the near-future period for all seasons, and across the ensemble. The amplitudes of the projected changes are generally somewhat higher though, for the mid-future compared to the near-future. Most ensemble members project rainfall decreases for the south-western Cape, for all seasons. This pattern of drying is projected to extend to the all-year rainfall region of the Cape south coast. The summer rainfall region is projected to become generally drier, with relatively large decreases projected for Limpopo. The 90th percentile of the projections indicates that slight to moderate increases in rainfall are also plausible over the central interior.

These patterns of projected changes remain similar for the far-future, with further general increases in amplitude. Physically significant rainfall decreases are projected for the south-western Cape and Cape south coast for the important winter, spring and autumn periods. Strong drying is projected for Limpopo, for spring, summer and autumn. Moderate increases in rainfall are plausible over the central interior, extending to the south-eastern coastal areas, during spring and summer. The general pattern of drying is projected to be particularly uniform during autumn and winter. This has been shown to be consistent with a projected strengthening of mid-level anti-cyclones over southern Africa, and a strengthening of anti-cyclonic circulation to the south of the country, which occurs in conjunction with a southward displacement of the westerly wind regime (e.g. Engelbrecht et al., 2009; Malherbe et al., 2013).

5.1.3 Key messages from the ensemble of CCAM A2 SRES scenario projections

Temperature increases of more than 4°C are plausible under the A2 scenario, over the central and northern interior regions of South Africa, for the period 2080–2100 relative to the baseline period 1971–2005. Autumn and winter are the seasons that are projected to warm most.

Significant reductions in rainfall are plausible over Limpopo, already in the near-future, with the pattern of drying projected to increase over time. The projections of decreasing rainfall totals are consistent with projected increases in the occurrence of mid-level highs over the eastern parts of southern Africa, a strengthening of the Indian Ocean High to the southeast of the subcontinent, and an associated northward displacement of tropical lows and cyclones (Engelbrecht et al., 2009; Malherbe et al., 2013).

Strong drying is plausible over the south-western Cape in the near-future, amplifying in time, and extending to the Cape south coast. These changes are consistent with a projected southward displacement of the westerlies and cold fronts.

Moderate to strong increases in rainfall are plausible over the central interior of South Africa in the far-future, extending to the southeast coast. Slight to moderate rainfall increases are projected over these regions for the near and mid-futures. These rainfall increases are projected to occur in spring and summer, in association with a deepening of the heat low over the western interior (Engelbrecht et al., 2009).

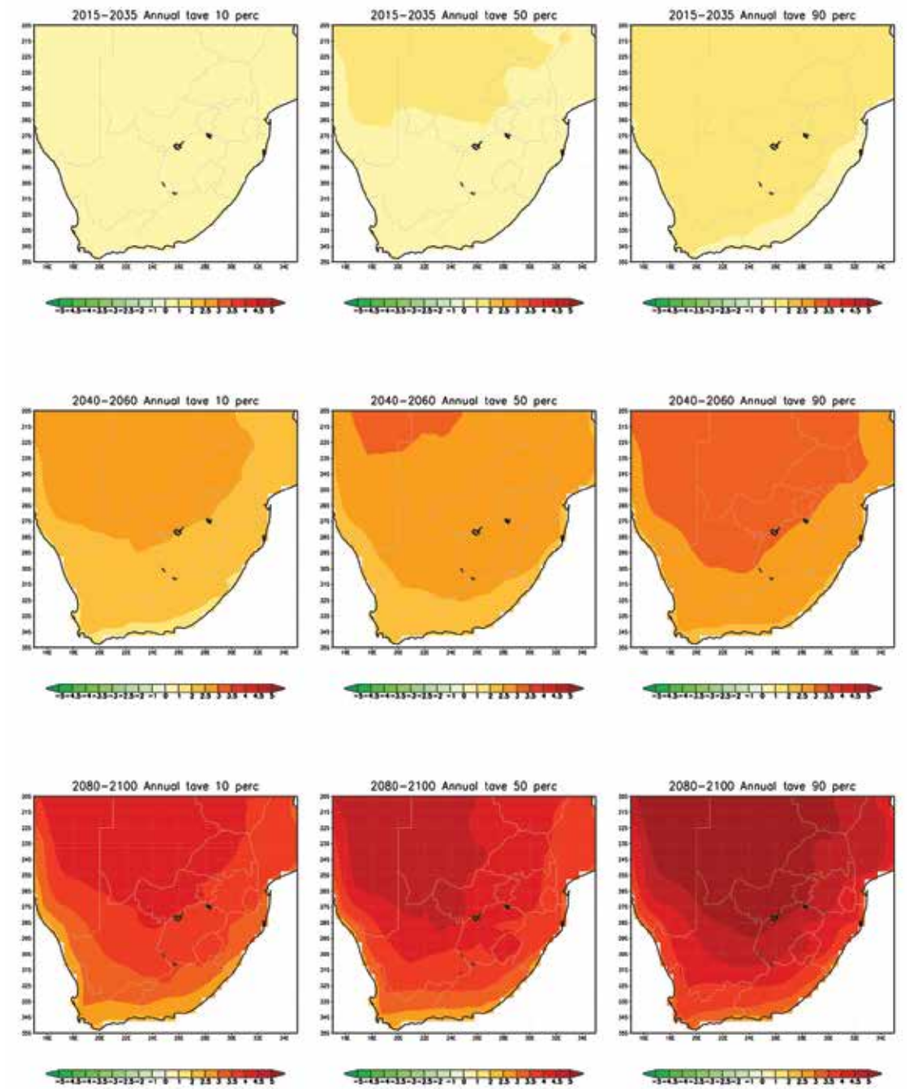

Figure 64. Projected change in the annual average temperature (°C) over South Africa, for the time periods 2015–2035, 2040–2060 and 2080–2100, relative to 1970–2005. The 10th percentile (left), median (middle) and 90th percentile (right) are shown for the ensemble of downscalings of six CGCM projections, for each of the time periods. The downscalings were performed using the regional model CCAM. All the CGCM projections contributed to CMIP3 and AR4 of the IPCC, and are for the A2 SRES scenario.

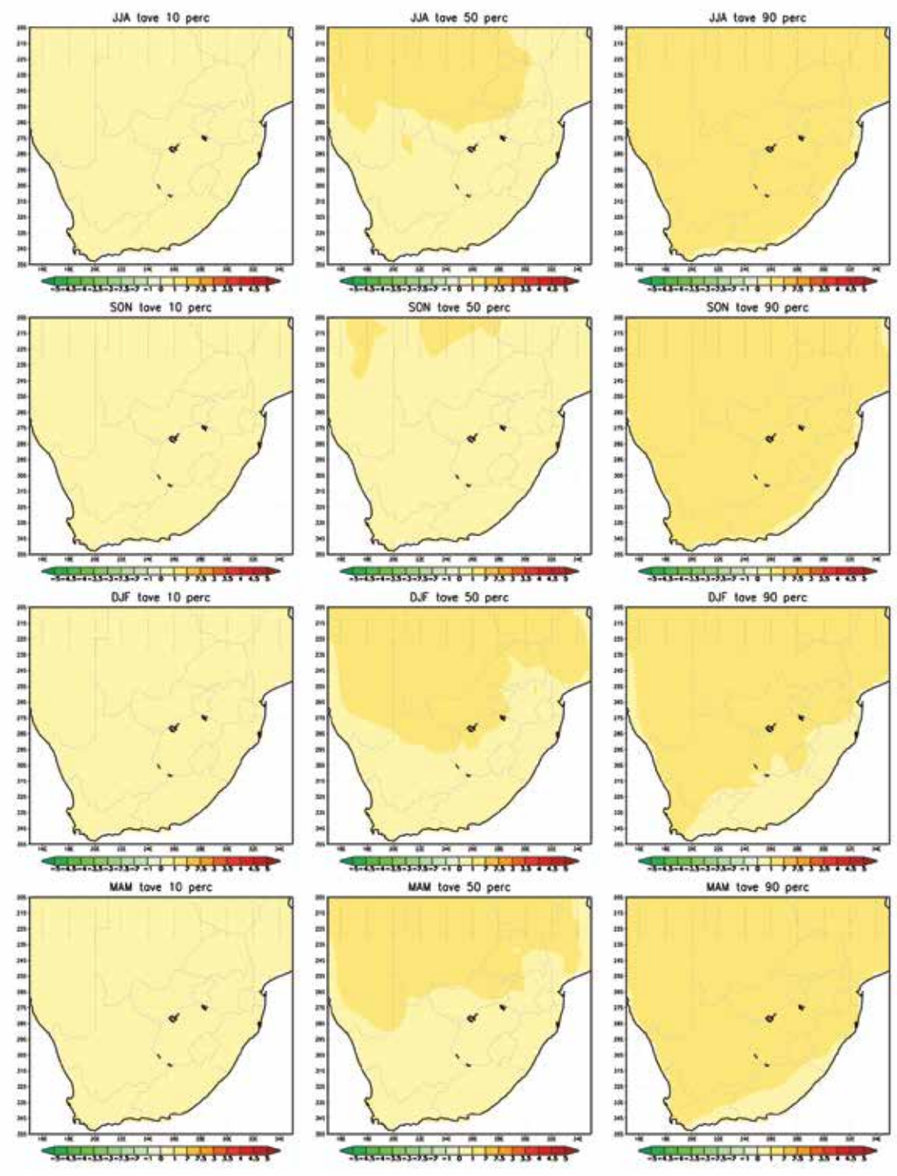

Figure 65. Projected change in the average seasonal temperatures (°C) over South Africa for JJA, SON, DJF and MAM, for the period 2015–2035 relative to 1971–2005. The 10th percentile (left), median (middle) and 90th percentile (right) are shown for an ensemble of downscalings of six CGCM projections, for each of the seasons. The downscalings were generated using the regional model CCAM. All the CGCM projections contributed to CMIP3 and AR4 of the IPCC, and are for the A2 SRES scenario.

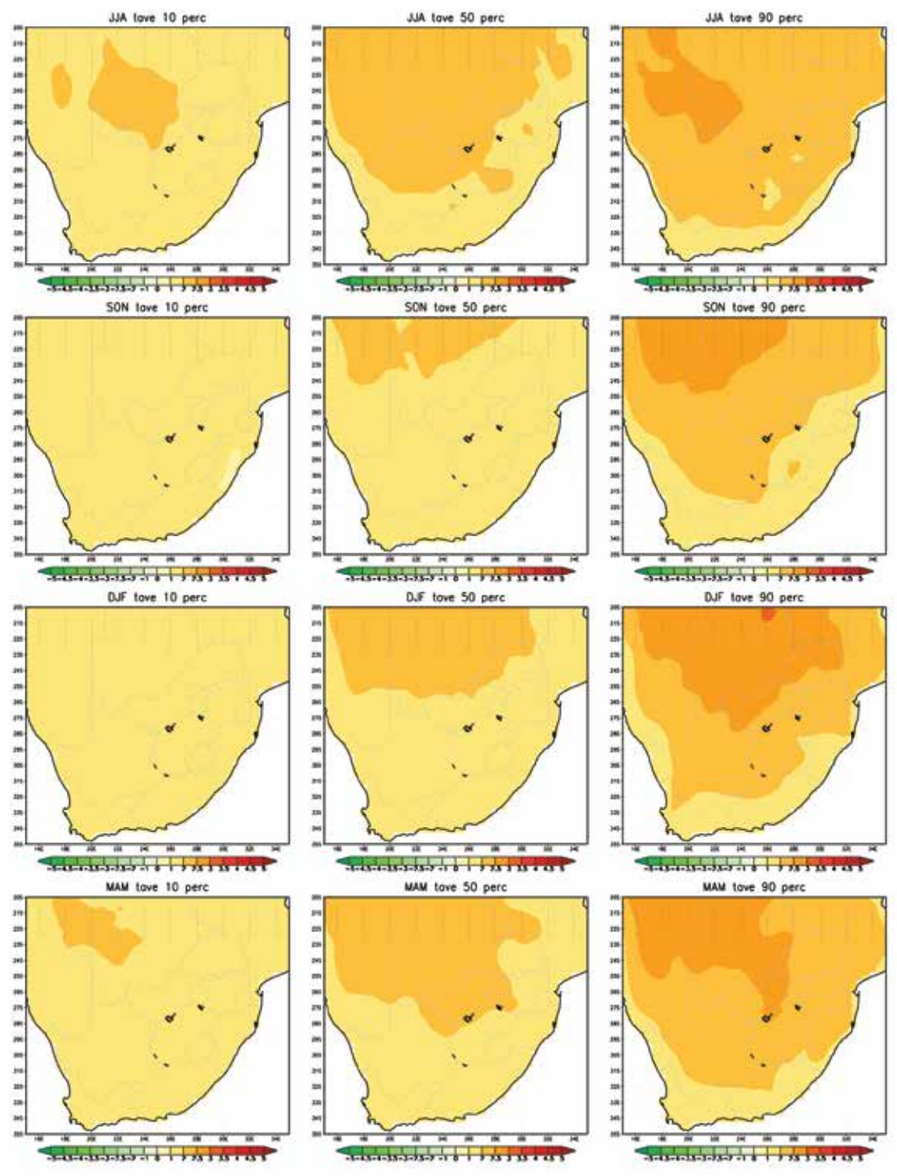

Figure 66. Projected change in the average seasonal temperatures (°C) over South Africa for JJA, SON, DJF and MAM, for the period 2040–2060 relative to 1971–2005. The 10th percentile (left), median (middle) and 90th percentile (right) are shown for an ensemble of downscalings of six CGCM projections, for each of the seasons. The downscalings were generated using the regional model CCAM. All the CGCM projections contributed to CMIP3 and AR4 of the IPCC, and are for the A2 SRES scenario.

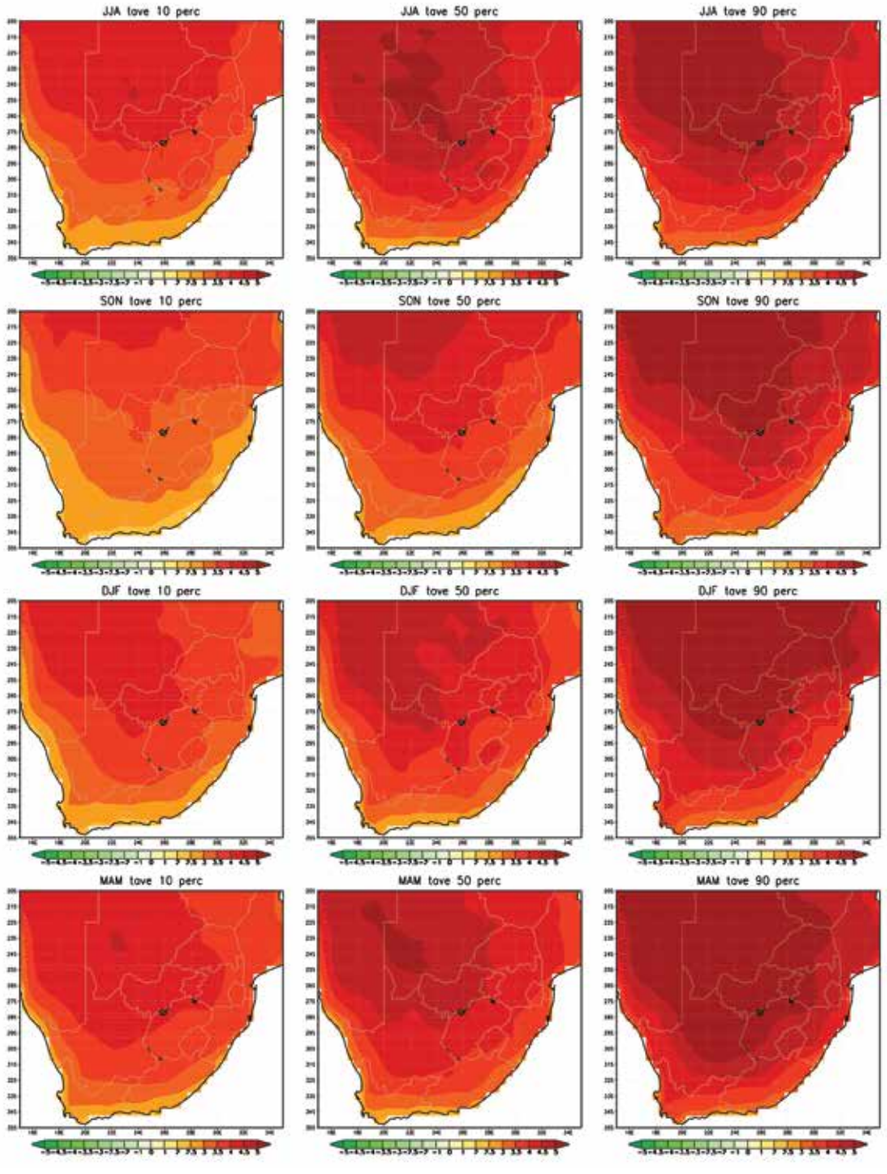

Figure 67. Projected change in the average seasonal temperatures (°C) over South Africa for JJA, SON, DJF and MAM, for the period 2080–2100 relative to 1971–2005. The 10th percentile (left), median (middle) and 90th percentile (right) are shown for an ensemble of downscalings of six CGCM projections, for each of the seasons. The downscalings were generated using the regional model CCAM. All the CGCM projections contributed to CMIP3 and AR4 of the IPCC, and are for the A2 SRES scenario.

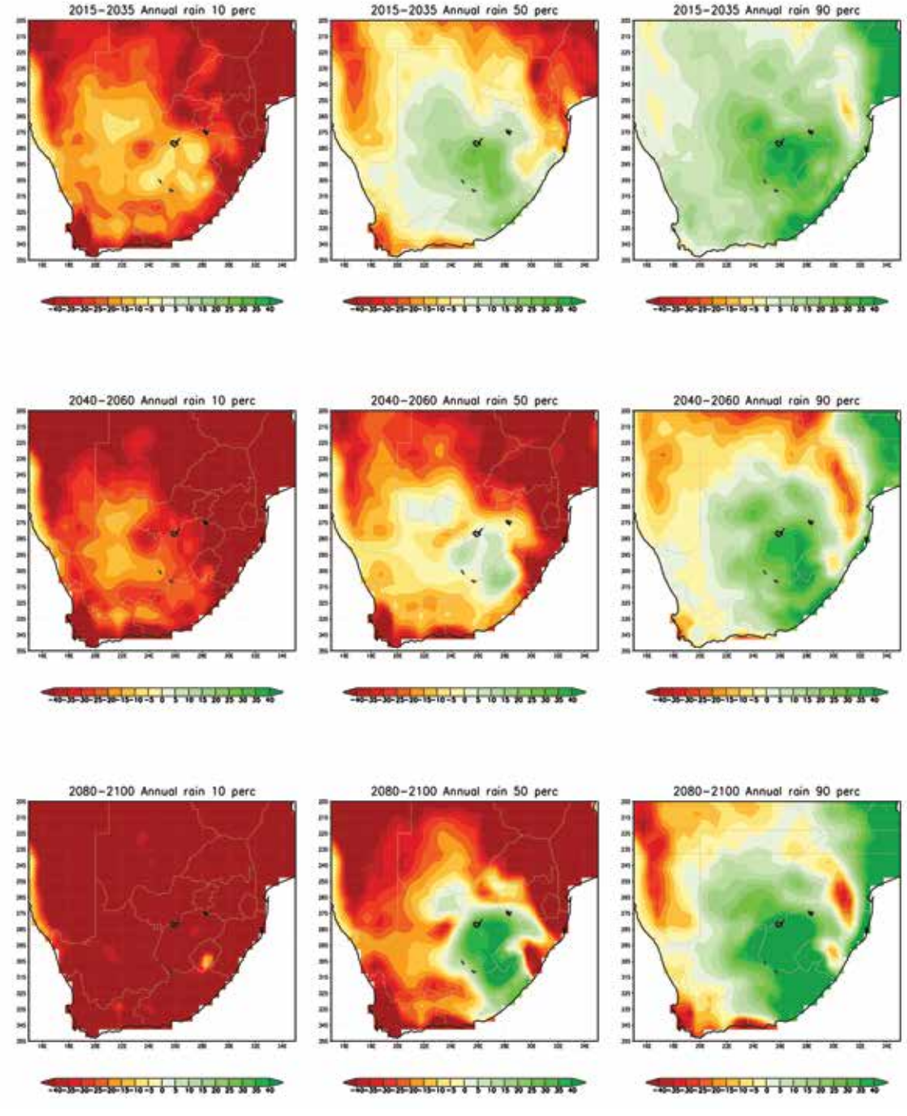

Figure 68. Projected change in the average annual rainfall (mm) over South Africa, for the time periods 2015–2035, 2040–2060 and 2080–2100, relative to 1970–2005. The 10th percentile (left), median (middle) and 90th percentile (right) are shown for the ensemble of downscalings of six CGCM projections, for each of the time periods. The downscalings were performed using the regional model CCAM. All the CGCM projections contributed to CMIP3 and AR4 of the IPCC, and are for the A2 SRES scenario.

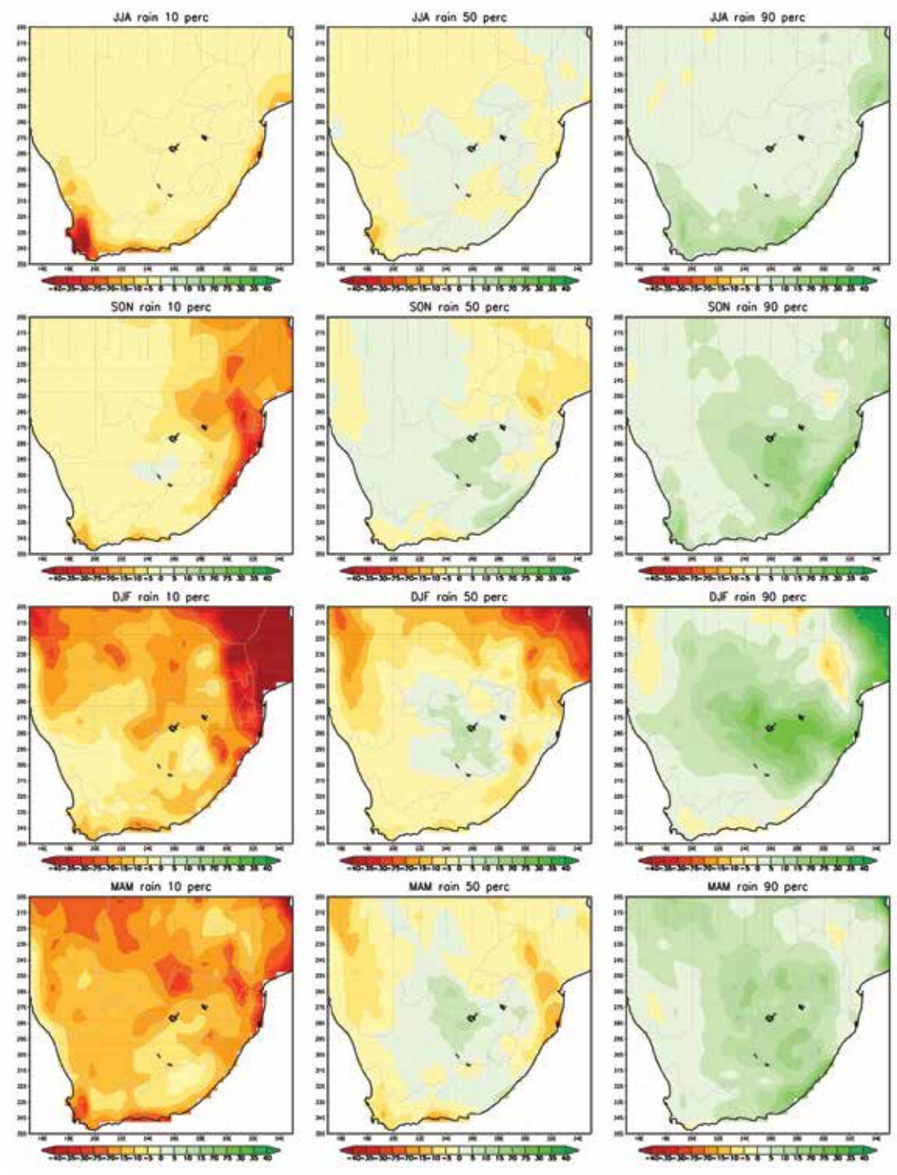

Figure 69. Projected change in the average seasonal rainfall (mm) over South Africa for JJA, SON, DJF and MAM, for the period 2015–2035 relative to 1971–2005. The 10th percentile (left), median (middle) and 90th percentile (right) are shown for an ensemble of downscalings of six CGCM projections, for each of the seasons. The downscalings were generated using the regional model CCAM. All the CGCM projections contributed to CMIP3 and AR4 of the IPCC, and are for the A2 SRES scenario.

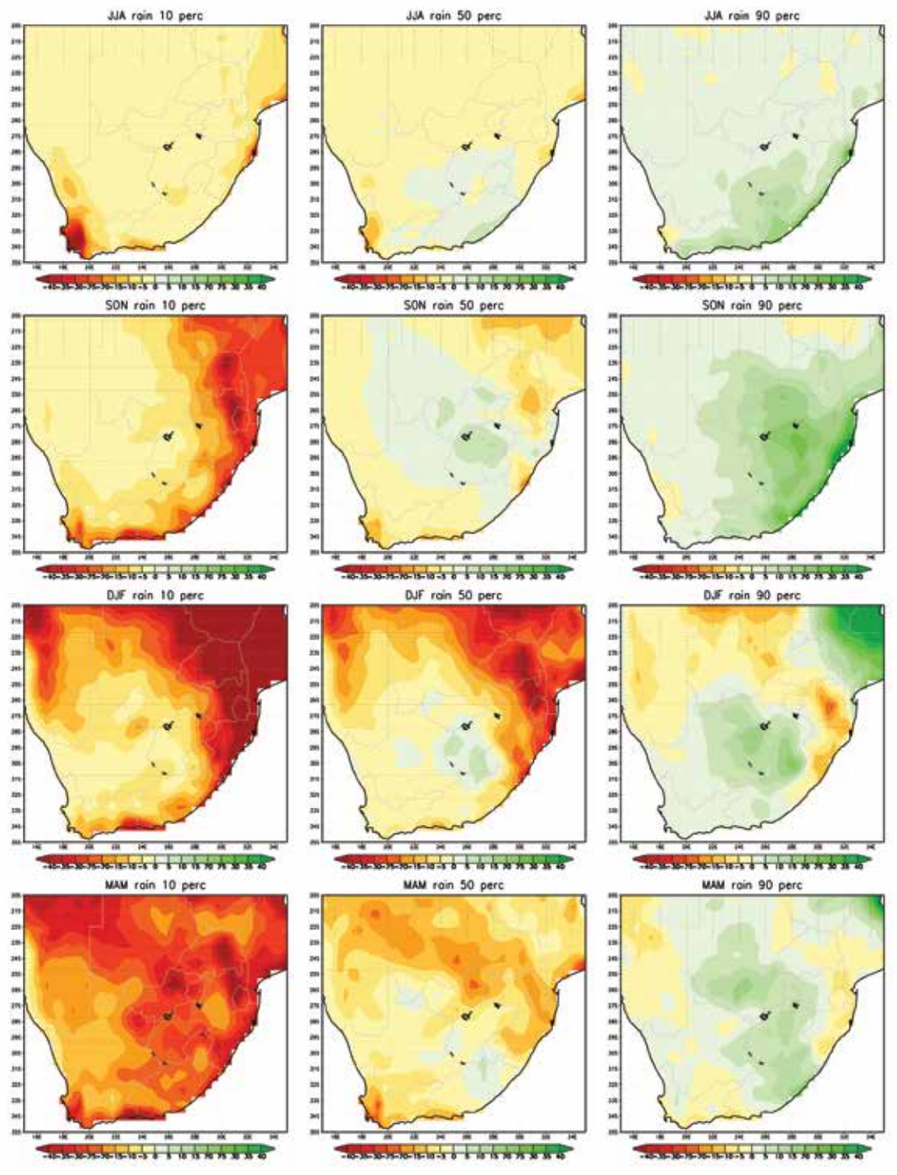

Figure 70. Projected change in the average seasonal rainfall (mm) over South Africa for JJA, SON, DJF and MAM, for the period 2040–2060 relative to 1971–2005. The 10th percentile (left), median (middle) and 90th percentile (right) are shown for an ensemble of downscalings of six CGCM projections, for each of the seasons. The downscalings were generated using the regional model CCAM. All the CGCM projections contributed to CMIP3 and AR4 of the IPCC, and are for the A2 SRES scenario.

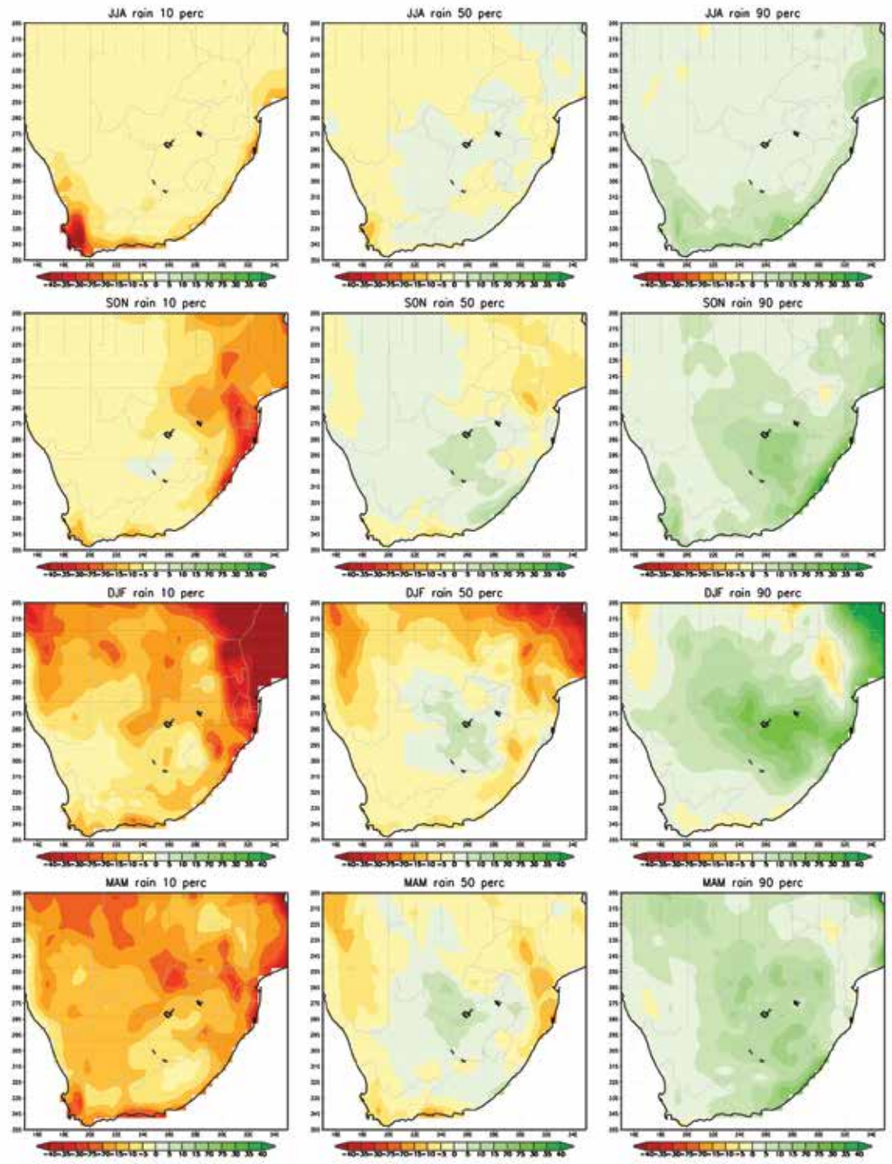

Figure 71. Projected change in the average seasonal rainfall (mm) over South Africa for JJA, SON, DJF and MAM, for the period 2080–2100 relative to 1971–2005. The 10th percentile (left), median (middle) and 90th percentile (right) are shown for an ensemble of downscalings of six CGCM projections, for each of the seasons. The downscalings were generated using the regional model CCAM. All the CGCM projections contributed to CMIP3 and AR4 of the IPCC, and are for the A2 SRES scenario.

5.2 CCAM projections for RCP8.5

5.2.1 Temperature

Rapid rises in the annual average near-surface temperature are projected to occur over southern Africa during the 21st century under RCP8.5. The projected changes are shown in Figure 72 for the future time periods 2015–2035 (near-future), 2040–2060 (mid-future) and 2080–2100 (far-future), relative to the baseline period 1971–2005. For each time period, the 10th, 50th (median) and 90th percentiles are shown, for the ensemble of projected changes. For the near-future, temperature increases of between 1 and 2°C are projected by most ensemble members (slightly higher than in the case of the CCAM A2 downscalings). For the period 2040–2060, annual average temperatures are projected to rise by more than 4°C over most of the central and western interior, relative to the baseline period. Substantial temperature increases, of more than 3°C are projected for the southern interior and coastal areas. Drastic increases in average annual temperatures are projected for the far-future period. Increases of more than 5°C are projected across the southern African interior. Substantial temperature increases of more than 3°C are projected for the coastal areas. Generally, the pattern and amplitude of projected temperature increases shows close correspondence across the different ensemble members, indicating that the projected signal is robust. It may also be noted that for the mid- and far-futures, substantially larger increases in temperature are projected for RCP8.5 compared to the A2 SRES scenario – in correspondence to the relatively higher equivalent CO_2e concentrations described by RCP8.5.

The projected changes in winter, spring, summer and autumn average temperatures are displayed for the various time periods in Figure 73, Figure 74 and Figure 75. For each season within each time period, the 10th, 50th (median) and 90th percentiles of the projected changes are shown. For the near-future period of 2015–2035, the projected temperature signal is similar across the different seasons (Figure 73). Most ensemble members project increases of between 1 and 2°C for all seasons. Winter and spring are projected to warm somewhat less than summer and autumn, consistent with the CCAM A2 SRES scenario downscalings. For all seasons, warming of more than 4°C is projected for the northern interior regions, for the period 2040–2060. The southern interior and coastal regions are projected to have warmed by about 2.5°C for this period, relative to the baseline. Winter and spring are projected to warm somewhat more than the other seasons. The majority of ensemble members indicate warming of more than 5°C across the southern African interior for all seasons for 2080–2100 relative to the baseline (Figure 75). Somewhat smaller rises are projected for the southern interior and coastal areas.

5.2.2 Rainfall

The CCAM ensemble projects a diversity of plausible 21st century rainfall futures for South Africa under RCP8.5. These are displayed in Figure 76, which shows the projected change in the average annual rainfall (mm) for the time periods 2015–2035, 2040–2060 and 2080–2100, relative to 1970–2005. The 10th percentile (left), median (middle) and 90th percentile (right) are shown for the ensemble of downscalings of three CGCM projections, for each of the time-periods. For the near and far-futures, the projections indicate that wetter conditions are plausible over the central and eastern interior of South Africa, although a minority of ensemble members also project drying for this region. However, by the far-future, when the climate-change signal is best developed, the ensemble indicates general drying over eastern South Africa. Large rainfall reductions are projected to occur over the south-western Cape, already in the near- and mid-futures. The amplitude of the projected drying increases over time, and for the 2080–2100 time-period rainfall decreases of more than 40 mm/year are projected for the south-western Cape and large parts of the interior. Despite the general pattern of drying, most ensemble members project increases in the average annual rainfall over the

central interior of South Africa, eastern interior of South Africa (near- and mid-future) and Botswana. This pattern may be related dynamically to the strengthening of the heat low over the western interior (e.g. Engelbrecht et al., 2009), which is conducive to thunderstorm formation to the east of the trough axis, and is consistent with the A2 SRES scenario downscalings.

Projected changes in the average seasonal rainfall (mm) over South Africa for JJA, SON, DJF and MAM, for the periods 2015–2035, 2040–2060 and 2080–2100, relative to 1971–2005, are displayed in Figure 77, Figure 78, and Figure 79. The 90th percentile (left), median (middle) and 90th percentile (right) are shown for an ensemble of downscalings of three CGCM projections, for each of the seasons and each of the time-periods. For the winter rainfall region of the south-western Cape, most downscalings indicate drier conditions for the near-future, although slight increases in rainfall are also plausible. For most interior regions, the projected near-future changes in rainfall are small in amplitude, and physically insignificant. An exception is the east coast and adjacent interior region, where great uncertainty surrounds the projected changes: some ensemble members project substantial decreases in rainfall for all seasons, whilst others project substantial increases.

For the mid-future, most ensemble members project rainfall decreases for the south-western Cape for all seasons, and particularly in winter. This pattern of drying is projected to extend to the all-year rainfall region of the Cape south coast – consistent with the CCAM A2 SRES scenario downscalings. By the mid-future, a general pattern of drying manifests itself in most ensemble members over eastern South Africa, although a minority of ensemble members project rainfall increases over this region. Slight to moderate increases in rainfall are projected by most ensemble members for the central interior region of South Africa for the warmer seasons.

These patterns of projected changes remain similar for the far-future, with a general increase in amplitude. Physically significant rainfall decreases are projected for the south-western Cape and Cape south coast for the important winter, spring and autumn periods. Strong drying is projected for the central and eastern interior, for all seasons and by most ensemble members. Moderate increases in rainfall are plausible over the central and eastern interior during summer. The general pattern of drying is projected to be particularly uniform during autumn and winter. This has been shown (for the CCAM A2 SRES scenario downscalings) to be consistent with a projected strengthening of mid-level anti-cyclones over southern Africa, and a strengthening of anti-cyclonic circulation to the south of the country, which occurs in conjunction with a southward displacement of the westerly wind regime (e.g. Engelbrecht et al., 2009; Malherbe et al., 2013).

5.2.3 Key messages from the ensemble of CCAM RCP8.5 projections

Temperature increases of more than 5°C are plausible under RCP8.5 across the southern African interior for the period 2080–2100 relative to the baseline period 1971–2005.

Strong drying is plausible over the south-western Cape in the near-future, amplifying in time, and extending to the Cape south coast. These changes are consistent with a projected southward displacement of the westerlies and cold fronts and with the CCAM A2 SRES scenario downscalings.

For the mid- and far-future, significant drying is plausible over the central and eastern interior regions. Slight to moderate increases in rainfall are plausible over the central and eastern interior regions during summer, despite the general pattern of drying that is projected

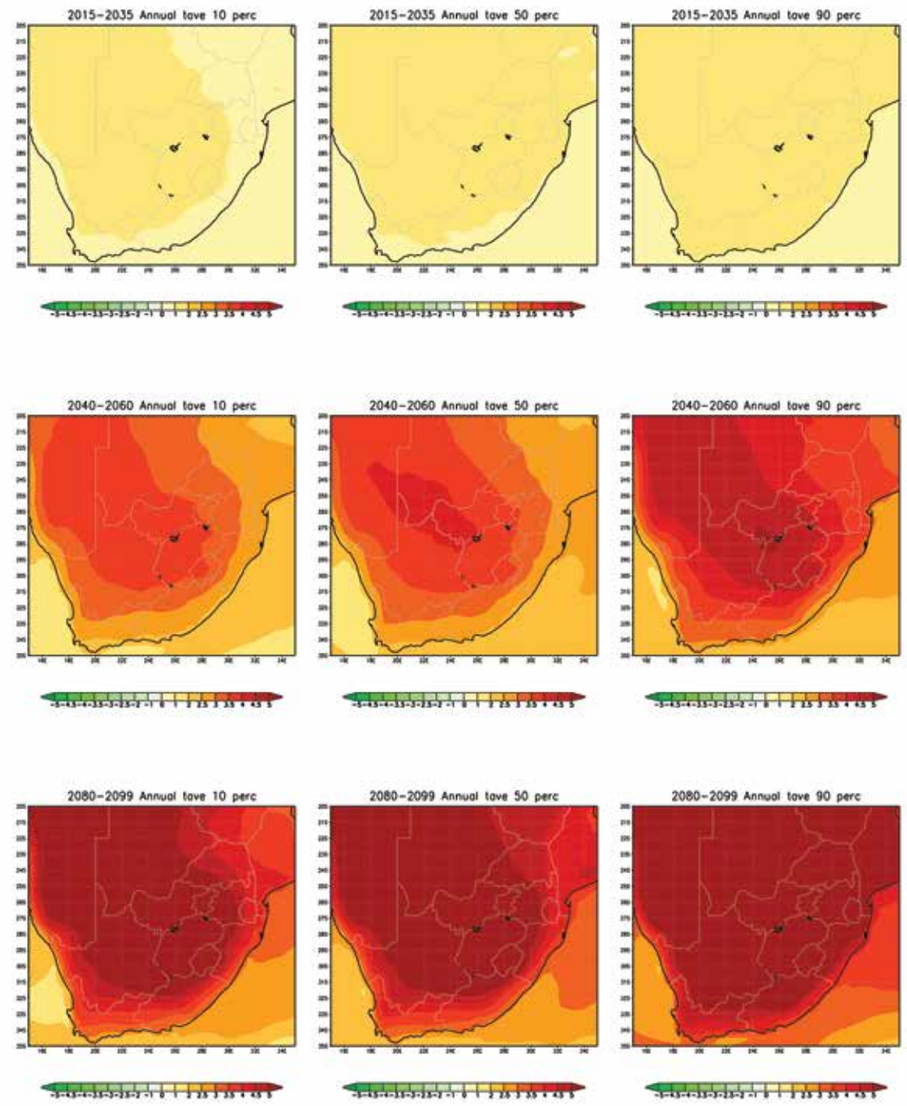

Figure 72. Projected change in the annual average temperature (°C) over South Africa, for the time-periods 2015–2035, 2040–2060 and 2080–2100, relative to 1970–2005. The 10th percentile (left), median (middle) and 90th percentile (right) are shown for an ensemble of downscalings of three CGCM projections, for each of the time-periods. The downscalings were performed using the regional model CCAM. All the CGCM projections are contributing to CMIP5 and AR5 of the IPCC, and are for RCP8.5.

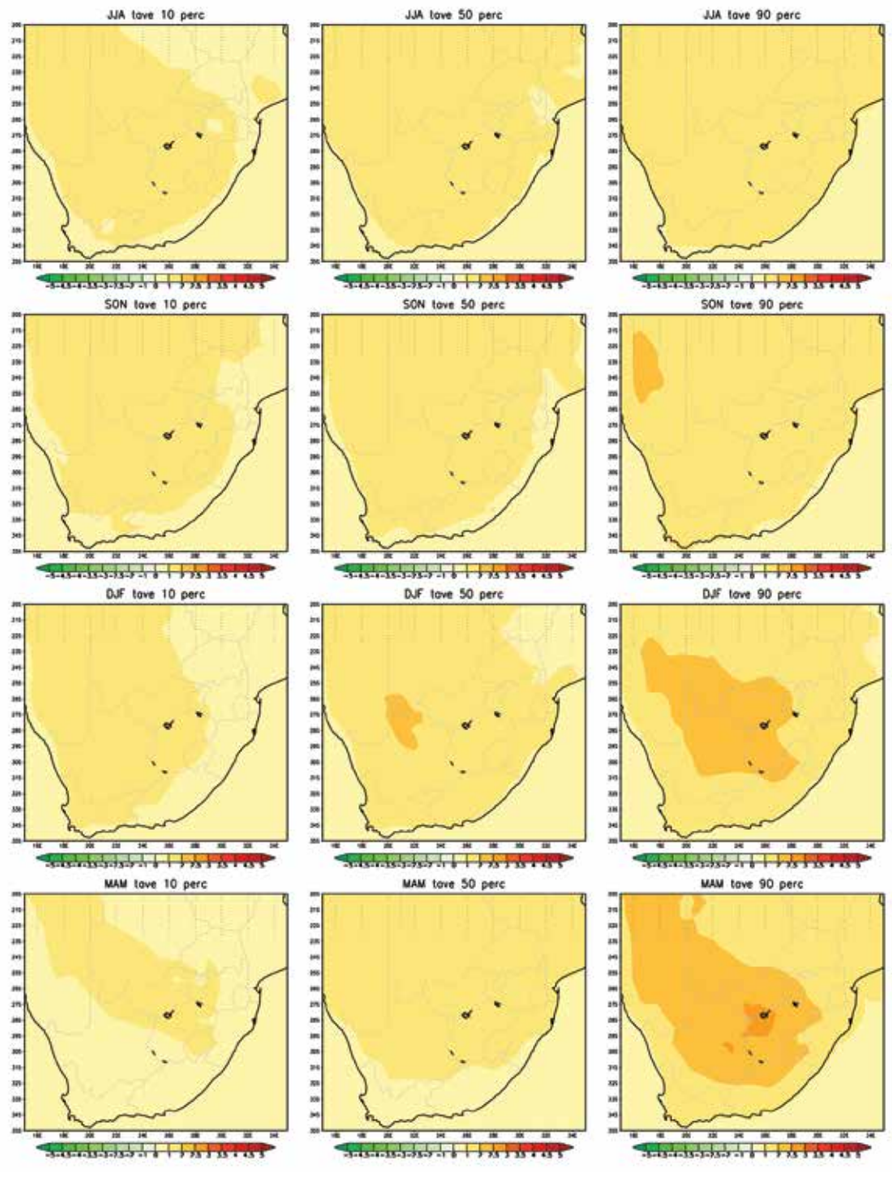

Figure 73. Projected change in the average seasonal temperatures (°C) over South Africa for JJA, SON, DJF and MAM, for the period 2015–2035 relative to 1971–2005. The 10th percentile (left), median (middle) and 90th percentile (right) are shown for an ensemble of downscalings of three CGCM projections, for each of the seasons. The downscalings were generated using the regional model CCAM. All the CGCM projections are contributing to CMIP5 and AR5 of the IPCC, and are for RCP8.5.

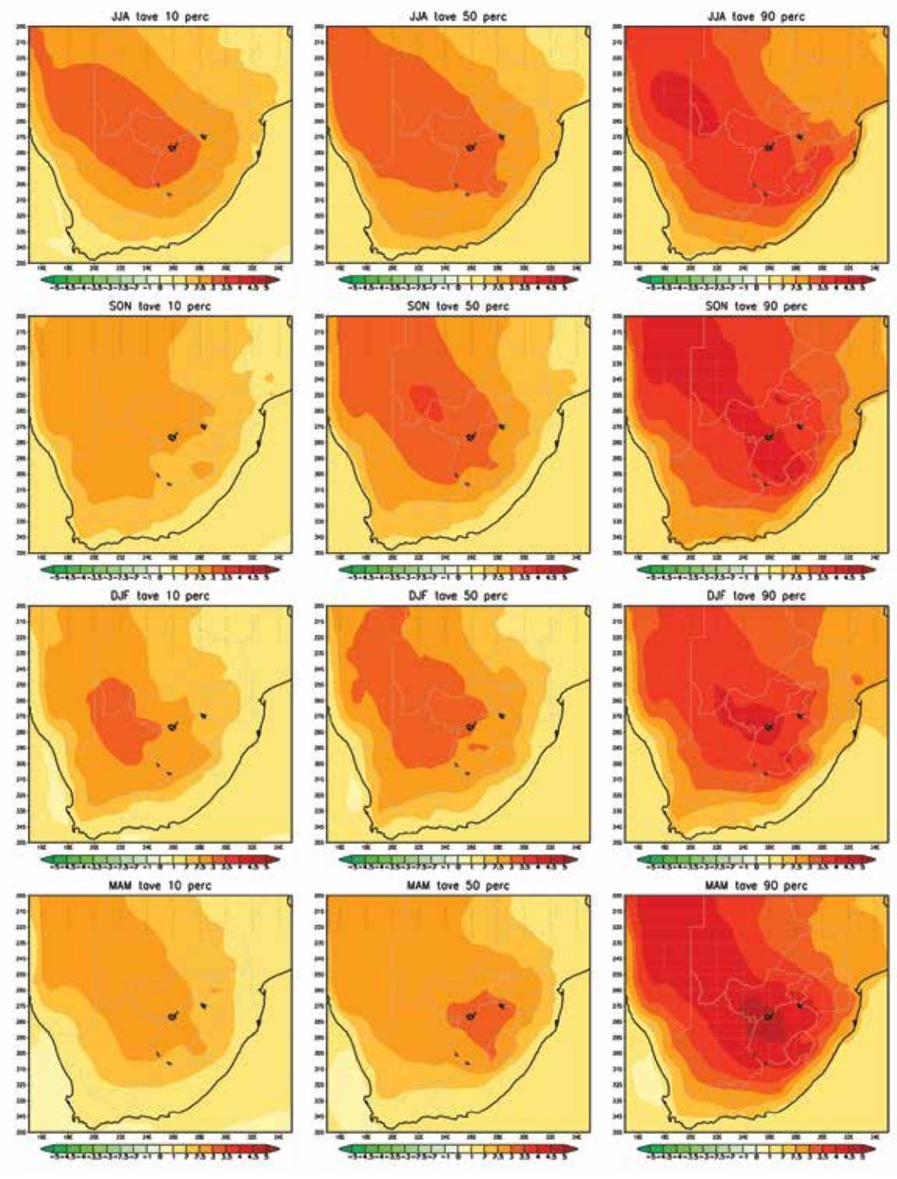

Figure 74. Projected change in the average seasonal temperatures (°C) over South Africa for JJA, SON, DJF and MAM, for the period 2040–2060 relative to 1971–2005. The 10th percentile (left), median (middle) and 90th percentile (right) are shown for an ensemble of downscalings of three CGCM projections, for each of the seasons. The downscalings were generated using the regional model CCAM. All the CGCM projections are contributing to CMIP5 and AR5 of the IPCC, and are for RCP8.5.

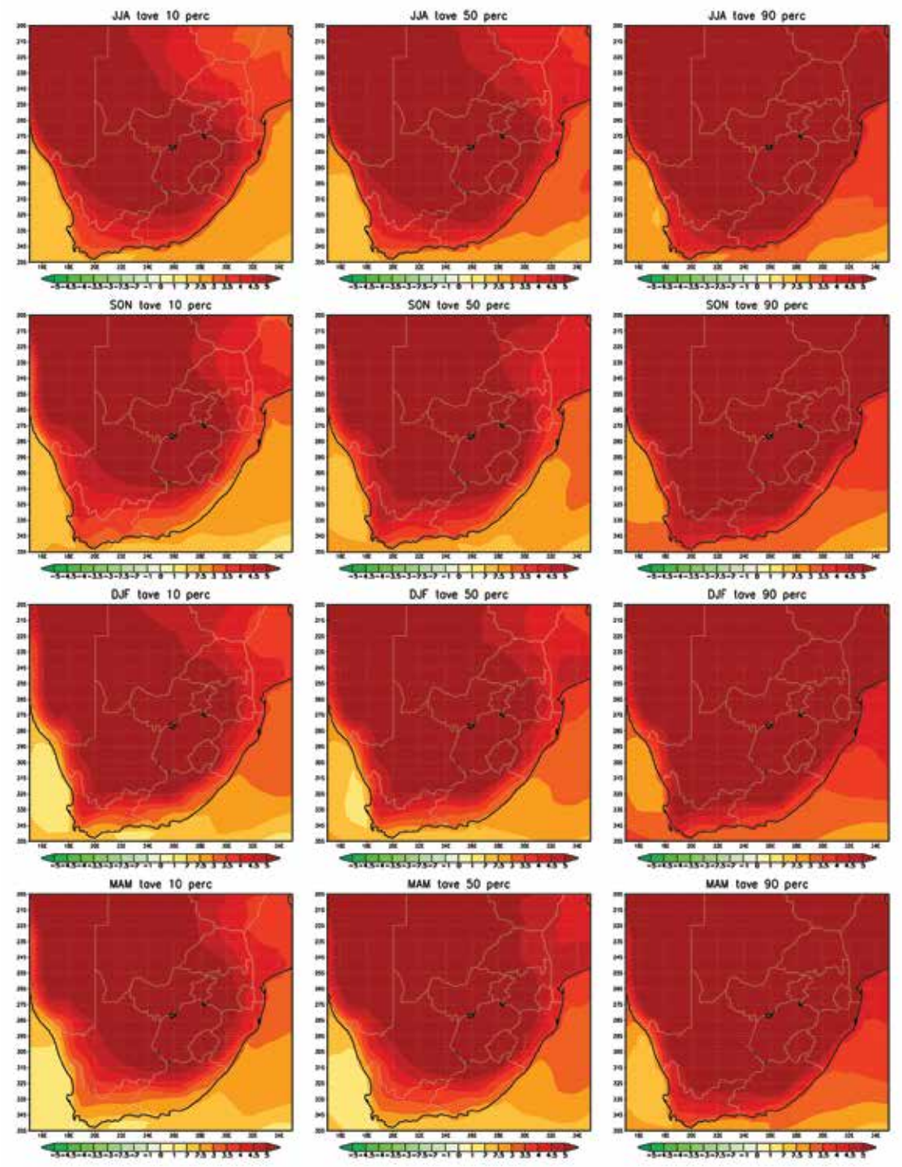

Figure 75. Projected change in the average seasonal temperatures (°C) over South Africa for JJA, SON, DJF and MAM, for the period 2080–2099 relative to 1971–2005. The 10th percentile (left), median (middle) and 90th percentile (right) are shown for an ensemble of downscalings of three CGCM projections, for each of the seasons. The downscalings were generated using the regional model CCAM. All the CGCM projections are contributing to CMIP5 and AR5 of the IPCC, and are for RCP8.5.

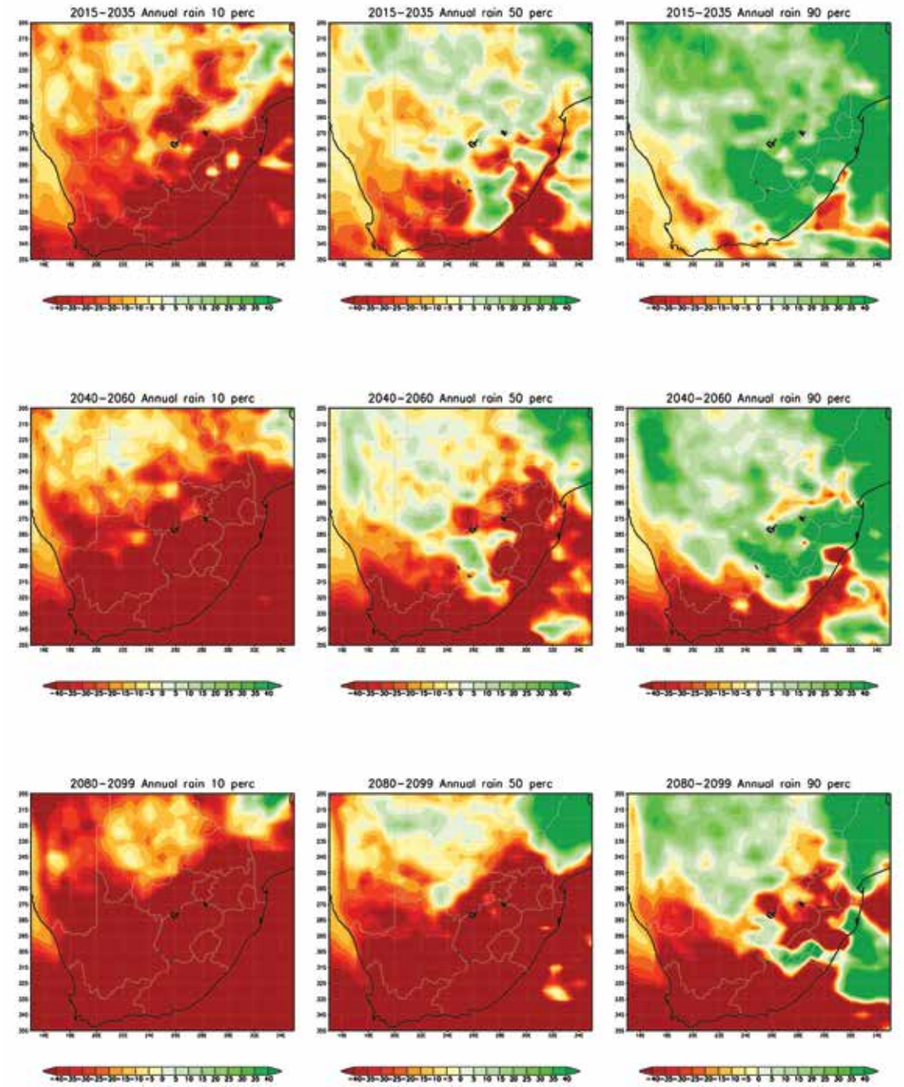

Figure 76. Projected change in the average annual rainfall (mm) over South Africa, for the time-periods 2015–2035, 2040–2060 and 2080–2100, relative to 1971–2005. The 10th percentile (left), median (middle) and 90th percentile (right) are shown for the ensemble of downscalings of three CGCM projections, for each of the time-periods. The downscalings were performed using the regional model CCAM. All the CGCM projections are contributing to CMIP5 and AR5 of the IPCC, and are for RCP8.5.

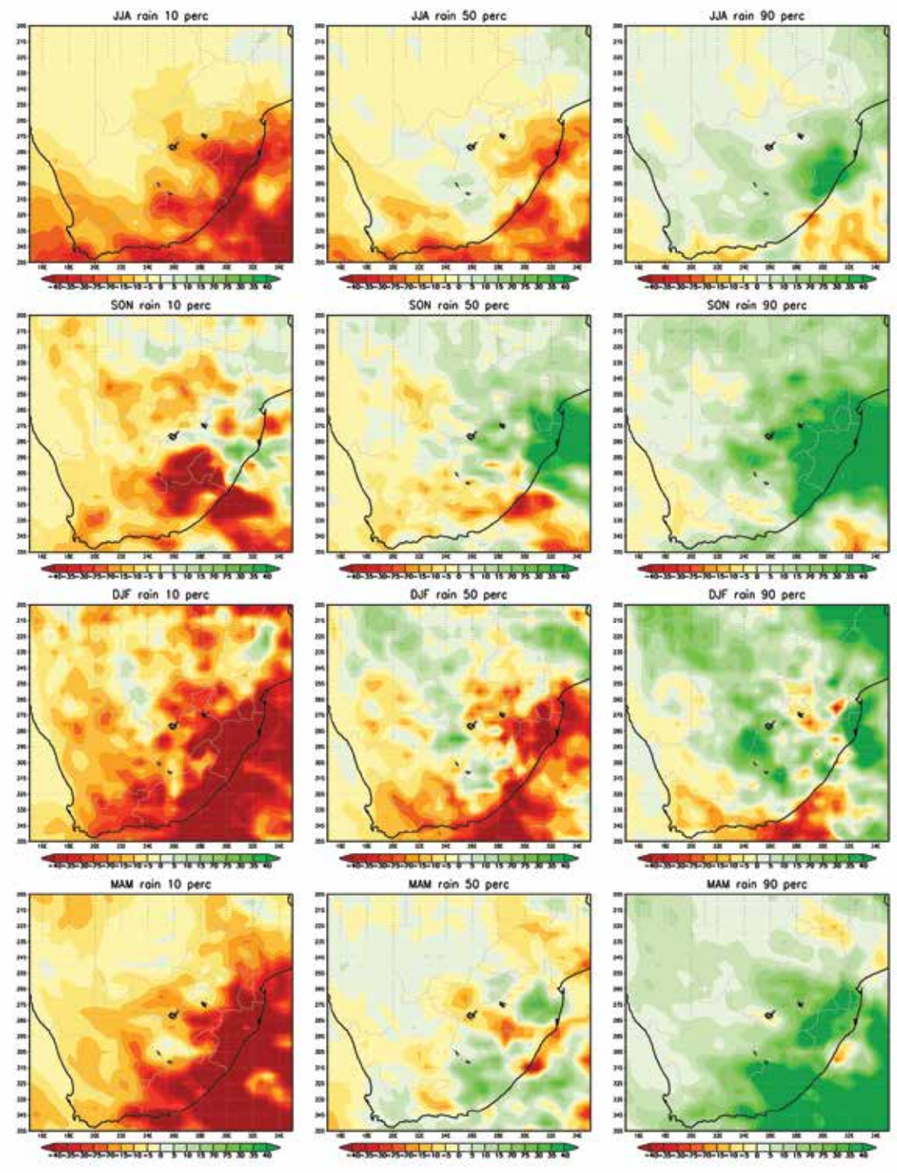

Figure 77. Projected change in the average seasonal rainfall (mm) over South Africa for JJA, SON, DJF and MAM, for the period 2015–2035 relative to 1971–2005. The 10th percentile (left), median (middle) and 90th percentile (right) are shown for an ensemble of downscalings of six CGCM projections, for each of the seasons. The downscalings were generated using the regional model CCAM. All the CGCM projections are contributing to CMIP5 and AR5 of the IPCC, and are for RCP8.5.

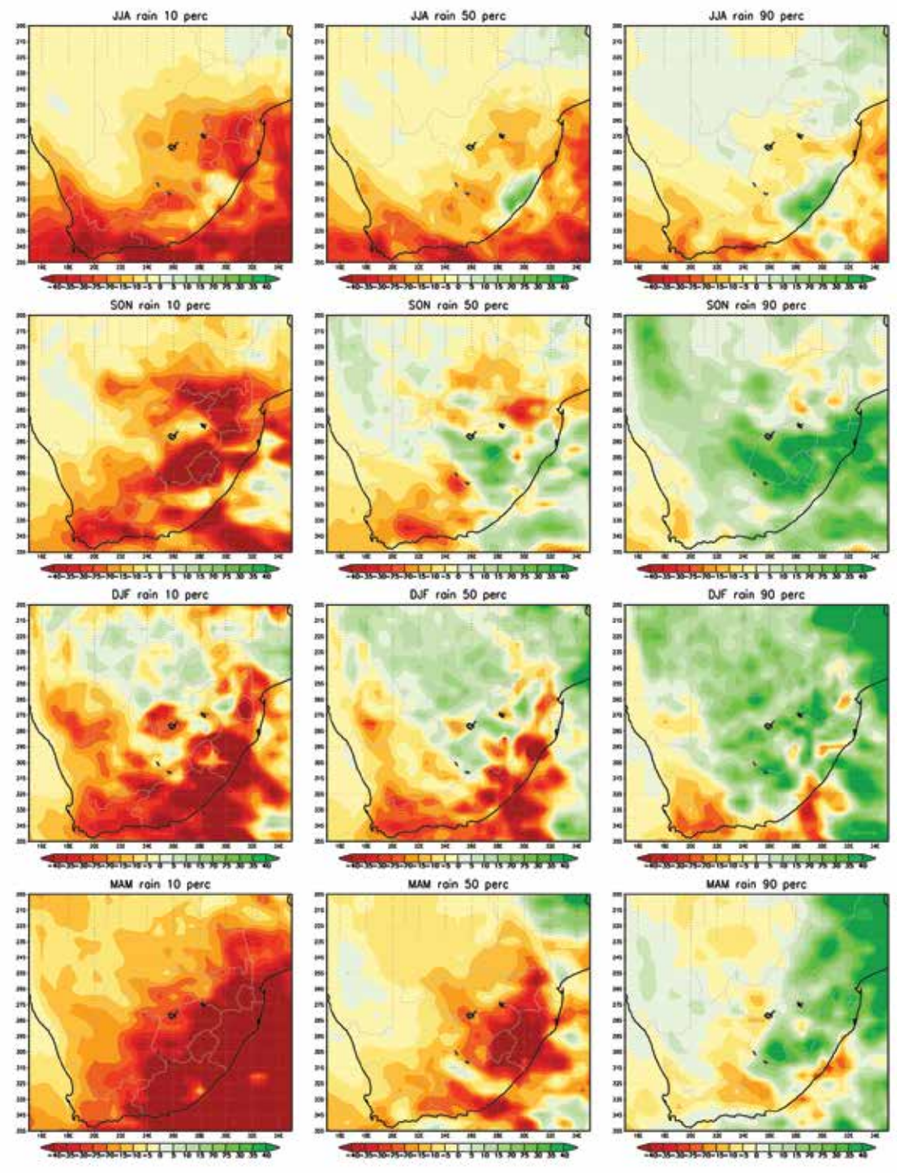

Figure 78. Projected change in the average seasonal rainfall (mm) over South Africa for JJA, SON, DJF and MAM, for the period 2040–2060 relative to 1971–2005. The 10th percentile (left), median (middle) and 90th percentile (right) are shown for an ensemble of downscalings of six CGCM projections, for each of the seasons. The downscalings were generated using the regional model CCAM. All the CGCM projections are contributing to CMIP5 and AR5 of the IPCC, and are for RCP8.5.

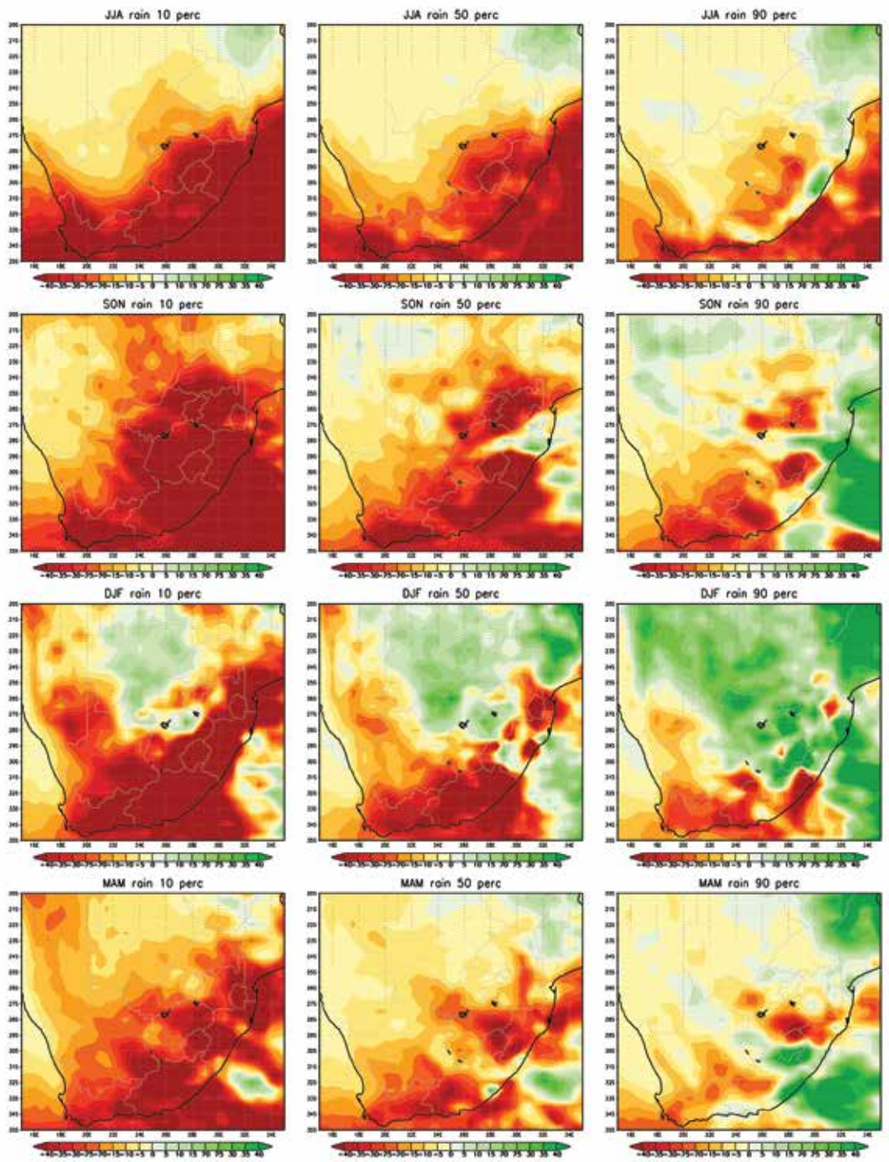

Figure 79. Projected change in the average seasonal rainfall (mm) over South Africa for JJA, SON, DJF and MAM, for the period 2080–2099 relative to 1971–2005. The 10th percentile (left), median (middle) and 90th percentile (right) are shown for an ensemble of downscalings of six CGCM projections, for each of the seasons. The downscalings were generated using the regional model CCAM. All the CGCM projections are contributing to CMIP5 and AR5 of the IPCC, and are for RCP8.5.

5.3 CCAM projections for RCP4.5

5.3.1 Temperature

Compared to the A2 SRES scenario and RCP8.5, RCP4.5 represents a future where the risks associated with temperature increases over southern Africa are significantly reduced. The projected changes are shown in Figure 80 for the future time-periods 2015–2035 (near-future), 2040–2060 (mid-future) and 2080–2100 (far-future), relative to the baseline period 1971–2005. For each time-period, the 10th, 50th (median) and 90th percentiles are shown, for the ensemble of projected changes. For the near-future, temperature increases of between 1 and 2°C are projected by most ensemble members (slightly higher than in the case of the CCAM A2 downscalings and similar to the RCP8.5 downscalings). However, for the period 2040–2060, annual average temperatures are projected to rise by only 2 to 3°C. Moreover, the projected increases for 2080–2100 are reduced to about 2.5 to 3.5°C, suggesting that the rises in regional temperatures are stabilising in a new climate regime, consistent with the stabilising greenhouse gas concentrations of RCP4.5. Although the projected increases of 2.5 to 3.5°C over the interior regions are still significant, the amplitude of temperature increase is about halved, compared to the RCP8.5 projections for 2080–2100.

The projected changes in winter, spring, summer and autumn average temperatures are displayed for the various time-periods in Figure 81, Figure 82, and Figure 83. For each season within each time-period, the 10th, 50th (median) and 90th percentiles of the projected changes are shown. For the near-future period of 2015–2035, the projected temperature signal is similar across the different seasons (Figure 81). Most ensemble members project increases of between 1 and 2°C over the northern interior and less than 1°C over the coastal areas and southern interior, for all seasons. Temperature increases are projected to be in the order of 2 to 2.5°C and 2.5 to 3.5°C, respectively, for 2040–2060 and 2080–2100, over the interior regions. Smaller increases are projected for the coastal areas.

5.3.2 Rainfall

Figure 84 shows the projected change in the average annual rainfall (mm) for the time-periods 2015–2035, 2040–2060 and 2080–2100, relative to 1970–2005, under RCP4.5. The 10th percentile (left), median (middle) and 90th percentile (right) are shown for the ensemble of downscalings of three CGCM projections, for each of the time-periods. The projected rainfall signal does not exhibit a significant amplification in time, contrary to the SRES A2 scenario and RCP8.5 CCAM downscalings.

A robust pattern of drying over the south-western Cape and along the Cape south coast is projected, consistent with the downscalings for the more negative emission scenarios. Another robust signal from the projections is the wetting that is projected for the western and central interior regions. For most of the summer rainfall region in the east, mixed signals of drying and wetting are projected by the various ensemble members.

Projected changes (under RCP4.5) in the average seasonal rainfall (mm) over South Africa for JJA, SON, DJF and MAM, for the periods 2015–2035, 2040–2060 and 2080–2100, relative to 1971–2005, are displayed in Figure 85, Figure 86, and Figure 87. The 10th percentile (left), median (middle) and 90th percentile (right) are shown for an ensemble of downscalings of six CGCM projections, for each of the seasons and each of the time-periods. For the near-future period, reductions in rainfall are projected for the south-western Cape and the east coast across all seasons, by both ensemble members. General rainfall increases are projected for the transition seasons of spring and autumn. It should be noted, however, that the number of CCAM RCP4.5 ensemble members is currently small, and that the uncertainty envelope of RCP4.5 rainfall futures may be expected to be better described once the ensemble size has increased. For the mid- and far-futures, a robust pattern of drying is projected for the south-western Cape and Cape south coast, in particular for the winter season. There are indications of both the central and eastern parts of the country being wetter under RCP4.5 during summer and autumn, for both the mid- and far-future periods.

5.3.3 Key messages from the ensemble of CCAM RCP4.5 projections

Temperature increases are drastically reduced under RCP4.5 compared to the RCP8.5 and SRES A2 scenarios, reaching values of only 2.5 to 3.5°C over the interior regions in the far-future.

Drying seems plausible over the south-western Cape across all time-periods under RCP4.5, extending to the Cape south coast. These changes are consistent with a projected southward displacement of the westerlies and cold fronts and with the CCAM A2 SRES scenario and RCP8.5 downscalings.

For the mid-and far future, wetter summers seem plausible over the east coast and central interior regions. However, it should be noted that the CCAM RCP4.5 ensemble currently consists of only two members – the uncertainty envelope of RCP4.5 rainfall futures may be expected to be better described once an extended set of simulations is available for analysis.

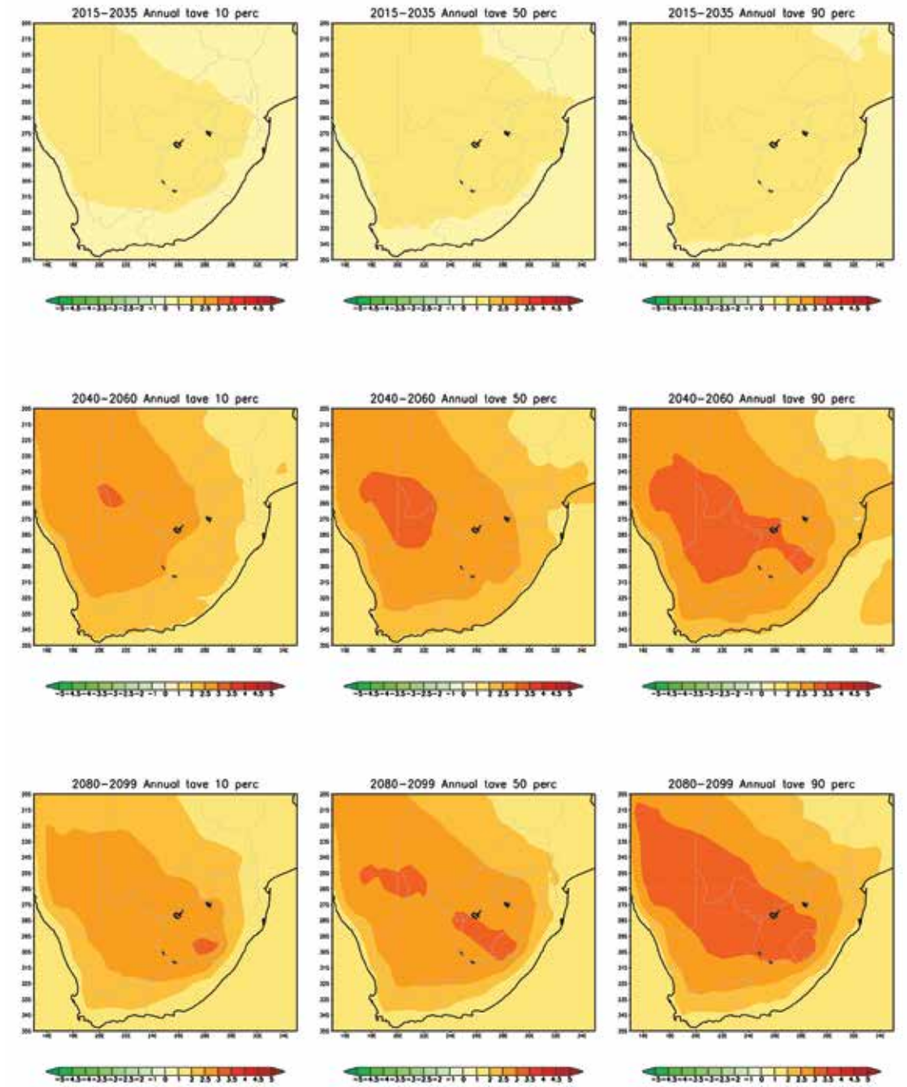

Figure 80. Projected change in the annual average temperature (°C) over South Africa, for the time-periods 2015–2035, 2040–2060 and 2080–2100, relative to 1970–2005. The 10th percentile (left), median (middle) and 90th percentile (right) are shown for an ensemble of downscalings of three CGCM projections, for each of the time-periods. The downscalings were performed using the regional model CCAM. All the CGCM projections are contributing to CMIP5 and AR5 of the IPCC, and are for RCP4.5.

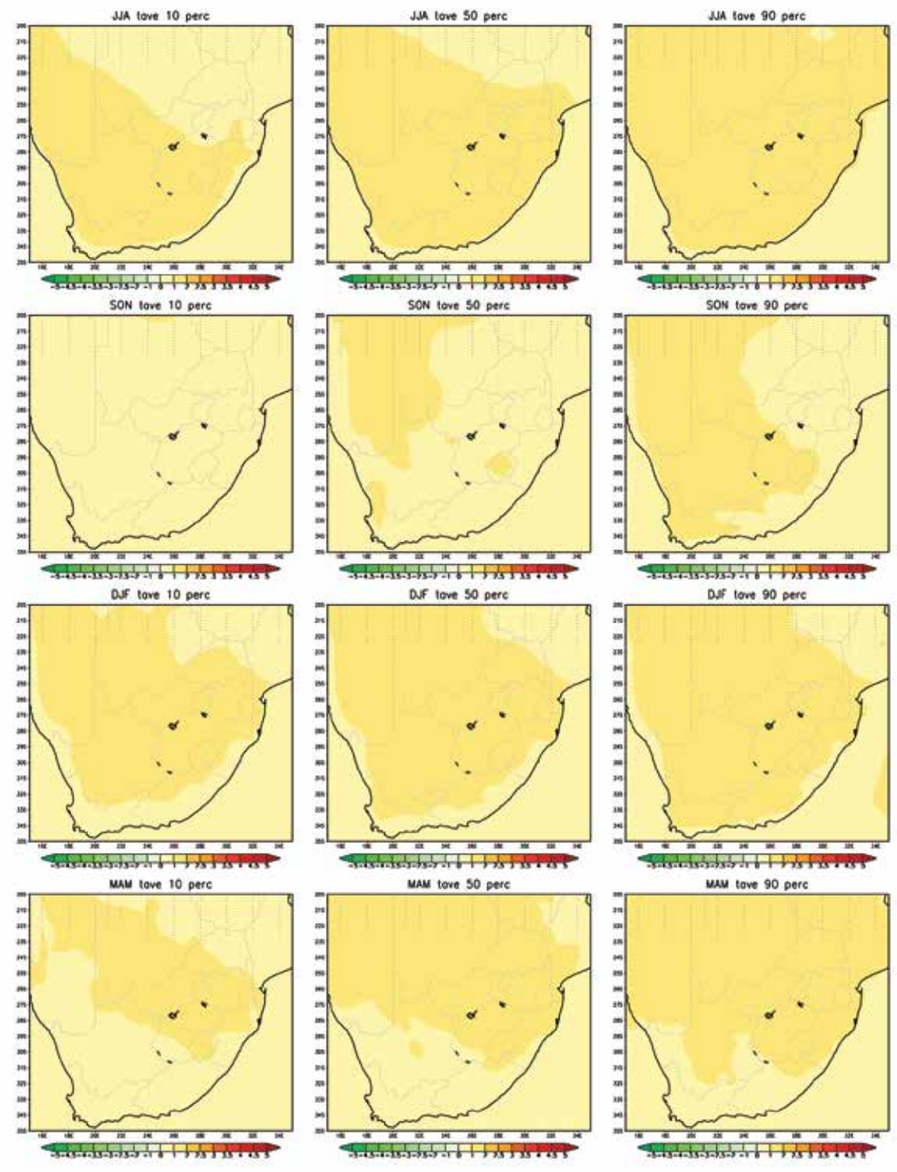

Figure 81. Projected change in the average seasonal temperatures (°C) over South Africa for JJA, SON, DJF and MAM, for the period 2015–2035 relative to 1971–2005. The 10th percentile (left), median (middle) and 90th percentile (right) are shown for an ensemble of downscalings of three CGCM projections, for each of the seasons. The downscalings were generated using the regional model CCAM. All the CGCM projections are contributing to CMIP5 and AR5 of the IPCC, and are for RCP4.5.

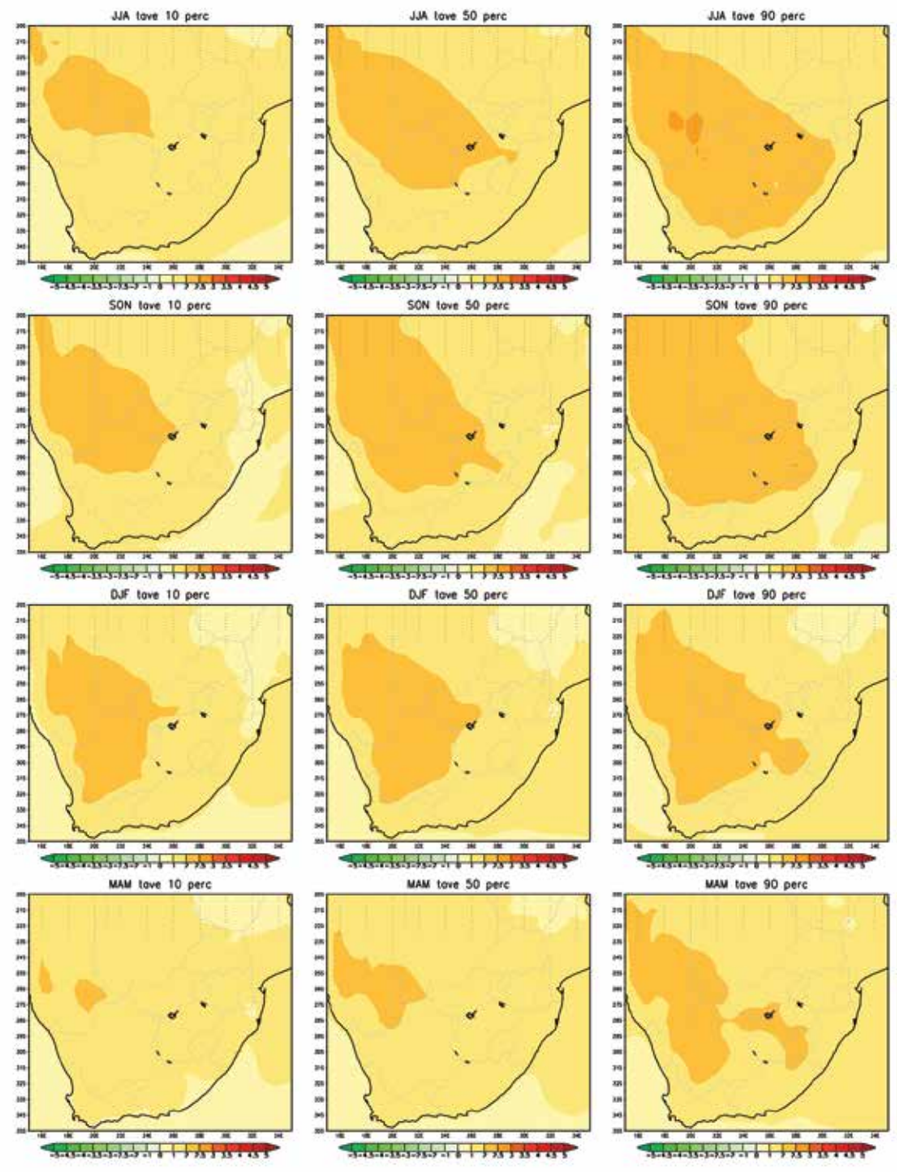

Figure 82. Projected change in the average seasonal temperatures (°C) over South Africa for JJA, SON, DJF and MAM, for the period 2040–2060 relative to 1971–2005. The 10th percentile (left), median (middle) and 90th percentile (right) are shown for an ensemble of downscalings of three CGCM projections, for each of the seasons. The downscalings were generated using the regional model CCAM. All the CGCM projections are contributing to CMIP5 and AR5 of the IPCC, and are for RCP4.5.

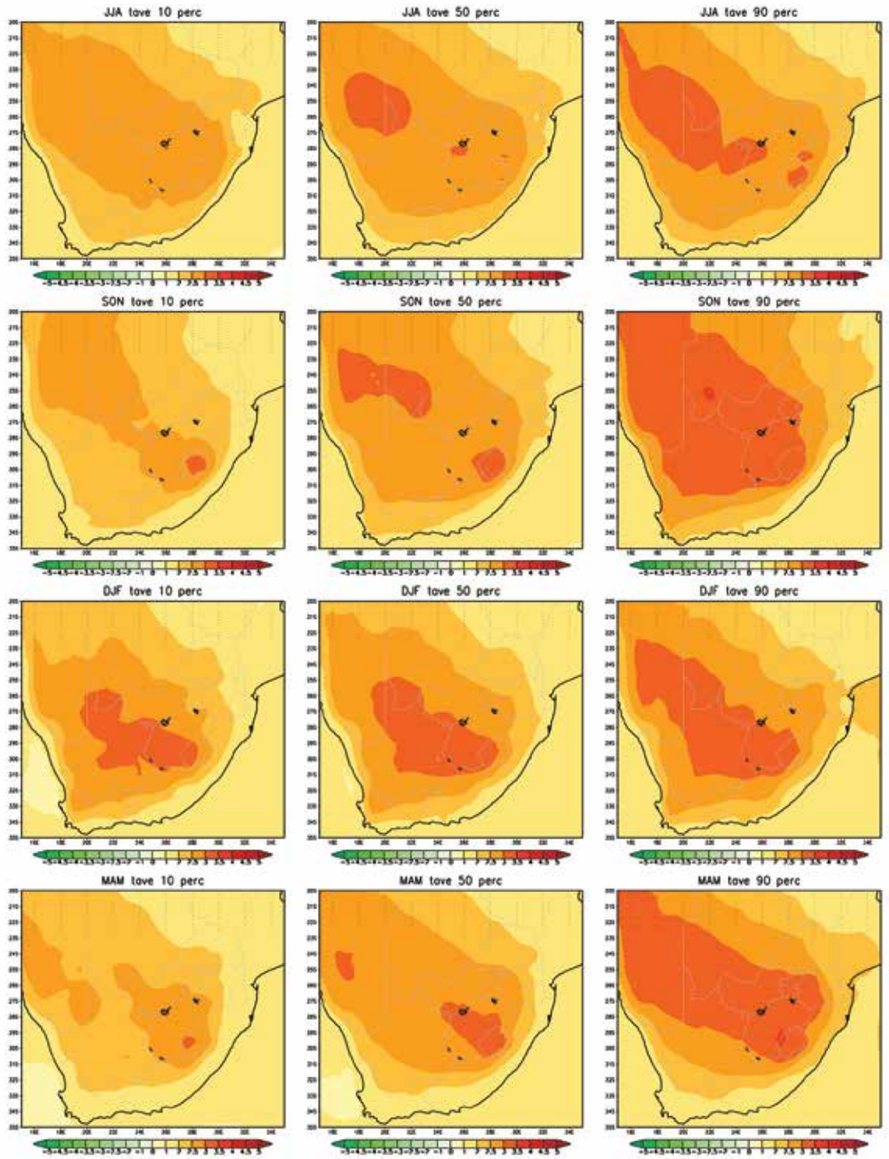

Figure 83. Projected change in the average seasonal temperatures (°C) over South Africa for JJA, SON, DJF and MAM, for the period 2080–2099 relative to 1971–2005. The 10th percentile (left), median (middle) and 90th percentile (right) are shown for an ensemble of downscalings of three CGCM projections, for each of the seasons. The downscalings were generated using the regional model CCAM. All the CGCM projections are contributing to CMIP5 and AR5 of the IPCC, and are for RCP4.5.

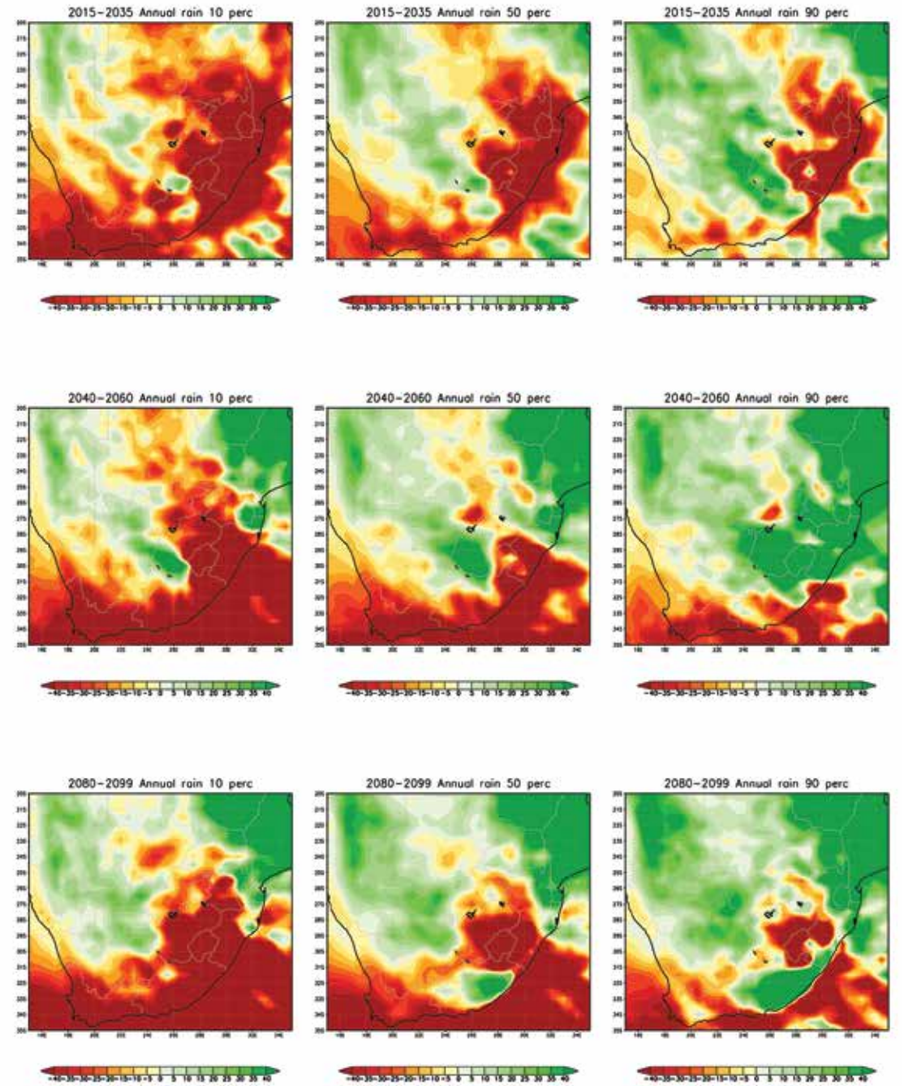

Figure 84. Projected change in the average annual rainfall (mm) over South Africa, for the time-periods 2015–2035, 2040-2060 and 2080–2100, relative to 1971–2005. The 10th percentile (left), median (middle) and 90th percentile (right) are shown for the ensemble of downscalings of three CGCM projections, for each of the time-periods. The downscalings were performed using the regional model CCAM. All the CGCM projections are contributing to CMIP5 and AR5 of the IPCC, and are for RCP4.5.

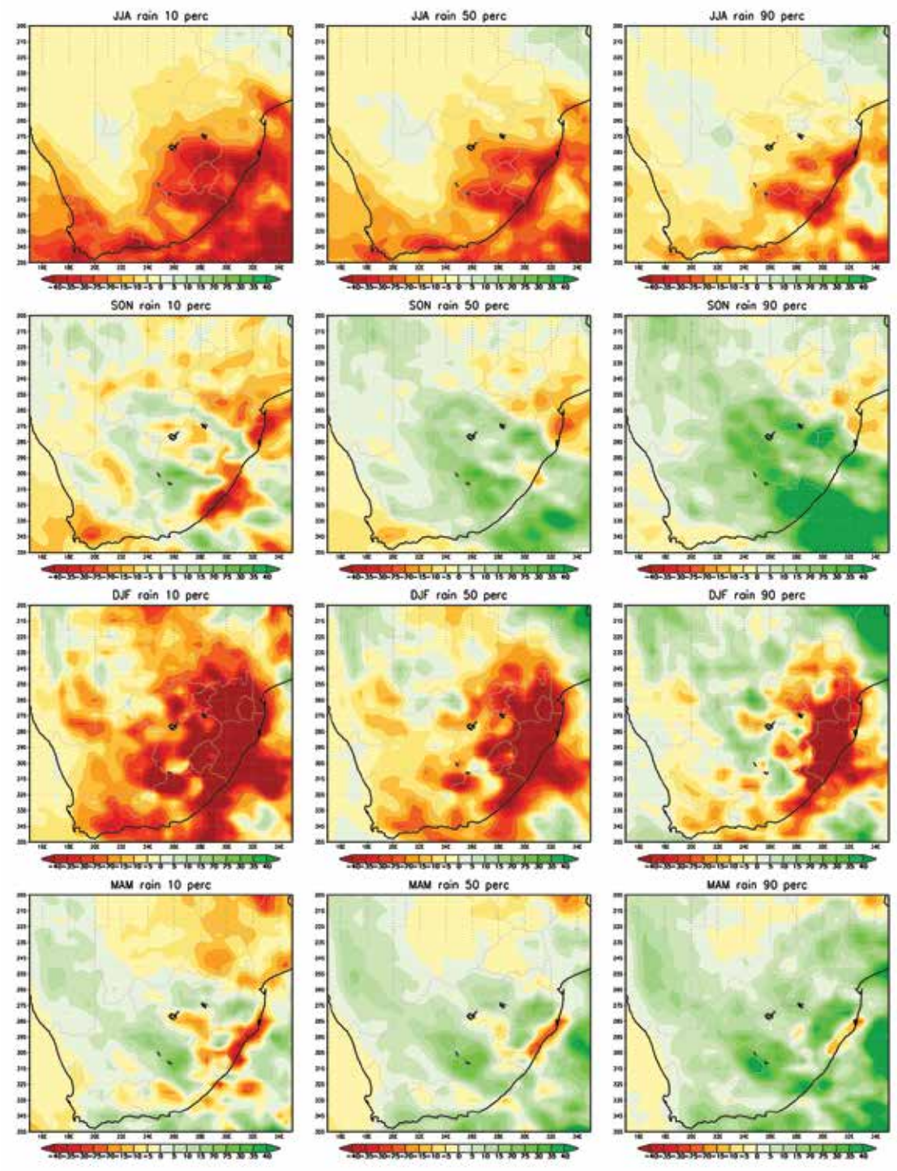

Figure 85. Projected change in the average seasonal rainfall (mm) over South Africa for JJA, SON, DJF and MAM, for the period 2015–2035 relative to 1971–2005. The 10th percentile (left), median (middle) and 90th percentile (right) are shown for an ensemble of downscalings of six CGCM projections, for each of the seasons. The downscalings were generated using the regional model CCAM. All the CGCM projections are contributing to CMIP5 and AR5 of the IPCC, and are for RCP4.5.

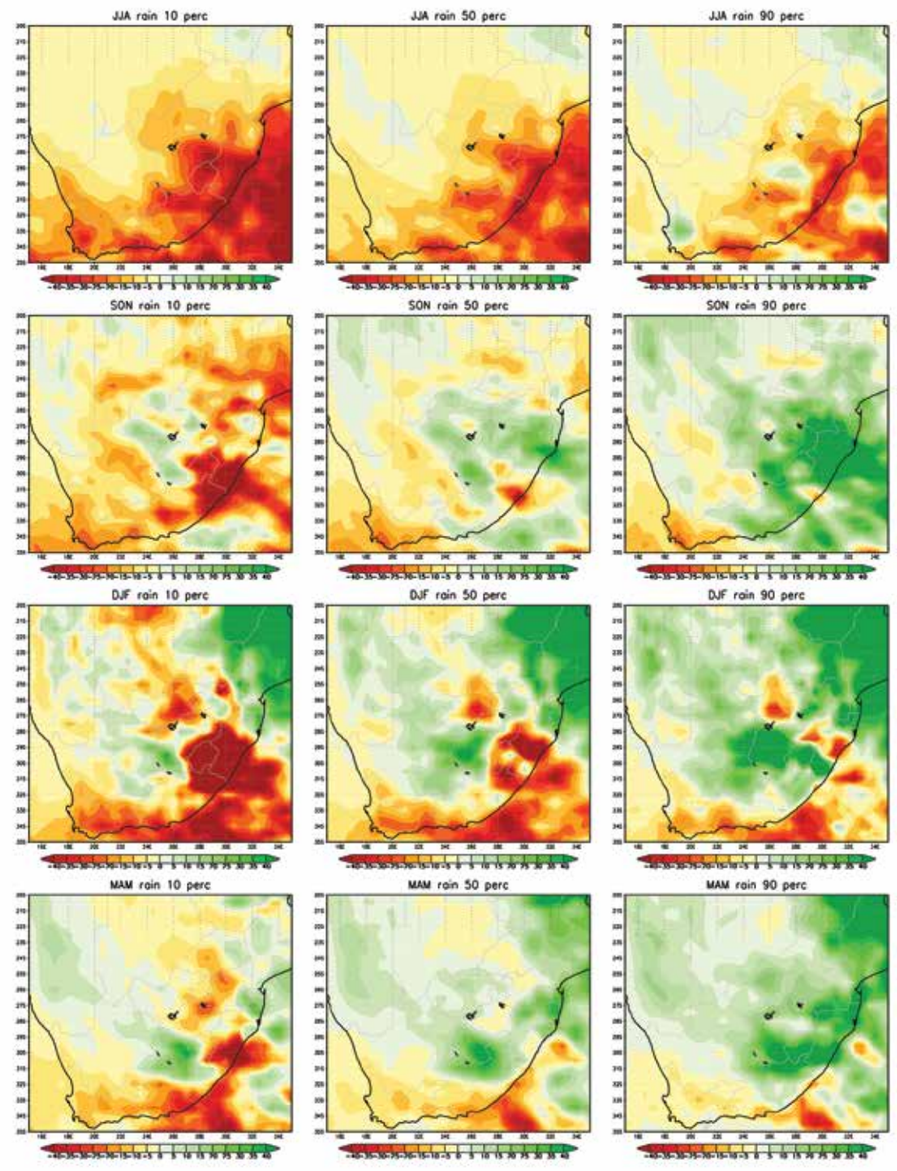

Figure 86. Projected change in the average seasonal rainfall (mm) over South Africa for JJA, SON, DJF and MAM, for the period 2040-2060 relative to 1971-2005. The 10th percentile (left), median (middle) and 90th percentile (right) are shown for an ensemble of downscalings of six CGCM projections, for each of the seasons. The downscalings were generated using the regional model CCAM. All the CGCM projections are contributing to CMIP5 and AR5 of the IPCC, and are for RCP4.5.

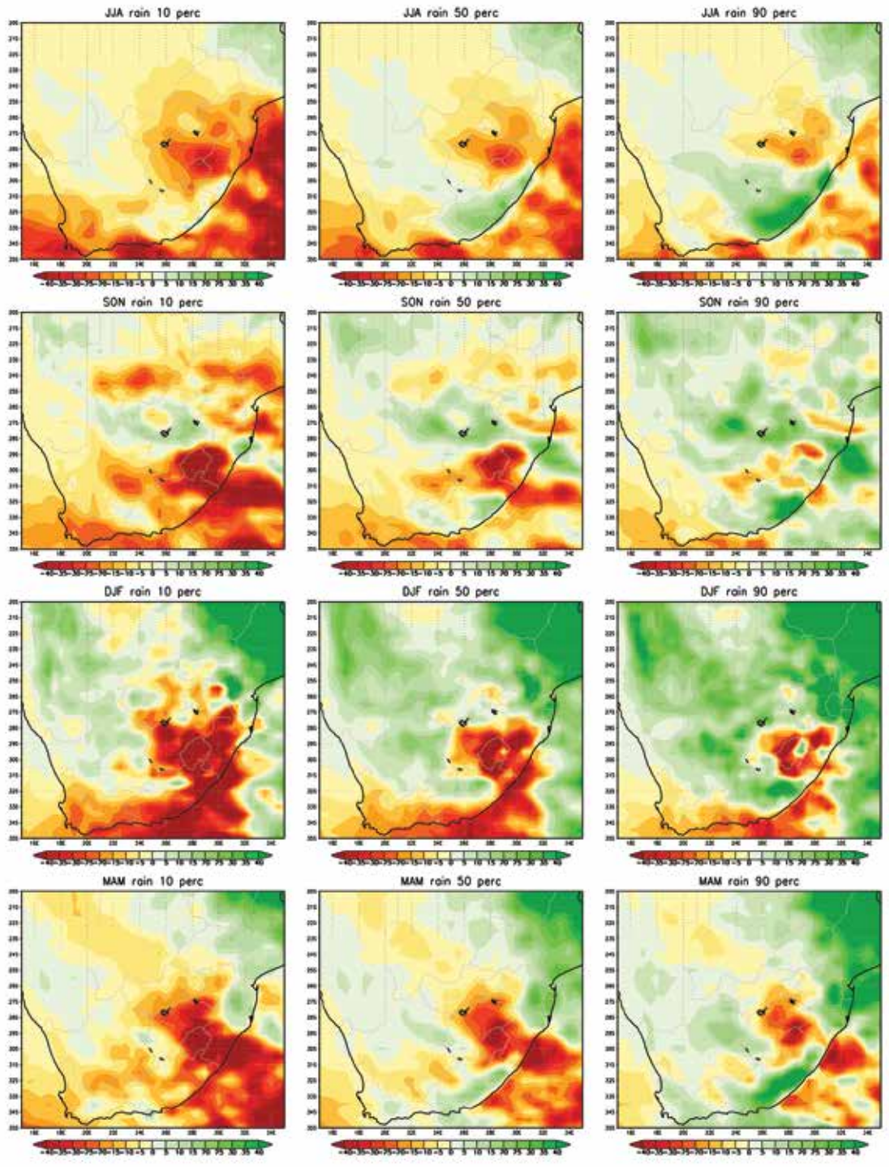

Figure 87. Projected change in the average seasonal rainfall (mm) over South Africa for JJA, SON, DJF and MAM, for the period 2080–2099 relative to 1971–2005. The 10th percentile (left), median (middle) and 90th percentile (right) are shown for an ensemble of downscalings of six CGCM projections, for each of the seasons. The downscalings were generated using the regional model CCAM. All the CGCM projections are contributing to CMIP5 and AR5 of the IPCC, and are for RCP4.5.

6. KEY MESSAGES AT NATIONAL AND SUB-NATIONAL SCALE

6.1 Key messages at national scale from the statistical and dynamical downscaling

The CCAM dynamic downscalings indicate that strong drying is plausible over the south-western Cape in the near-future under the A2 scenario, amplifying in time, and extending to the Cape south coast. These changes are consistent with a projected southward displacement of the westerlies and cold fronts in the model simulations (e.g. Christensen et al., 2007; Engelbrecht et al, 2009). These results to some extent contradict the CSAG B1 and A2 statistical downscalings, where the majority of ensemble members indicate moderate to significant rainfall increases over the winter rainfall region of the south-western Cape, extending to the Cape south coast, for the seasons autumn to spring, and for both the mid- and far-futures (a minority of the statistical downscaling ensemble members indicate significant drying over these regions). It has been proposed that thermodynamic considerations (more moisture in a warmer atmosphere – Hewitson, personal communication) may be the mechanism explaining the statistically downscaled projections indicating mostly wetter futures for the winter rainfall region. The signal of wetter futures is, however, of lesser amplitude in the CSAG downscalings for RCP 4.5 and 8.5, and it is only for winter and spring where most ensemble members indicate a wetting signal.

Dynamic downscaling indicates that significant reductions in rainfall are plausible over Limpopo and other parts of north-eastern South Africa, already in the near-future, with the pattern of drying projected to increase over time. The projections of decreasing rainfall totals are consistent with projected increases in the occurrence of mid-level highs over the eastern parts of southern Africa, a strengthening of the Indian Ocean High to the southeast of the subcontinent, and an associated northward displacement of tropical lows and cyclones (Engelbrecht et al., 2009; Malherbe et al., 2013). This signal of change is also evident in the majority of CSAG statistical downscalings, obtained for the B1 and A2 scenarios, for the summer and autumn seasons, and similarly in the CSAG downscalings for autumn for RCPs 4.5 and 8.5. Most RCP4.5 and 8.5 statistical downscalings indicate wetter futures over north-eastern South Africa, however, for summer.

The CCAM dynamic downscalings indicate that moderate to strong increases in rainfall are plausible over the central interior of South Africa in the far-future, extending to the southeast coast. Slight to moderate rainfall increases are projected over these regions for the near and mid-futures. These rainfall increases are projected to occur in spring and summer, in association with a deepening of the heat low over the western interior (Engelbrecht et al., 2009).

6.2 Downscaled sub-regional projections and key messages for SAs six hydrological zones

The projected envelope of changes in temperature and rainfall as a function of time is presented for each of the six hydrological zones below. The discussion of the regional messages is aided through the construction of graphs which show the ensemble of simulated annual anomalies in temperature and rainfall, for the period 1961–2100, relative to the 1971–2005 baseline period. The evolution of the climate system over time for each of the LTAS zones, as simulated by the CCAM downscalings, is depicted in this manner for the A2 (Figure 88), RCP8.5 (Figure 89) and RCP4.5 (Figure 90) scenarios.

6.2.1 Zone 1 (Limpopo/Olifants and Inkomati)

Annual average temperature increases of 3–6°C (4–7°C) are projected for Limpopo for the period 2080–2100, relative to the baseline period, under the A2 scenario (RCP8.5), by the respective CCAM ensembles (Figure

88 and Figure 89). These anomalies are well beyond the natural temperature variability of the region (as represented by the 1971–2005 blue dots in Figure 88 and Figure 89). That is, temperatures over Limpopo are projected to increase drastically, reaching a regime never observed before in the recorded climate of the region.

For the mid-future period (2040–2060) temperature anomalies of between 1 and 3°C (2 to 5°C) are projected under the A2 scenario (RCP8.5), by the respective CCAM ensembles (Figure 88 and Figure 89). The mid-future anomalies are already beyond the range of present-day climatology.

For the near-future period (2015–2035), annual temperature anomalies under the A2 and RCP8.5 scenarios are mostly within the realm of present-day climate, although drifting out of it towards the end of the period, reaching values of about 2°C.

Rainfall anomalies projected for Limpopo exhibit a clear pattern of drying under the A2 scenario, which strengthens over time. However, even for the far-future (2080–2100) the anomalies are within the range of present-day climate variability. Under the RCP8.5 scenario no clear pattern of drying is projected with simulated annual rainfall anomalies remaining within the range of present-day variability.

The RCP4.5 future implies significantly reduced increases in temperatures over Limpopo, with annual anomalies reaching only 2–3°C in the far-future (2080–2100). Rainfall anomalies are projected to remain within the realm of present-day climate (Figure 90).

6.2.2 Zone 2 (Pongola-Umzimkulu)

Annual average temperature increases of 3–5°C (4–6.5°C) are projected for Pongola-Umzimkulu for the period 2080–2100, relative to the baseline period, under the A2 scenario (RCP8.5), by the respective CCAM ensembles (Figure 88 and Figure 89). These anomalies are well beyond the natural temperature variability of the region (as represented by the 1971–2005 blue dots in Figure 88 and Figure 89). That is, temperatures over KwaZulu-Natal are projected to increase drastically, reaching a regime never observed before in the recorded climate of the region.

For the mid-future period (2040–2060) temperature anomalies of between 1 and 3°C (1 to 4°C) are projected under the A2 scenario (RCP8.5), by the respective CCAM ensembles (Figure 88 and Figure 89). The mid-future anomalies are already beyond the range of present-day climatology.

Even for the near-future (2015–2035), annual temperature anomalies under the A2 and RCP8.5 scenarios are drifting outside the present-day climatological regime of KwaZulu-Natal, reaching values of 1 to 2°C.

Rainfall anomalies projected for KwaZulu-Natal exhibit a clear pattern of drying under both the A2 scenario and RCP8.5, as is also clearly reflected by the medians of the projected changes (Figure 88 and Figure 89). Under the A2 scenario, the projected rainfall anomalies remain within the realm of present-day climate, but under RCP8.5, negative anomalies never observed under present-day conditions are projected to occur.

The RCP4.5 future implies significantly reduced increases in temperatures over KwaZulu-Natal, with annual anomalies reaching only 1 to 3°C in the far-future (2080–2100). Rainfall anomalies are projected to remain largely within the realm of present-day climate, with an indication of general, but modest drying (Figure 90).

6.2.3 Zone 3 (Vaal)

Drastic increases in annual average temperature of 3 to 6.5°C (5 to 8°C) are projected for zone 3 (North West) for the period 2080–2100, relative to the baseline period, under the A2 scenario (RCP8.5), by the respective CCAM ensembles (Figure 88 and Figure 89). These anomalies are well beyond the natural temperature variability of the region (as represented by the 1971–2005 blue dots in Figures 5.2 and 5.3). That is, temperatures over the north west are projected to increase drastically, reaching a regime never observed before in the recorded climate of the region.

For the mid-future period (2040–2060) temperature anomalies of between 1 and 3°C (2 to 5°C) are projected under the A2 scenario (RCP8.5), by the respective CCAM ensembles (Figure 88 and Figure 89). The mid-future anomalies are already beyond the range of present-day climatology.

Even for the near-future (2015–2035), annual temperature anomalies under the A2 and RCP8.5 scenarios are drifting outside the present-day climatological regime of north west, reaching values of 1 to 2.5°C.

Rainfall anomalies projected for north west exhibit a pattern of drying under both the A2 scenario and RCP8.5, as is reflected by the medians of the projected changes (Figure 88 and Figure 89). However, under both the A2 scenario and RCP8.5, the projected rainfall anomalies remain within the realm of present-day climate.

The RCP4.5 future implies significantly reduced increases in temperatures over north west, with annual anomalies remaining below 4°C in the far-future (2080–2100). There are indications of general but modest drying, with negative annual rainfall anomalies projected that are somewhat larger in amplitude than any of those simulated under present-day conditions (Figure 90).

6.2.4 Zone 4 (Orange)

Drastic increases in annual average temperature of 3–5.5°C (4–7.5°C) are projected for zone 4 (including a large part of the Northern Cape) for the period 2080–2100, relative to the baseline period, under the A2 scenario (RCP8.5), by the respective CCAM ensembles (Figure 5.2 and 5.3). These anomalies are well beyond the natural temperature variability of the region (as represented by the 1971–2005 blue dots in Figure 88 and Figure 89). That is, temperatures over zone 4 are projected to increase drastically, reaching a regime never observed before in the recorded climate of the region.

For the mid-future period (2040–2060) temperature anomalies of between 1 and 3°C (2 to 4°C) are projected under the A2 scenario (RCP8.5), by the respective CCAM ensembles (Figure 88 and Figure 89). The mid-future anomalies are already beyond the range of present-day climatology.

Even for the near-future (2015–2035), annual temperature anomalies under the A2 and RCP8.5 scenarios are drifting outside the present-day climatological regime for zone 4, reaching values of up to 2.5°C.

Rainfall anomalies projected for zone 4 exhibit a pattern of drying under both the A2 scenario and RCP8.5, as reflected by the medians of the projected changes (Figure 88 and Figure 89). However, under both the A2 and the RCP8.5 scenarios the projected rainfall anomalies remain within the realm of present-day climate.

The RCP4.5 future implies significantly reduced increases in temperatures over zone 4, with annual anomalies remaining below 4°C in the far-future (2080–2100). The pattern of drying projected for zone 4 under the more negative scenarios is absent under RCP4.5, with the simulated anomalies remaining within the realm of present-day climate (Figure 90).

6.2.5 Zone 5 (Mzimvubu Tsitsikamma)

Drastic increases in the annual average temperature of 2 to 5°C (4 to 6°C) are projected for the Eastern Cape

for the period 2080–2100, relative to the baseline period, under the A2 scenario (RCP8.5), by the respective CCAM ensembles (Figure 88 and Figure 89). These anomalies are well beyond the natural temperature variability of the region (as represented by the 1971–2005 blue dots in Figure 88 and Figure 89). That is, temperatures over zone 4 are projected to increase drastically, reaching a regime never observed before in the recorded climate of the region.

For the mid-future period (2040–2060) temperature anomalies of between 1 and 2°C (1 to 3.5°C) are projected under the A2 scenario (RCP8.5), by the respective CCAM ensembles (Figure 88 and Figure 89). The mid-future anomalies are already beyond the range of present-day climatology.

Even for the near-future (2015–2035), annual temperature anomalies under the A2 and RCP8.5 scenarios are drifting slightly outside the present-day climatological regime for zone 4, reaching values of just more than 2°C.

Rainfall anomalies projected for zone 5 exhibit a pattern of drying under both the A2 scenario and RCP8.5, as reflected by the medians of the projected changes (Figure 88 and Figure 89). For both the A2 and RCP8.5 scenarios the projected negative rainfall anomalies attain values that are well outside those associated with the present-day climatological regime.

The RCP4.5 future implies significantly reduced increases in temperatures over zone 4, with annual anomalies remaining below 3°C in the far-future (2080–2100). The pattern of drying projected for zone 5 under the more negative scenarios is significantly reduced under RCP4.5, with the simulated anomalies remaining within the realm of present-day climate (Figure 90).

6.2.6 *Zone 6 (Breede-Gouritz/Berg)*

Increases in the annual average temperature of 2 to 4°C (2 to 5°C) are projected for the south-western Cape for the period 2080–2100 relative to the baseline period, under the A2 scenario (RCP8.5), by the respective CCAM ensembles (Figure 88 and Figure 89). These anomalies are well beyond the natural temperature variability of the region (as represented by the 1971–2005 blue dots in Figure 88 and Figure 89). That is, temperatures over zone 4 are projected to increase drastically, reaching a regime never observed before in the recorded climate of the region.

For the mid-future period (2040–2060) temperature anomalies of between 1 and 2°C (1 to 2.5°C) are projected under the A2 scenario (RCP8.5), by the respective CCAM ensembles (Figure 88 and Figure 89). The mid-future anomalies are already beyond the range of present-day climatology.

Even for the near-future (2015–2035), annual temperature anomalies under the A2 and RCP8.5 scenarios are drifting slightly outside the present-day climatological regime for zone 6, reaching values of about 1.5°C (Figure 88 and Figure 89).

Rainfall anomalies projected for zone 6 exhibit a pattern of drying under both the A2 scenario and RCP8.5, as reflected by the medians of the projected changes (Figure 88 and Figure 89). For both the A2 and RCP8.5 scenarios the projected negative rainfall anomalies attain values that are well outside those associated with the present-day climatological regime.

The RCP4.5 future implies significantly reduced increases in temperatures over zone 6, with annual anomalies remaining below 3°C in the far-future (2080–2100). The pattern of drying projected for zone 6 under the more negative scenarios is well established even under RCP4.5, with the simulated anomalies outside the realm of present-day climate (Figure 90).

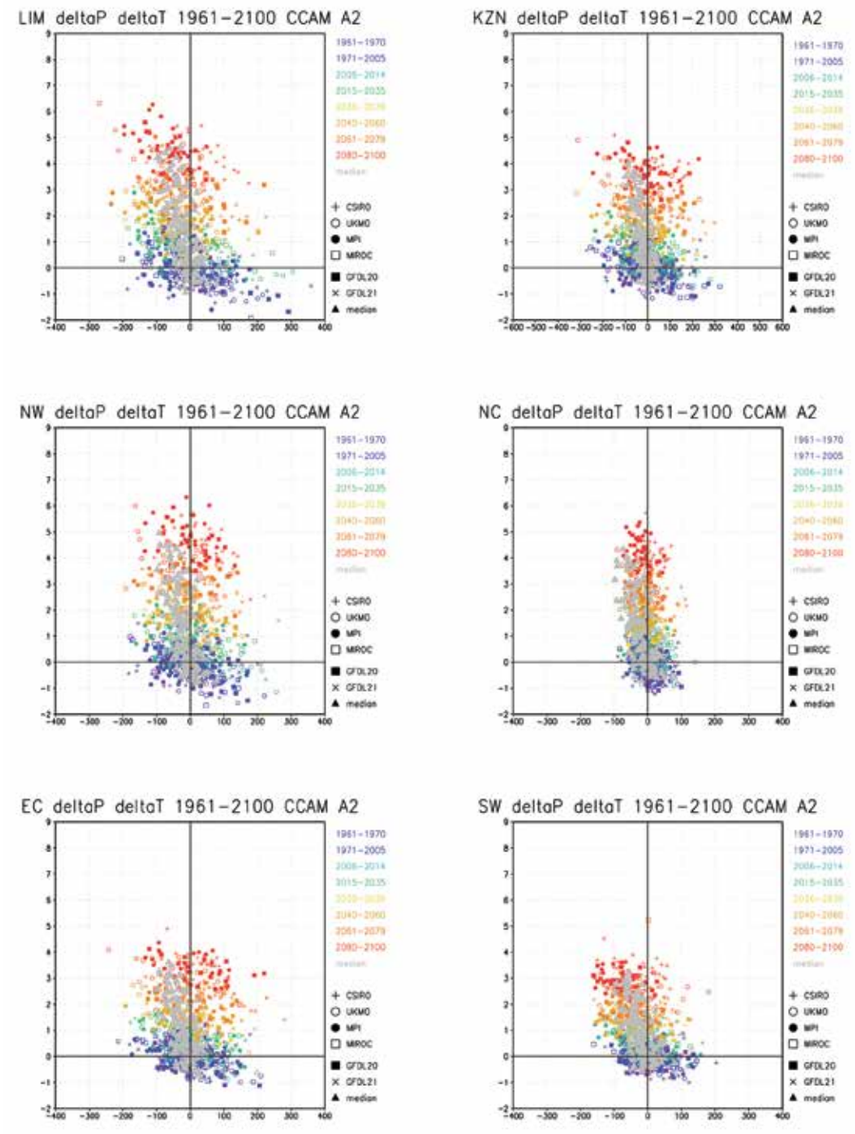

Figure 88. Projected annual temperature (°C, x-axis) and rainfall (mm, y-axis) anomalies for the period 1961–2100 over the six LTAS zones, relative to the 1971–2005 baseline climatology, for the six CCAM downscalings under the A2 scenario. For each year, the median of the ensemble of projected changes is shown in grey.

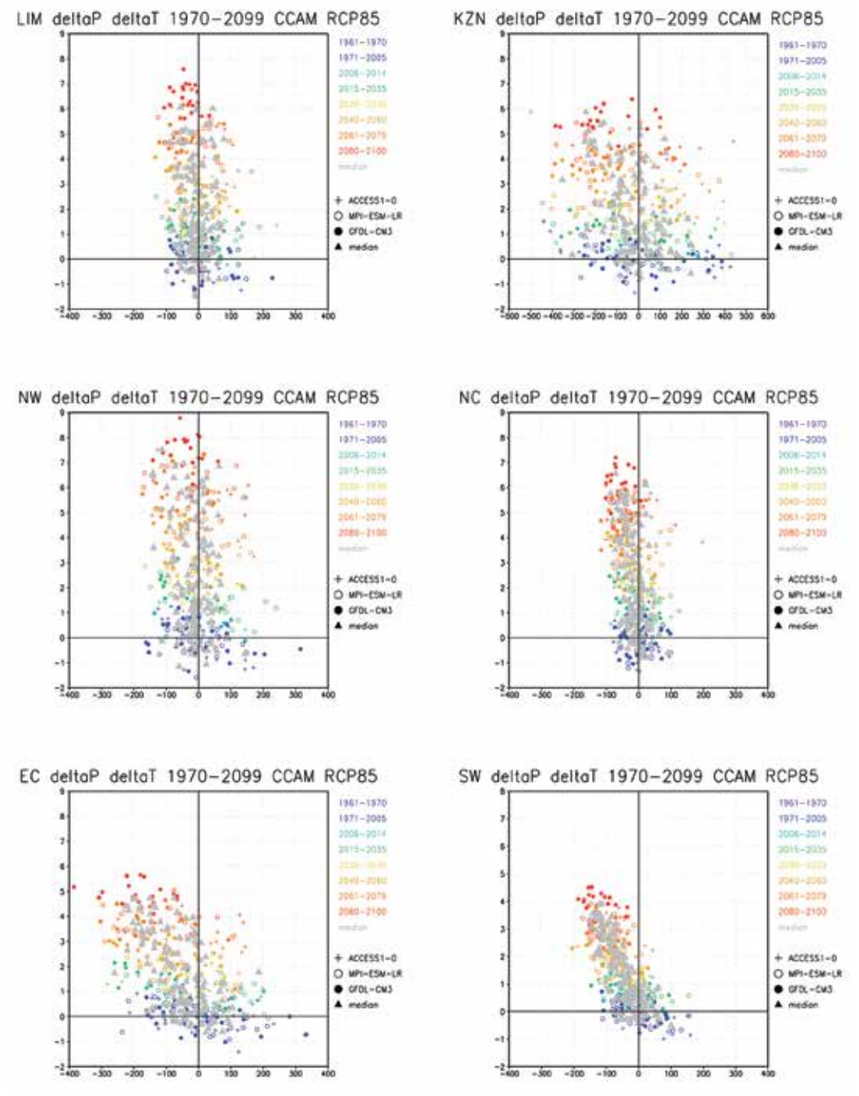

Figure 89. Projected annual temperature (°C, x-axis) and rainfall (mm, y-axis) anomalies for the period 1971–2099 over the six LTAS zones, relative to the 1971–2005 baseline climatology, for the six CCAM downscalings under the RCP8.5 scenario. For each year, the median of the ensemble of projected changes is shown in grey.

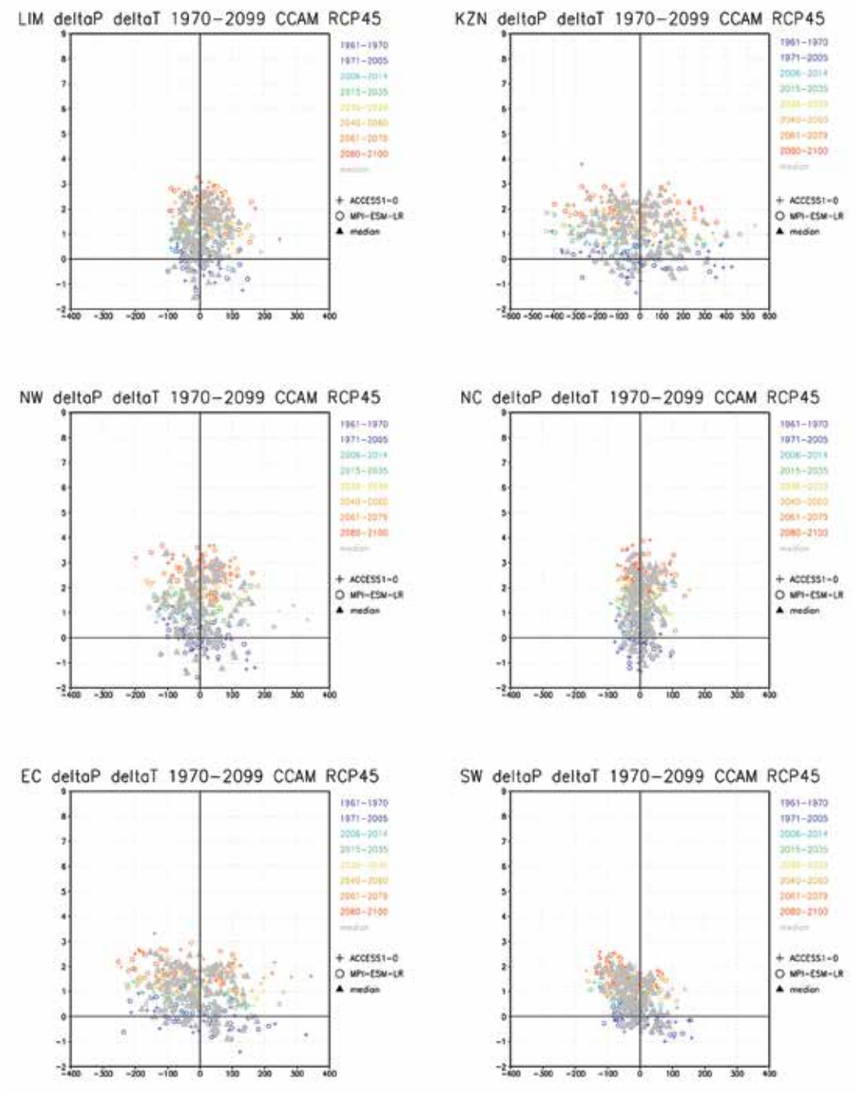

Figure 90. Projected annual temperature (°C, x-axis) and rainfall (mm, y-axis) anomalies for the period 1971–2099 over the six LTAS zones, relative to the 1971–2005 baseline climatology, for the six CCAM downscalings under the RCP4.5 scenario. For each year, the median of the ensemble of projected changes is shown in grey.

7. MIT PATTERN-SCALING PROJECTIONS AND COMPARISON TO THE HIGH-RESOLUTION REGIONAL DOWNSCALINGS

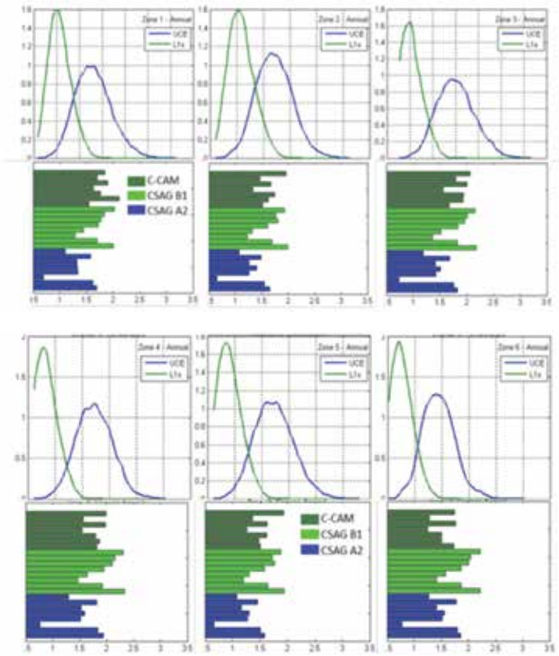

Figure 91. Probability density functions (PDFs) based on results of a global climate model that shows the spread of projected temperature changes as a probability curve (upper panels) under two emissions scenarios (unmitigated and mitigated) for each of the 6 water management zones, and temperature changes generated by statistically downscaled model projections (CCAM = mechanistically downscaled A2 emissions scenario, CSAG = statistically downscaled A2 and B1 emissions scenarios).

The Massachusetts Institute of Technology (MIT) procedure (Schlosser et al., 2011) allows for the construction of meta-ensembles of regional climate outcomes, combining the ensembles of the MIT Integrated Global System Model — which produce global and latitudinal climate projections, with uncertainty, under different global climate policy scenarios — with regionally resolved patterns from archived IPCC AR4 climate-model projections. These projections will be used during Phase 2 of the LTAS to derive a top-down view of the economic impacts of climate change on the South African economy. It is important to compare the MIT IGSM results with those produced by the locally generated downscaled results to ensure that the methodologies do not produce divergent projections, which would then propagate into divergent projections of impacts. Frequency distributions of future increases in temperature over the six LTAS zones are presented in Figure 91, for mitigated and unmitigated emissions, and compared with selected locally produced downscaled results. Qualitatively, the MIT results portray a similar message to those generated by the downscaling methods reported above. However, the MIT methodology more clearly indicates the potential reduction in risk due to global mitigation of large temperature increases over the country that is better quantified in the frequency distributions than by the relatively few realisations modelled in the locally generated projections. In other words, the MIT IGSM based methodology provides a useful additional view of the potential value of global mitigation for local impacts, and the potential avoided damages.

8. CLIMATE SCENARIOS FOR SOUTH AFRICA

Based on an assessment of the above climate change projections at national level under both the unconstrained and constrained pathways, South Africa's climate future up to 2050 and beyond can be described using four fundamental climate scenarios at national scale, with different degrees of change and likelihood that capture the impacts of global mitigation and the passing of time.

1. **warmer (<3°C above 1961–2000) and wetter** with greater frequency of extreme rainfall events.
2. **warmer (<3°C above 1961–2000) and drier**, with an increase in the frequency of drought events and somewhat greater frequency of extreme rainfall events.
3. **hotter (>3°C above 1961–2000) and wetter** with substantially greater frequency of extreme rainfall events.
4. **hotter (>3°C above 1961–2000) and drier**, with a substantial increase in the frequency of drought events and greater frequency of extreme rainfall events.

The effect of strong international mitigation responses would be to reduce the likelihood of scenarios 3 and 4, and increase the likelihood of scenarios 1 and 2 during the course of this century. In both wetter and drier futures, a higher frequency of flooding and drought extremes is projected, with the range of extremes exacerbated significantly under unconstrained emissions scenarios. These scenarios can be further elaborated in terms of rainfall projections at sub-national level e.g. for South Africa's six hydrological zones (see Table 1).

Table 2. Rainfall projections for each of South Africa's six hydrological zones

Scenario	Limpopo/ Olifants/ Inkomati	Pongola-Umzimkulu	Vaal	Orange	Mzimvubu-Tsitsikamma	Breede-Gouritz/ Berg
1: warmer/ wetter	↑ spring and summer	↑ spring	↑ spring and summer	↑ in all seasons	↑ in all seasons	↓ autumn, ↑ winter and spring
2: warmer/drier	↓ summer, spring and autumn	↓ spring and strongly ↓ summer and autumn	↓ summer and spring and strongly ↓ autumn	↓ summer, autumn and spring	↓ in all seasons, strongly ↓ summer and autumn	↓ in all seasons, strongly ↓ in the west
3: hotter/wetter	Strongly ↑ spring and summer	Strongly ↑ spring	↑ spring and summer	↑ in all seasons	Strongly ↑ in all seasons	↓ autumn, ↑ winter and spring
4: hotter/ drier	Strongly ↓ summer, spring and autumn	↓ spring and strongly ↓ summer and autumn	↓ summer and spring and strongly ↓ autumn	↓ summer, autumn and spring	↓ all seasons, strongly ↓ in summer and autumn	↓ all seasons, strongly ↓ in the west

9. CONCLUSION

The climate trends and scenario work conducted as part of LTAS Phase 1 represents the most significant step forward since the work of the Initial National Communication in consolidating locally relevant data that is available for South African climate change modelling. It is clear that climate changes have been observed over the last five decades, and include the fact that mean annual temperatures have increased by at least 1.5 times the observed global average of 0.65°C reported by IPCC AR4, that maximum and minimum temperatures show significant increases annually, and in almost all seasons. High temperature extremes have increased significantly in frequency, and low temperatures have decreased significantly in frequency annually and in most seasons across the country. Rainfall has shown high inter-annual variability, with rainfall being above average in the 1970s, the late 1980s, and the mid to late 1990s, and below average in the 1960s and in the early 2000s, reverting to mean towards 2010. Annual rainfall trends overall over the last five decades are weak and non-significant, but there is a tendency towards a significant decrease in the number of rain days in almost all hydrological zones. This implies a tendency towards an increase in the intensity of rainfall events and increased dry spell duration.

Based on comparisons of observed and modelled trends for 1960–2010, some key climatic processes relevant for South Africa appear not to be adequately represented by the GCMs or the downscaling methods currently in use. Key findings in this regard are that observed temperature trends are more closely matched by modelled simulations than are rainfall trends, a tendency noted in the IPCC fifth Assessment Report. It is also noteworthy that observed temperature trends since 2000 have not increased as steeply as projected by model simulations.

Overall, there is far less uncertainty in temperature than in rainfall projections over the coming century. All modelling approaches project warming trends until the end of this century, but most approaches project the possibility of both drying and wetting trends in almost all parts of South Africa. Climate change projections for South Africa up to 2050 and beyond under high emission scenarios include very significant warming, as high as 5–8°C, over the South African interior by the end of this century. Warming would however be somewhat reduced over coastal zones. A general pattern of a risk of drier conditions to the west and south of the country and a risk of wetter conditions over the east of the country is projected. Many of the projected changes are within the range of historical natural variability, and uncertainty in the projections is high. Nonetheless, global climate model ensembles summarised for South Africa suggest a significant benefit from effective mitigation responses (global CO_2e stabilisation at between 450 and 500 ppm) relative to unconstrained emission pathways by as early as mid-century. Effective global mitigation efforts would halve median warming at the regional level from just under 2°C to about 1°C by as early as 2050, and would reduce the risk of high regional warming and extreme changes in rainfall.

Even under effective international mitigation responses, significant socio-implications are expected for vulnerable groups and communities in South Africa under both wetter and drier climate futures. These implications will largely be felt through impacts on water resources, such as changes in water resource availability and a higher frequency of natural disasters (flooding and drought), with cross-sectoral effects on human settlements, disaster risk management and food security. There is a need to explore the cross-sectoral socio-implications of future climate scenarios on water and food security and to develop adaptation scenarios to inform national and sub-regional response strategies.

REFERENCES

Behera, S.K., Yamagata, T., 2001. Subtropical SST dipole events in the southern Indian Ocean. *Geophysical Research Letters* 28(2), 327–330.

Christensen, J.H., Hewitson, B., Busuioc, A., Chen, A., Gao, X., Held, I., Jones, R., Kolli, R.K., Kwon, W.-T., Laprise, R., Rueda, V.M., Mearns, L., Menéndez, C.G., Räisänen, J., Rinke, A., Sarr, A., Whetton, P., 2007. Regional climate projections. In: S. Solomon, D. Qin, M. Manning, Z. Chen, M. Marquis, K.B. Averyt, M. Tignor, H.L. Miller (Editors), Climate Change 2007: The Physical Science Basis. Contribution of Working Group I to the Fourth Assessment Report of the Intergovernmental Panel on Climate Change. Cambridge University Press, Cambridge, United Kingdom and New York, NY, USA, pp. 847–940.

Department of Environmental Affairs (DEA) 2011. National Climate Change Response White Paper (NCCRP). Department of Environmental Affairs, Pretoria.

Easterling, D.R., et al., 1997. Maximum and Minimum Temperature Trends for the Globe. *Science* 277(5324), 364–367.

Easterling, D.R., Evans, J.L., Groisman, P.Y., Karl, T.R., Kunkel, K.E., Ambenje, P., 2000. Observed Variability and Trends in Extreme Climate Events: A Brief Review. *Bulletin of the American Meteorological Society* 81, 417–425.

Engelbrecht C.J., Engelbrecht F.A. and Dyson L.L., 2012. High-resolution model-projected changes in mid-tropospheric closed-lows and extreme rainfall events over southern Africa. *International Journal of Climatology* 33, 173–187. doi: 10/1002/joc.3420.

Engelbrecht, F., W. Landman, C. Engelbrecht, S. Landman, M. Bopape, G. Roux, J. McGregor, and M. Thatcher. 2011. Multi-scale climate modelling over Southern Africa using a variable-resolution global model. *Water SA* 37(5), 647–658.

Engelbrecht, F. A., J. L. McGregor, and C. J. Engelbrecht. 2009. Dynamics of the conformal-cubic atmospheric model projected climate-change signal over southern Africa. *International Journal of Climatology* 29(7),1013–1033.

Fauchereau, N., Pohl, B., Reason, C.J.C., Rouault, M., Richard, Y., 2008. Recurrent daily OLR patterns in the Southern Africa/Southwest Indian Ocean region, implications for South African rainfall and teleconnections. *Climate Dynamics* 32(4), 575–591.

Groisman, P.Y., Knight, R.W., Easterling, D.R., Karl, T.R., Hegerl, G.C., Razuvaev, V.N., 2005. Trends in Intense Precipitation in the Climate Record. *Journal of Climate* 18, 1326–1350.

Hansingo, K., Reason, C.J.C., 2008. Modelling the atmospheric response to SST dipole patterns in the South Indian Ocean with a regional climate model. *Meteorology and Atmospheric Physics* 100(1–4), 37–52.

Hewitson, B. C. and R. G. Crane. 2006. Consensus between GCM climate change projections with empirical downscaling: Precipitation downscaling over South Africa. *International Journal of Climatology* 26(10),1315-1337.

Hughes, W.S., Balling, R.C., 1996. Urban influences on South African temperature trends. *International Journal of Climatology* 16(8), 935–940.

Hulme, M., Doherty, R., Ngara, T., New, M., Lister, D., 2001. African climate change: 1900–2100. *Climate Research* 17, 145–168.

Hulme, M., J. Mitchell, W. Ingram, J. Lowe, T. Johns, M. New, and D. Viner. 1999. Climate change scenarios for global impacts studies. *Global Environmental Change* 9, S3-S19.

IPCC, 2007: Climate Change (2007): *Synthesis Report.* Contribution of Working Groups I, II and III to the

Fourth Assessment Report of the Intergovernmental Panel on Climate Change [Core Writing Team, Pachauri, R.K and Reisinger, A. (eds.)]. IPCC, Geneva, Switzerland, 104 pp.

Kruger, A.C., 1999. The influence of the decadal-scale variability of summer rainfall on the impact of El Niño and La Niña events in South Africa. *International Journal of Climatology* 19(1), 59–68.

Kruger, A.C., 2006. Observed trends in daily precipitation indices in South Africa: 1910–2004. *International Journal of Climatology* 26(15), 2275–2285.

Kruger, A.C., Sekele, S.S., 2013. Trends in extreme temperature indices in South Africa: 1962–2009. International *Journal of Climatology* 33(3), 661–676.

Kruger, A.C., Shongwe, S., 2004. Temperature trends in South Africa: 1960-2003. *International Journal of Climatology* 24(15), 1929–1945.

Landman, W.A., Beraki, A., 2012. Multi-model forecast skill for mid-summer rainfall over southern Africa. *International Journal of Climatology* 32(2), 303–314.

Lindesay, J.A., 1988. South African rainfall, the Southern Oscillation and a Southern Hemisphere semi-annual cycle. *Journal of Climatology* 8(1), 17–30.

Mason, S. J. and Jury, M.R. (1997). Climatic change and inter-annual variability over Southern Africa: a reflection on underlying processes. *Progress in Physical Geography*, 21, 24-50.

Mason, S.J., Waylen, P.R., Mimmack, G.M., Rajaratnam, B., Harrison, J.M., 1999. Changes in extreme rainfall events in South Africa. *Climatic Change* 41(2), 249–257.

Malherbe J., Engelbrecht F.A. and Landman W.A., 2013. Projected changes in tropical cyclone climatology and landfall in the Southwest Indian Ocean under enhanced anthropogenic forcing. *Climate Dynamics* 40(11-12), 2867–2886. doi: 10.1007/s00382-012-1635-2.

Nel, W., 2009. Rainfall trends in the KwaZulu-Natal Drakensberg region of South Africa during the twentieth century. *International Journal of Climatology* 29(11), 1634–1641.

New, M., Hewitson, B., Stephenson, D.B., Tsiga, A., Kruger, A., Manhique, A., Gomez, B., Coelho, C.A.S., Masisi, D.N., Kululanga, E., Mbambalala, E., Adesina, F., Saleh, H., Kanyanga, J., Adosi, J., Bulane, L., Fortunata, L., Mdoka, M.L., Lajoie, R., 2006. Evidence of trends in daily climate extremes over southern and west Africa. *Journal of Geophysical Research* 111. doi: 10.1029/2005JD006289

Pohl, B., Richard, Y., Fauchereau, N., 2007. Influence of the Madden–Julian Oscillation on Southern African summer rainfall. *Journal of Climate* 20(16), 4227–4242.

Pohl, B., Fauchereau, N., Reason, C.J.C., Rouault, M., 2010. Relationships between the Antarctic Oscillation, the Madden–Julian Oscillation, and ENSO, and consequences for rainfall analysis. *Journal of Climate* 23(2), 238–254.

Reason, C.J.C., Allan, R.J., Lindesay, J.A., Ansell, T.J., 2000. ENSO and climatic signals across the Indian Ocean Basin in the global context: part I, interannual composite patterns. *International Journal of Climatology* 20(11), 1285–1327.

Reason, C.J.C., 2001. Subtropical Indian Ocean SST dipole events and southern African rainfall. *Geophysical Research Letters* 28, 2225–2227.

Reason, C. J. C., W. Landman, M. Tadross, W. Tennant, and M.-J. Kagatuke. 2004. Seasonal to decadal predictability and prediction of southern African climate. OceanDocs. http://hdl.handle.net/1834/403:41.

Reason, C. J. C. and M. Rouault. 2002. ENSO-like decadal variability and South African rainfall. *Geophysical Research Letters* 29(13),16-11–16-14.

Reason, C.J.C., Rouault, M., 2005. Links between the Antarctic Oscillation and winter rainfall over western South Africa. *Geophysical Research Letters* 32, L07705, doi:10.1029/2005GL022419

Richard, Y., Fauchereau, N., Poccard, I., Rouault, M., and Trzaska, S.: 2001. 20th century droughts in Southern Africa – spatial and temporal variability, teleconnections with oceanic and atmospheric conditions, *International Journal of Climatology* 21, 873–895.

Richard, Y., Trzaska, S., Roucou, P., Rouault, M., 2000. Modification of the southern African rainfall variability/ ENSO relationship since the late 1960s. *Climate Dynamics* 16(12), 883–895.

Tadross, M.A., Jack C., and Hewitson B.C., 2005: On RCM-based projections of change in southern African summer climate. *Geophysical Research Letters*, 32(23), L23713, doi: 10.1029/2005GL024460

Thomas, D.S.G., Twyman, C., Osbahr, H., Hewitson, B., 2007. Adaptation to climate change and variability: farmer responses to intra-seasonal precipitation trends in South Africa. *Climatic Change* 83(3), 301–322

Tyson, P.D., 1986. *Climatic change and variability in southern Africa.* Oxford University Press, Cape Town.

Tyson, P. D., T. G. J. Dyer, and M. N. Mametse. 1975. Secular changes in South African rainfall: 1880 to 1972. *Quarterly Journal of the Royal Meteorological Society* 101, 817–833.

Tyson, P.D., Cooper, G.R.J., McCarthy, T.S., 2002. Millennial to multi-decadal variability in the climate of southern Africa. *International Journal of Climatology* 22(9), 1105–1117

NOTES

315 Pretorius Street
cnr Pretorius & van der Walt Streets
Fedsure Forum Building
North Tower
2nd Floor (Departmental reception) or
1st Floor (Departmental information centre) or
6th Floor (Climate Change Branch)
Pretoria, 0001

Postal Address
Private Bag X447
Pretoria
0001

Publishing date: October 2013

www.environment.gov.za

S-1159-A www.studio112.co.za